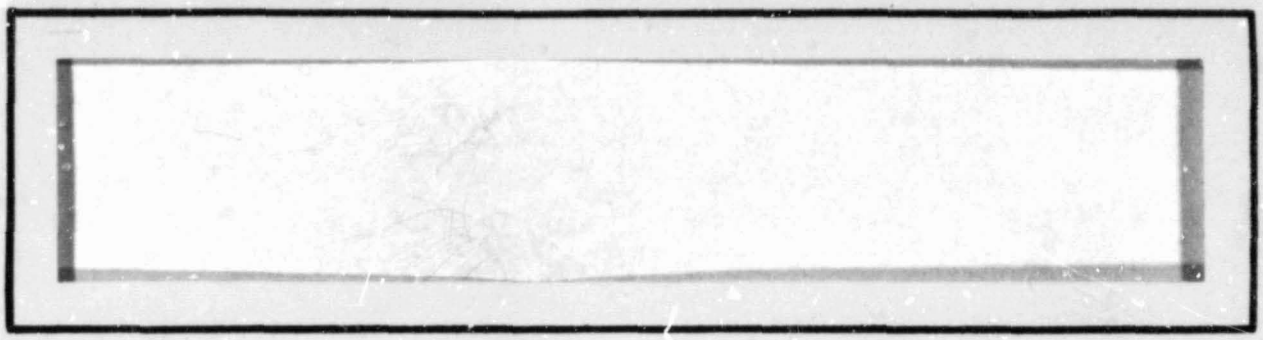

Axiomatix

PRELIMINARY CENTAUR SYSTEMS ANALYSIS

FINAL REPORT

Contract No. NAS9-16067, Exhibit B

Technical Monitor: William Teasdale

Prepared for

NASA Lyndon B. Johnson Space Center
Houston, Texas 77058

Prepared by

Robert G. Maronde
Dr. Jack K. Holmes
Dr. Richard S. Iwasaki

Axiomatix
9841 Airport Blvd., Suite 912
Los Angeles, California 90045

Axiomatix Report No. R8112-2
December 10, 1981

TABLE OF CONTENTS

1.0 INTRODUCTION

The purpose of this report is to summarize the Axiomatix activities to date on the Shuttle/Centaur program. This document contains both new findings and those previously discussed in Axiomatix Interim Report No. R8109-2, dated September 15, 1981.

2.0 BACKGROUND

The Centaur is stored in the Orbiter payload bay on the Centaur Integrated Support System (CISS), as shown in Figure 2.1. The CISS not only cradles the Centaur prior to deployment but also provides any signal conditioning required to make the Centaur/Orbiter hardwire interfaces compatible. In addition, the CISS provides other Centaur functions such as controlling all the avionics safety features and providing all the helium supplies for tank pressurizations.

Upon deployment, the Centaur is raised up and mechanically spring ejected from the CISS which returns with the Orbiter for future use. After arming the reaction control motors, the Centaur is stabilized and, for thermal reasons, has a roll imparted to it. Sometime prior to Centaur/payload separation, the initial roll is significantly increased. The roll rates are still under discussion but, originally, the initial roll rate was 1 RPM at Centaur/Orbiter separation. Just prior to Centaur/paylaod separation, the 1-RPM rate was to have been increased to 2.9 RPM. Currently, General Dynamics (GD) feels that the initial roll rate will be 0.1 RPM and will be increased to 0.33 RPM prior to Centaur/payload separation.

Once separated from the Orbiter, the Centaur RF links will be either between the Centaur and the Orbiter utilizing the Orbiter Payload Interrogator (PI) or between the Centaur and the ground stations via the TDRSS. The Centaur transponder under consideration by GD is a NASA standard transponder manufactured by Motorola which was previously used by the Goddard Spaceflight Center. Since this particular transponder possesses no false-lock discrimination circuits, the payload specialist aboard the Orbiter must employ a manual acquisition process, as illustrated in Figure 2.2.

Briefly, the payload specialist must transmit an unmodulated carrier to the Centaur, achieve return link lock and modulate the carrier. In order to verify proper lock, the operator should also examine the

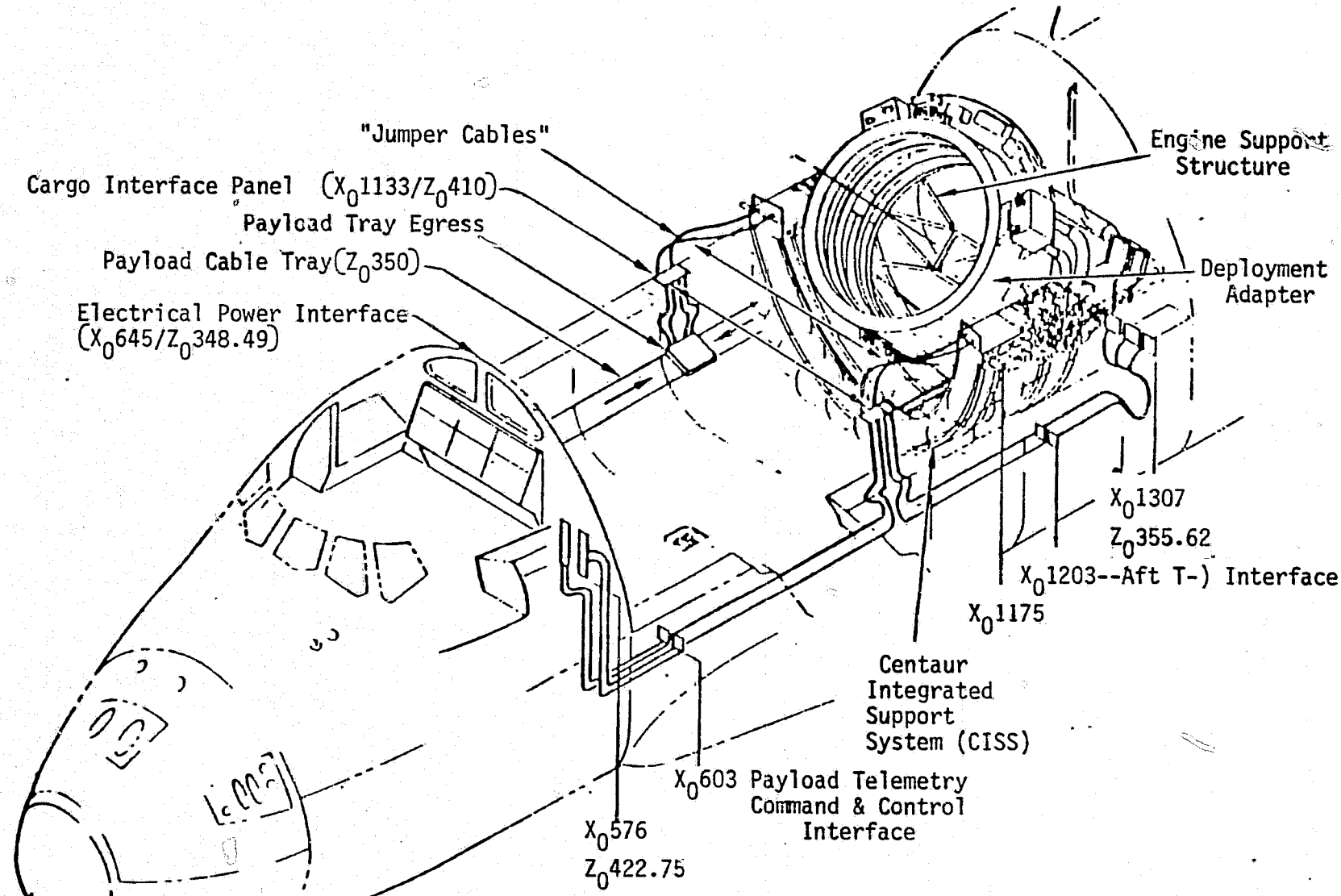

Figure 2.1. Centaur/Payload Bay Interface Overview

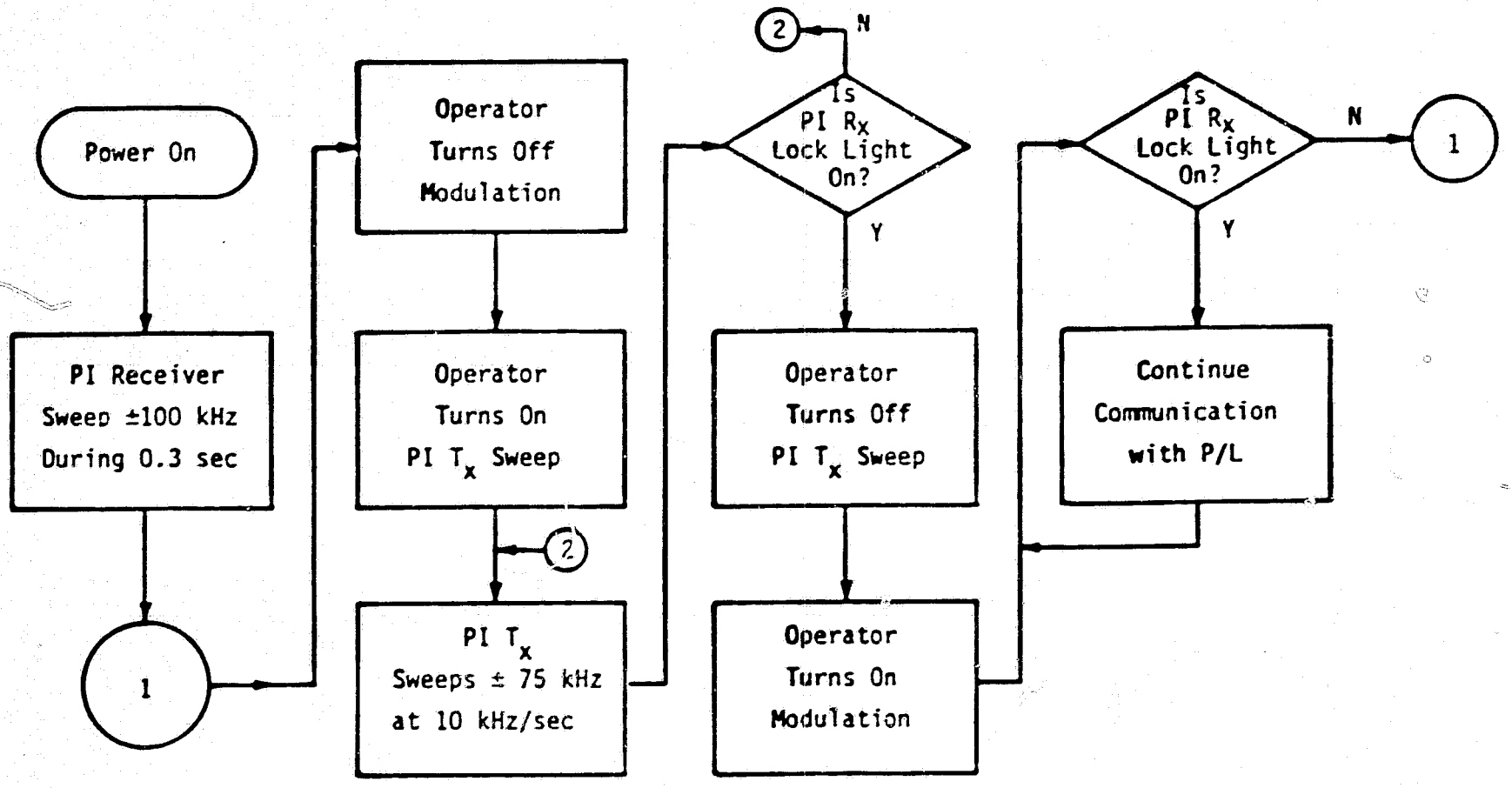

Note 1. PI Receiver can tolerate 50-ms signal dropout without reinitiating the sweep

Note 2. Standard transponder's receiver has ±1400-Hz instantaneous acquisition range

Figure 2.2. Orbiter Payload Interrogator/Payload Transponder Link Acquisition Sequence

return link telemetry. It has been estimated that this manual acquisition procedure could take as long as 30 seconds.

In order to provide full spherical RF coverage for the Centaur, the initial antenna concept was to employ two S-band switchable hemispherical antennas on 1-to-2-foot booms, as shown in Figure 2.3. Since each antenna provides hemispherical coverage, the antennas will switch from one to another and back every Centaur revolution. For example, each antenna will switch every 300 seconds for a roll rate of 0.1 RPM, every 30 seconds for a roll rate of 1 RPM and every 10 seconds for a roll rate of 3 RPM.

3.0 FINDINGS

There are a number of very serious potential problems associated with a Centaur design concept using the Motorola transponder and the two switchable-hemispherical antennas.

3.1 Problem 1

The first problem is the manual acquisition sequence previously described. At the present time, the Orbiter software does not display the Centaur telemetry on the crew CRT to determine if the telemetry is valid. Without verifying the telemetry, it is possible to be false locked on a sideband and not be aware of the situation. It is also possible for the Shuttle/Centaur link to be in the noncoherent mode, i.e., the return link locked on the Centaur TCXO instead of the VCXO, and have no indication of the problem.

3.1.1 Solution to Problem 1

One possible solution is to implement in the Orbiter software the ability to display the Centaur telemetry for the payload specialist on the crew CRT. A second possible solution is to design antifalse-lock circuits into the Motorola transponder.

3.2 Problem 2

The second potential problem dealt with is the ability of the transponder to hold lock in the presence of transients. The GD Functional

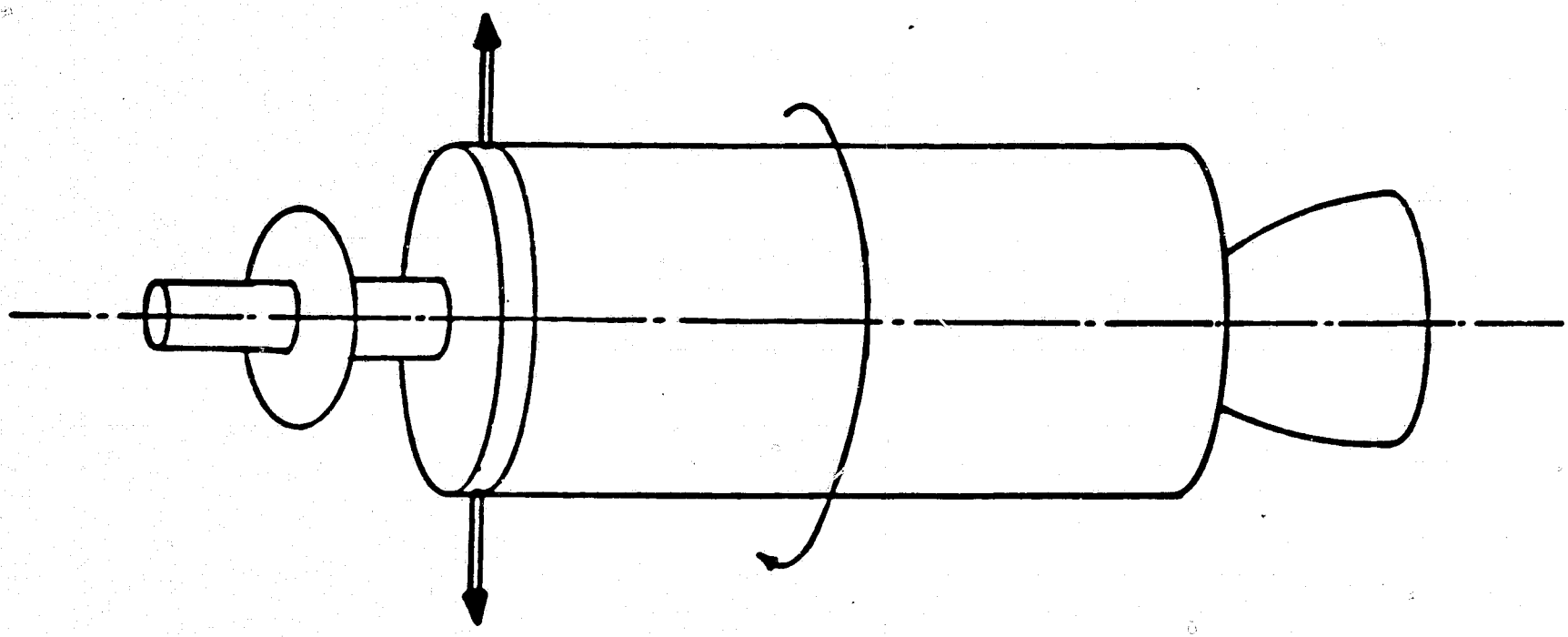

Figure 2.3. Initially Proposed GD Centaur Antenna System

Requirements Document (FRD) 65-03001, Specification for Transponder-Shuttle/Centaur states in paragraph 3.2.1.3.1.8 that antenna-switching transients of 1 to 40 ms shall be accommodated without loss of lock.

3.2.1 Solution to Problem 2

When Axiomatix initially examined the transponder FRD, it appeared that the transponder would lose lock in the presence of transients. After a detailed analysis by Axiomatix with follow-up testing verification by Motorola, however, Axiomatix now feels that the transponder can tolerate 40-ms transients.

Appendix A, Sections 1 and 2, are the results of the Axiomatix transponder analysis. Appendix A, Section 3, is a Motorola analysis, while Sections 4 and 5 are the TDRS mode and STDN mode, respectively, Motorola test results.

The conclusion reached is that, in the presence of 1-to-40-ms transients, the transponder will not lose lock but, of course, any data acquired during the transient will be lost.

3.3 Problem 3

The third problem concerns the phase transients produced when switching from one antenna to another and the low gain of the hemispherical antennas which contribute to a marginal RF link. Since both antennas are many wavelengths apart from each other physically, the geometric differences between the two phase centers will produce a phase transient when the antennas are switched.

Depending on the Centaur roll rate, a very serious potential problem may occur. Consider the magnitude of the impact upon the Shuttle/Centaur RF link should loss of lock occur with the Centaur rolling at a rate of 1 to 3 RPM, which means that the antennas switch every 30 to 10 seconds, respectively. The time for the manual acquisition sequence to establish lock between the Orbiter and Centaur is 30 seconds maximum. The worst-case situation is that, with the long acquisition sequence and the relatively fast antenna switching, the phase transients may be such that Shuttle/Orbiter lock may never be established or, if it is, the payload specialist has no real method with which to determine if true lock has occurred since there is no telemetry to analyze.

3.3.1 Solution to Problem 3

It can easily be seen that, should the roll rates be decreased to the order of 0.1 to 0.33 RPM, the potential problem of not being able to establish lock is resolved. If the roll rates are sufficiently high, however, another antenna concept may be used--not only to minimize switching--but to improve the antenna gain as well.

Appendix B, Section 1, discusses the various GD antenna approaches. Appendix B, Section 2, describes an initial concept which Axiomatix presented at the Centaur Communications Panel meeting at Lewis Research Center, held September 30 to October 1, 1981. After addressing a number of criticisms, Axiomatix presents a second approach for consideration which is discussed in Appendix B, Section 3.

3.4 Additional Tasks

Additional tasks performed by Axiomatix included determining acceptable interface circuits between the Centaur and the payload recorder and the Payload Data Interleaver (PDI). Figures 3.1 and 3.2 show interface circuits that are being used successfully by Boeing for the Inertial Upper Stage (IUS) program, and these circuits should be adaptable for Centaur use.

Also, generation of a hardware Interface Control Document (ICD) was required. Rockwell, working with Axiomatix, produced the hardline ICD shown in Appendix C.

3.5 Conclusions

Axiomatix feels that the Orbiter crew needs some indication that the Centaur/Orbiter link is coherent and, therefore, recommends that the Orbiter software be modified to display Centaur telemetry. Axiomatix has concluded that 1-to-40-ms transients will not cause the transponder to lose lock but, of course, any data during the transient will be lost.

Lastly, Axiomatix is very concerned about the impact that high Centaur roll rates will have on the ability to maintain the Centaur link. Axiomatix has proposed an antenna approach to minimize this problem but also recommends that the required roll rates be established as soon as possible in order to study their effects on link integrity.

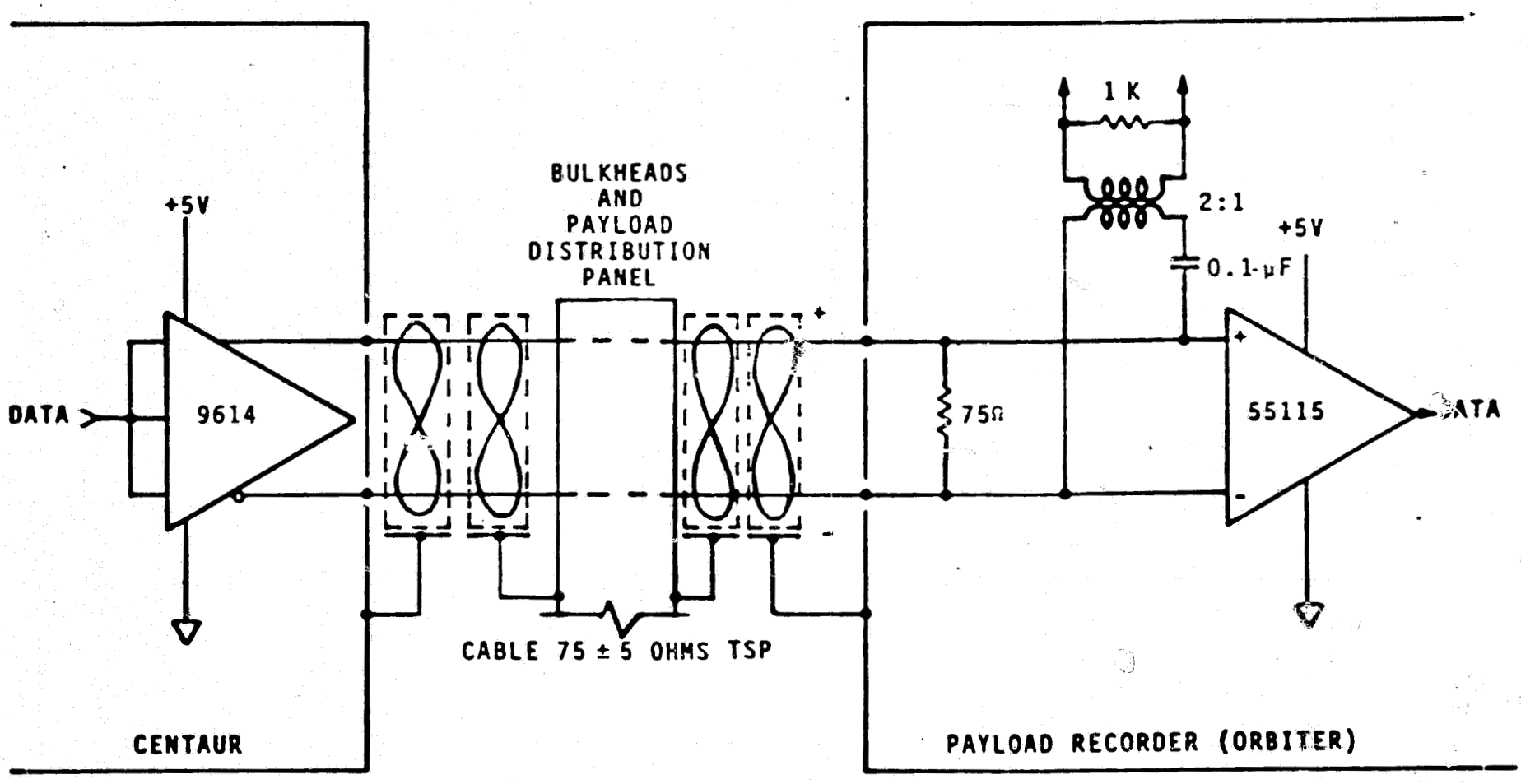

Figure 3.1. Centaur/Payload Recorder Hardline Interface

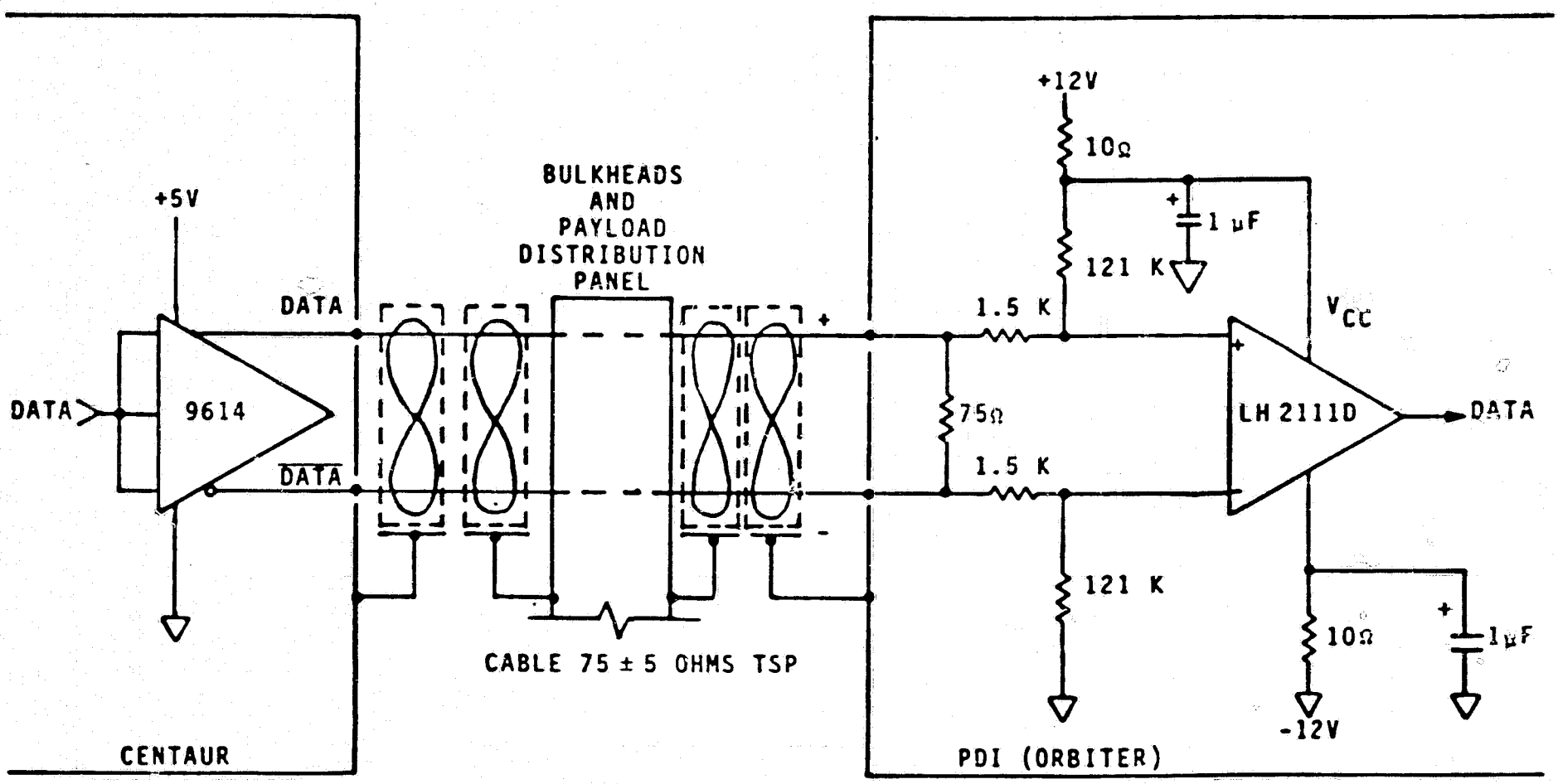

Figure 3.2. Centaur/PDI Hardline Interface

APPENDIX A

MOTOROLA TRANSPONDER RESPONSE TO ONE-TO-40-MS TRANSIENTS

APPENDIX A.1

FREQUENCY DRIFT OF CENTAUR TRANSPONDER VCO FREQUENCY DUE TO ANTENNA SWITCHING

Axiomatix

9841 Airport Boulevard • Suite 912 • Los Angeles, California 90045 • Phone (213) 641-8600

TECHNICAL MEMORANDUM NO. M8109-2

TO: B. Maronde

DATE: September 25, 1981

FROM: J. K. Holmes

COPIES: R. Iwasaki
16067"B" File

SUBJECT: Frequency Drift of Centaur Transponder VCO Frequency Due to Antenna Switching

---

1.0 SUMMARY

The Centaur carrier loop dropout problem has been investigated by considering how far the carrier loop VCO would change frequency from the initial position of one-half the tracking range (50-kHz offset) to its rest position of 0-kHz offset due to a signal dropout. It was found that, for a dropout of a few milliseconds, loss of lock would not occur with high probability. However, for a dropout of 40 ms, the drift would be about 5100 Hz, or over 10 times the closed-loop bandwidth of 500 Hz. Under this amount of drift, it is felt that the loop will, with very high probability, lose lock.

It was also determined that the carrier phase shift induced by antenna switching and occuring after the signal dropout was not important for dropouts greater than about 4 ms. The reason for this is that the typical VCO frequency drift during dropouts causes the phase error to be on the order of cycles so that any additional phase error due to antenna switching is unimportant because phase errors are important only on the modulo 2π.

2.0 ANALYSIS

Consider a PLL model that has a noise only input as shown in Figure 1.

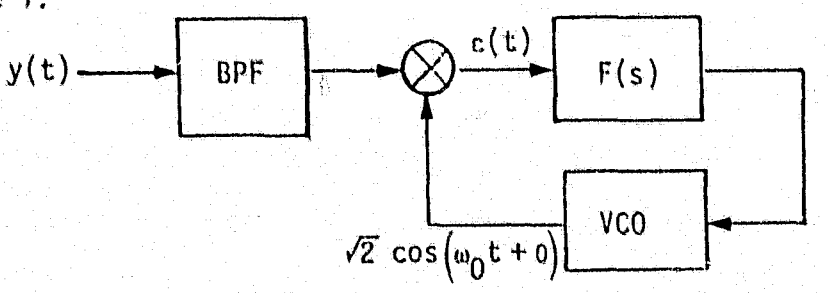

Figure 1. Phase-Locked-Loop Model Used for Analysis

Just after dropout, the noise-only input is given by

$$y(t) = \sqrt{2}\, N_c(t) \cos\left(\omega_0 t + 0\right) + \sqrt{2}\, N_s(t) \sin\left(\omega_0 t + 0\right) \tag{1}$$

which is an in-phase and quadrature noise representation of bandpass noise centered at angular frequency ω_0. After heterodyning by the VCO frequency, the error signal is of the form

$$\varepsilon(t) = N_c(t) \cos\phi + N_s(t) \sin\phi + V_{dc} \tag{2}$$

where ϕ is the phase difference between the VCO frequency and the reference phase angle of the noise process. The multiplier offset bias is denoted by V_{dc}. It can be shown that $\varepsilon(t)$ has the statistics of $N_c(t)$ or $N_s(t)$, i.e., bandlimited white Gaussian noise. Therefore, we model the error signal by

$$\varepsilon(t) = N'(t) + V_{dc} \tag{3}$$

where $N'(t)$ has the same statistics as $N_c(t)$. Using Heaviside operator notation in the variable s, for the VCO phase estimate, we have

$$\hat{\theta}(t) = \frac{K_m K_{VCO} F(s)}{s} \left(N'(t) + V_{dc}\right) \tag{4}$$

where K_m is the multiplier gain and K_{VCO} is the VCO gain constant having units of radians per second per volt. Since the Centaur transponder loop is specified as a second-order loop, we can model the loop filter as a passive second-order loop filter

$$F(s) = \frac{1 + \tau_2 s}{1 + \tau_1 s} \tag{5}$$

where τ_1 and τ_2 are the time constants of the loop filter. This can be rewritten as

$$F(s) = F_0\left[1 + \frac{\frac{1}{\tau_2} - \frac{1}{\tau_1}}{s + \frac{1}{\tau_1}}\right] \tag{6}$$

where

$$F_0 = \frac{\tau_2}{\tau_1} \tag{7}$$

Denoting $K_m K_{VCO}$ by K and using (6) in (4) yields

$$\dot{\hat{\theta}}(t) = \left\{KF_0 + KF_0\left[\frac{\frac{1}{\tau_2} - \frac{1}{\tau_1}}{s + \frac{1}{\tau_1}}\right]\right\}\left\{V_{dc} + N'(t)\right\} \tag{8}$$

Now since

$$\frac{1}{s + \frac{1}{\tau_1}} \; g(t) \leftrightarrow \int_0^t e^{-(t-\tau)/\tau_1} \, g(\tau)d\tau + C_0 e^{-t/\tau_1} \tag{9}$$

where the third term is due to the homogeneous solution associated with the differential equation

$$e_i(t) = \dot{e}_0(t) + \frac{1}{\tau_1} e_0(t) \tag{10}$$

We have that

$$\dot{\hat{\theta}}(t) = \left\{KF_0V_{dc} + KF_0N'(t) + KF_0\int_0^t e^{-(t-\tau)/\tau_1}\left(V_{dc} + N'(\tau)\right)d\tau + C_0e^{-t/\tau_1}\right\} \tag{11}$$

Since V_{dc} is unknown, we will assume that it is negligible*, thus allowing us to approximate (10) by

---

*This assumption minimizes the worst-case out-of-lock VCO drift rate.

$$\dot{\hat{\theta}}(t) = KF_0N'(t) + KF_0 \frac{\frac{1}{\tau_2} - \frac{1}{\tau_1}}{s + \frac{1}{\tau_1}} \int_0^t e^{-(t-\tau)/\tau_1} N'(t)d\tau + C_0e^{-t/\tau_1} \quad (12)$$

implied by (9).

From (12), we see that the value of $\dot{\hat{\theta}}(t)$ at any time t is composed of the original noise process N'(t) plus a filtered version of the noise process. Consequently, the noise is large compared to the dc loop control voltage (nominally zero in lock). Furthermore, it appears that the VCO noise voltage changes appreciably with time, whereas the dc component of the VCO voltage changes slowly, with a time constant τ_1. When the loop is in lock (signal is present), the thermal noise is again quite large; however, the loop can tolerate this condition since phase tracking "sees" one more integration than frequency tracking. Therefore, we consider the dc voltage on the VCO as the important parameter in reacquisition. At t = 0, the dc value of the VCO frequency is $\Delta\omega_0$ (relative to the rest VCO frequency) so that, at t = 0,

$$C_0 = \Delta\omega_0 \quad (13)$$

and the change, or error, in the VCO frequency is given by

$$\delta\omega(t) = \Delta\omega_0 - \Delta\omega_0e^{-t/\tau_1} \quad (14)$$

In order to estimate the parameter τ_1, we must estimate* some loop parameters. First, since B_L = 500 Hz, we can determine the value of ω_n via

$$\omega_n = \frac{2B_L}{\left(\zeta + \frac{1}{4\zeta}\right)} \text{ rad/sec} \quad (15)$$

*The parameters were unknown at the time of this writing.

Using $\zeta = 0.707$ in (15) yields

$$\omega_n = 942.9 \quad \text{rad/sec} \tag{16}$$

From [1], we have that

$$\omega_n = \sqrt{\frac{AK}{\tau_1}} \quad \text{rad/sec} \tag{17}$$

A typical value of AK, the open-loop gain, is 3.25×10^5, so that τ_1 can be solved to be

$$\tau_1 = \frac{\sqrt{AK}}{\omega_n} \tag{18}$$

or

$$\tau_1 = 0.367 \quad \text{sec} \tag{19}$$

Now, if the VCO swing is ± 100 kHz (from [1], subsection 3.2.1.3.2.9) and the frequency offset is one-half the maximum, or 50 kHz, then $\Delta\omega_0 = 2\pi$ (50 kHz). From (14), we can write

$$\delta f(t) = \Delta f_0 - \Delta f_0 \, e^{-t/\tau_1} \qquad \left(\Delta f_0 = \frac{\Delta W_0}{2\pi}\right) \tag{20}$$

Hence, at time t, we have

$$\delta f(t) = 50 \text{ kHz} \left[1 - e^{-2.72t}\right] \tag{21}$$

For various values of t, $\delta f(t)$ is tabulated in Table 1.

We see from Table 1 that, at 40 ms, the frequency generated with a 50-kHz off-rest frequency is 5,155 Hz, or over 10 loop bandwidths, It is very improbable that a phase-lock-loop will reacquire when it drifts 10 loop bandwidths away from the carrier since the practical limit is something like one loop bandwidth away. However, a few millisecond dropout would probably not cause loss of lock.

Table 1. Mean Frequency Offsets as a Function of Dropout Time

t (ms)	δf (Hz)
1	135.3
2	271.3
3	406.3
4	675.4
10	1,341.7
20	2,647.3
30	3,918
40	5,154.5

It is to be noted that, under large dropout time conditions (40 ms), the carrier phase shift due to switching Centaur antennas is not an additional concern since the frequency drift is about 5000 Hz!

Also note that, if the frequency drift is 5155 Hz in 0.04 seconds, the drift rate is $\dot{f} \approx 129{,}000$ Hz/s. Therefore, the phase change assuming a linear drift rate is

$$\Delta\theta(t) = \int_0^t 129000u \, du = 64500t^2 \text{ cycles}$$

so that, after about 4 ms, the carrier phase has drifted by one cycle. Hence, the phase shift due to the VCO drift during dropout is as important as the antenna-induced phase shifts for dropouts greater than 4 ms. Furthermore, only phase shifts of modulo-one cycle are important.

REFERENCES

1. W. C. Lindsey, Synchronization Systems in Communication and Control, Chapter 4, Prentice-Hall, 1972.

APPENDIX A.2

POTENTIAL CENTAUR CARRIER-LOOP FALSE-LOCK PROBLEM DUE TO ANTENNA SWITCHING

Axiomatix

9841 Airport Boulevard • Suite 912 • Los Angeles, California 90045 • Phone (213) 641-8600

TECHNICAL MEMORANDUM NO. M8110-2 REV. A: November 5, 1981

TO: B. Maronde DATE: October 15, 1981

FROM: J. K. Holmes COPIES: 16067"B" File
R. Iwasaki

SUBJECT: Potential Centaur Carrier-Loop
False-Lock Problem due to Antenna Switching

1.0 SUMMARY

This memorandum addresses the potential carrier-loop false-lock problem that exists in the Centaur receiver when the 1-Kbps command channel from the Shuttle is operating in the idle pattern, which is a 500-Hz square-wave signal.

It was found that, although sidebands from the Shuttle idle pattern exist and are not negligible, the Centaur PLL should drift only about 250 Hz during antenna-induced dropouts, which is well within the loop bandwidth of 500 Hz. Therefore, it is believed that false lock will not occur during 40-ms dropouts and further loss of lock is also quite unlikely during these dropouts. It was assumed that the lock detector did not drop below threshold during this signal dropout.

2.0 ANALYSIS--MODULATION

To determine where potential carrier-loop false-lock points occur, it is necessary to determine the spectral distribution of the modulated signal. The signal can be modeled as

$$y(t) = \sqrt{2A}\,\sin\left(\omega_0 t + o\ sq\left(\omega_1 t\right)\ \sin\ \omega_2 t\right) \qquad (1)$$

where o is the modulation index (nominally 1.0) and $sq(\omega_1 t)$ is a square-wave signal at 500 Hz which models the idle pattern when no data is sent. The $\sin\ \omega_2 t$ term represents the subcarrier which operates at 16 kHz.

Expand (1) to the form

$$y(t) = \sqrt{2A}\sin\omega_0 t\ \cos\left[o\sin\omega_2 t\right] + \sqrt{2A}\cos\omega_0 t\ sq\left(\omega_1 t\right)\sin\left[o\sin\omega_2 t\right] \qquad (2)$$

Note that

$$\cos\left[\theta \sin \omega_2 t\right] = J_0(\theta) + \sum_{\substack{n=2 \\ n \text{ even}}}^{\infty} J_n(\theta) \cos\left(n \omega_2 t\right) \tag{3}$$

$$\sin\left[\theta \sin \omega_2 t\right] = \sum_{\substack{n=1 \\ n \text{ odd}}}^{\infty} 2 J_n(\theta) \sin\left(n \omega_2 t\right) \tag{4}$$

$$sq\left(\omega_1 t\right) = \frac{4}{\pi} \cos \omega_1 t - \frac{4}{3\pi} \cos 3\omega_1 t + \frac{4}{5\pi} \cos 5\omega_1 t + \cdots \tag{5}$$

Using (3), (4) and (5) in (2) yields

$$\begin{aligned} y(t) = \sqrt{2}A \sin \omega_0 t \left\{J_0(\theta) + \sum_{\substack{n=2 \\ n \text{ even}}}^{\infty} J_n(\theta) \cos n\omega_2 t\right\} + \sqrt{2}A \cos \omega_0 t \\ \times \left\{\frac{4}{\pi} J_1(\theta) \sin\left[\left(\omega_1 + \omega_2\right)t\right] - \frac{4}{\pi} J_1(\theta) \sin\left[\left(\omega_1 - \omega_2\right)t\right]\right. \\ - \frac{4}{3\pi} J_1(\theta) \sin\left[\left(\omega_1 + 3\omega_2\right)t\right] + \frac{4}{3\pi} J_1(\theta) \sin\left[\left(\omega_1 - 3\omega_2\right)t\right] \\ \left. + \frac{4}{5\pi} J_1(\theta) \sin\left[\left(\omega_1 + 5\omega_2\right)t\right] + \frac{4}{5\pi} J_1(\theta) \sin\left[\left(\omega_1 - 5\omega_2\right)t\right] + \cdots\right\} \end{aligned} \tag{6}$$

In (6), we have indicated only the significant terms between the carrier frequency and the 16-kHz subcarrier frequency. Figure 1 illustrates the spectral distribution of the Shuttle-to-Centaur link when the data is on the idle pattern (which is a square wave of 500 Hz).

Using a nominal value of θ of 1 radian yields

$$\frac{P_{f_0 - f_1}}{P_c} = -8.7 \text{ dB} \qquad \frac{P_{f_0 - 3f_1}}{P_c} = -18.2 \text{ dB} \; ; \; \frac{P_{f_0 - 5f_1}}{P_c} = -22.7 \text{ dB} \tag{7}$$

Thus, we see that the sideband power diminishes quite rapidly as we approach the carrier from the upper 16-kHz subcarrier, but the main sidebands are down only 8.7 dB from the carrier.

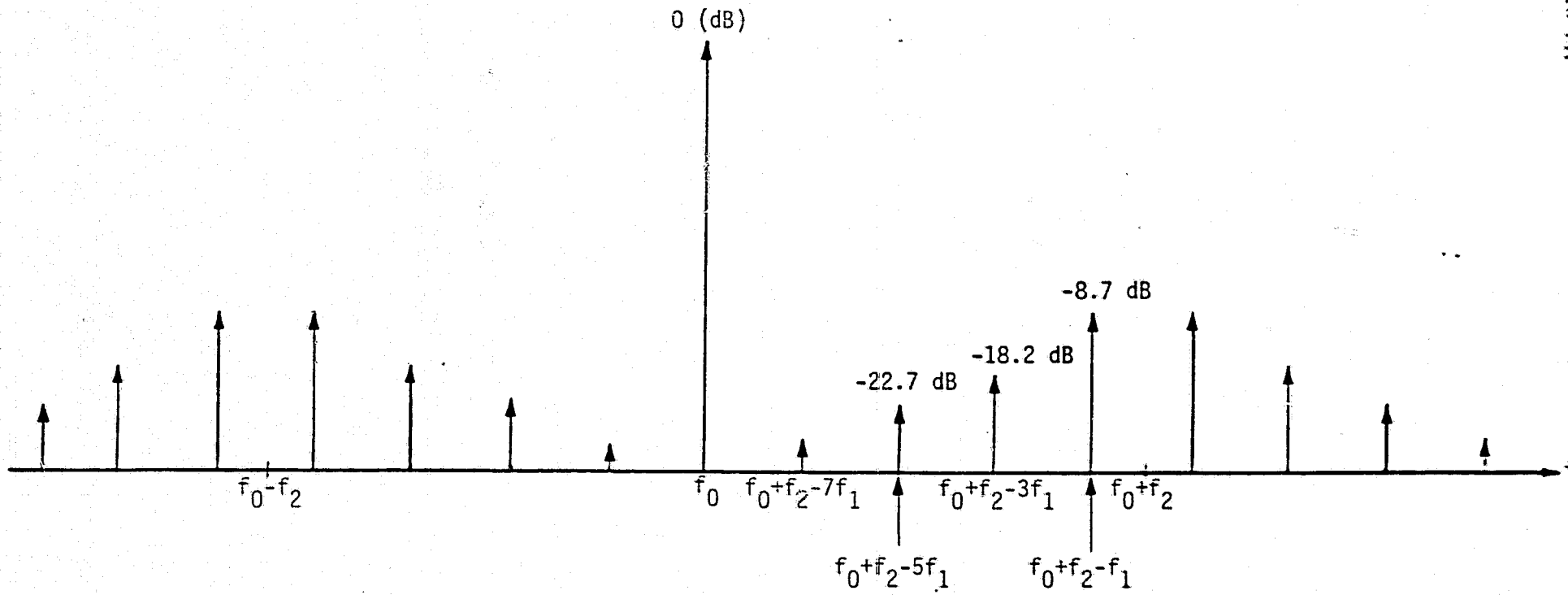

f_2 = 16 kHz

f_1 = 500 Hz

f_0 = Carrier Frequency

Figure 1. Spectral Distribution Near f_0 in the Idle Pattern (relative levels)

3.0 ANALYSIS--VCO DRIFT

We can now determine how far the Centaur loop VCXO can drift during a 40-ms dropout. Using the method discussed in [1] and the actual* closed-loop parameter values of [2], we can determine the VCXO frequency drift during the (maximum time) 40-ms dropout due to antenna switching. Consider the assumed second-order passive loop filter of the form

$$F(s) = G\,\frac{1 + \tau_2 s}{1 + \tau_1 s} \tag{8}$$

which is illustrated in Figure 2. For this loop filter, when the input e_i was nonzero and constant for a long time, then suddenly drops to zero, the output voltage drops quickly to $(R_3)/(R_2+R_3)\ V_0$, where V_0 is the previous (before dropout) voltage, then decays from $(R_3)/(R_2+R_3)\ V_0$ to zero, as shown in Figure 3.

For the Centaur loop, we have the following loop parameters [2]:

B_L	= 500 Hz	K_{DC}	= 69.1
ζ	= 0.707	τ_1	= 16.2 sec
ω_n	= 943 rad/sec	Loop gain	= 1.44×10^7

By calculation,

$$\frac{\tau_2}{\tau_3} << 1 \implies \frac{R_2}{R_2 + R_3} \cong 0 \tag{9}$$

therefore, the frequency decays in the form

$$\delta f(t) = \Delta f\left[1 - e^{-t/\tau_1}\right] \tag{10}$$

Using 100 kHz as the nominal maximum value of Δf along with τ_1 = 16.2 seconds yields, after 40 ms,

---

*As opposed to the estimated time constant values of [1].

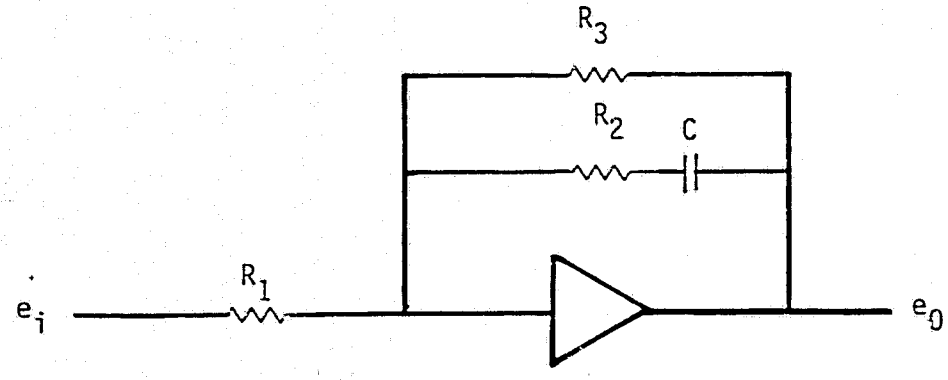

$$F(s) = \frac{R_3}{R_1} \frac{(1+\tau_2 s)}{1+\tau_1 s}$$

$$\tau_2 = R_2 C$$

$$\tau_1 = (R_3+R_2)C$$

Figure 2. Passive Second-Order Loop Filter Model

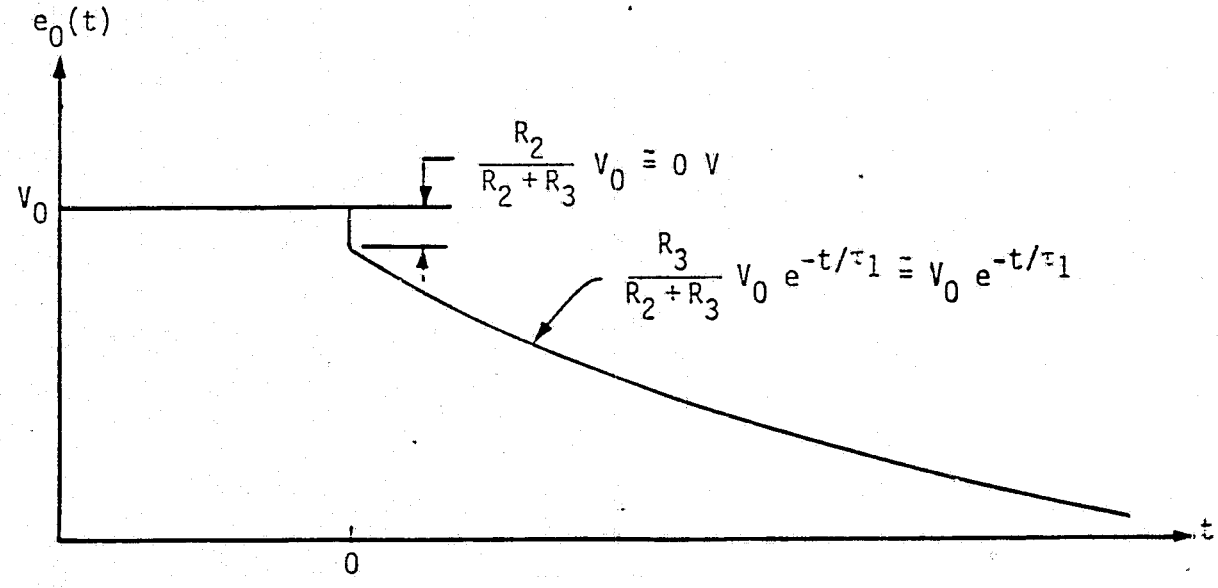

Figure 3. Output Loop Filter Response Due to a Sudden Zeroing of the Input

$$\delta f(0.04) = 100 \times 10^3 \left| 1 - e^{-(0.04)/16.2} \right| = 246.6 \text{ Hz} \qquad (11)$$

Since this value is about one-half the loop bandwidth, it is very likely that the loop will acquire in a few milliseconds after the signal reappears. Also, since the nearest significant spectral line is at 13.5 kHz from the center frequency, false lock is quite unlikely.

4.0 CONCLUSION

Although the false-lock potential exists (see Figure 1), the loop should drift only about 250 Hz in the worst-case 40-ms outage during the antenna switching. Since this frequency offset (247 Hz) is only one-half the loop bandwidth, and far from any potential false-lock points, the loop should reacquire in a few milliseconds.

References

1. J. K. Holmes, "Frequency Drift of Centaur Transponder VCO Frequency Due to Antenna Switching," Axiomatix Technical Memo No. M8109-2, September 25, 1981.

2. J. R. Nelson, "Shuttle/Centaur TDRSS User Transponder Response To Antenna Switching Transients," Motorola Report No. PIA 3123-709, September 22, 1981.

APPENDIX A.3

SHUTTLE/CENTAUR TDRSS USER TRANSPONDER RESPONSE TO ANTENNA-SWITCHING TRANSIENTS

22 September 1981

PIA 3123-700

SHUTTLE/CENTAUR TDRSS USER TRANSPONDER RESPONSE TO ANTENNA SWITCHING TRANSIENTS

Prepared for
GENERAL DYNAMICS/CONVAIR

Prepared by
John R. Nelson

MOTOROLA • Government Electronics Division • 8201 E. McDOWELL ROAD, SCOTTSDALE, ARIZ. 85252

SHUTTLE/CENTAUR
TDRSS USER TRANSPONDER
RESPONSE TO ANTENNA SWITCHING TRANSIENTS

The TDRSS User Transponder will accommodate antenna switching transients of up to 40 milliseconds duration without indicating loss-of-lock and without requiring initiation of the receiver acquisition sequence. A transient is considered to be a momentary loss of forward link signal where the phase of the re-established signal is random (0^{o}-360^{o}) relative to the previously received signal.

The antenna switching transient will cause the receiver tracking phase-locked loop (PLL) to drop lock. When the signal is re-established after 40 msec or less, the PLL will relock within milliseconds (as detailed in the appendix). The RECEIVER LOCK telemetry signal has an out-of-lock sensor time constant of approximately two seconds. The 40 msec transient will therefore not cause an out-of-lock indication and will not re-initiate the receiver acquisition sequence.

The forward link command data will, of course, be lost during the switching transient. Depending on the duration of the transient, the command detector unit (CDU) LOCK INDICATOR may or may not indicate loss of CDU lock for STDN mode operation. In the TDRSS mode the CDU will remain locked to the internally generated 16 kHz command subcarrier and the CDU LOCK INDICATOR will not indicate loss of lock. In either mode, however, the CDU may not be able to maintain internal bit synchronization during the transient drop-out period. It will therefore be necessary to supply the 132 bit minimum alternate one/zero command acquisition sequence following the antenna switching transient.

APPENDIX

ANALYSIS OF RECEIVER TRACKING LOOP RELOCK FOLLOWING ANTENNA SWITCHING TRANSIENTS

The accommodation of antenna switching transients of up to 40 msec duration is based on the fact that the receiver tracking phase-locked loop (PLL) will immediately relock after the switching transient. The PLL will relock if the frequency error is within the pull-in range of the loop, regardless of the phase relationship between the pre-transient and post-transient signals. Since the received signal frequency is the same before and after the transient*, the only potential source for frequency error is receiver VCXO frequency drift during the switching transient. These parameters must be examined separately for the STDN and TDRSS modes.

---

* If the forward link signal is changing frequency (sweeping) at the time of the antenna switching transient, then the post-transient frequency will actually be different from the pre-transient frequency. For TDRSS mode operation, the maximum sweep rate is only 70 Hz/sec and the PLL will still relock practically instantaneously following the transient. In the STDN mode, however, the analysis becomes quite complicated because the PLL must pull in and lock to a signal which is sweeping farther away in frequency. It is estimated that the 40 msec antenna switching transients can be accommodated for STDN sweep rates up to approximately 13 kHz/sec.

STDN MODE

The STDN mode tracking loop parameters are as follows:

Bandwidth (β_L)	= 500 Hz
Damping factor (ζ)	= .707
Natural frequency (ω_n)	= 943 rad/sec
Loop filter DC gain (K_{DC})	= 69.1
Loop filter pole time constant (τ_p)	= 16.2 sec
VCXO gain constant (K_v)	= 66300 Hz/v at 22F1F
Loop gain (A)	= $1.44X10^7$

Worst case frequency drift during the antenna switching transient will take place when the forward link frequency is at a tracking range extreme ($\pm$ 150 kHz). If the VCXO exhibits worst case temperature stability ($\pm$ 14 ppm), the static phase error (SPE) to the VCXO under quiescent conditions would be

(150000 Hz + 29650 Hz)/(66300 Hz/V) = 2.710 Vdc

and the input to the loop filter amplifier would be

2.710 Vdc/69.1 = 39.2 mVdc

If the loop filter input voltage takes a step from V_1 to V_2, the output (V_{SPE}) responds as follows:

$$\Delta V_{SPE}(t) = K_{DC} (V_2-V_1) (1-e^{-t/\tau p})$$

As indicated above, worst case V_1 is 39.2 mVdc. Worst case V_2 would be an input offset voltage of -20 mVdc. Therefore,

$$\Delta V_{SPE} = 69.1 (.020 + .0392)(1-e^{-.040/16.2})$$
$$= 4.09 (1-.9975)$$
$$= .010 \text{ Vdc}$$

STDN MODE—Continued

This ΔV_{SPE} will produce a frequency drift in the loop of (.010 Vdc)(66300 Hz/V) = 663 Hz. The loop will relock practically instantaneously for frequency offsets less than $2\zeta f_n$ = 212 Hz. The loop will pull in to lock for offsets within $\left[\frac{2}{\pi}\zeta f_n A\right]^{\frac{1}{2}}$ = 31180 Hz, and will pull into lock from 663 Hz with pull-in time $\frac{(\Delta f)^2}{4\pi\zeta f_n^3}$ = 14.7 msec. The time for the PLL to relock is therefore much less than the lock detector time constant of two seconds and the receiver will not give an out-of-lock indication.

TDRSS MODE

The TDRSS mode tracking loop parameters at or above the nominal 1000 bps command threshold (-126 dBm) are as follows:

Bandwidth (β_L)	= 42 Hz
Damping factor (ζ)	= .90
Natural frequency (ω_n)	= 77 rad/sec
Loop filter integrator time constant (τ)	= 24.3 sec
VCXO gain constant (K_V)	6300 Hz/V at 221F1
Loop gain (A)	= 1.42×10^5

Worse case frequency drift during the antenna switching transient corresponds to worst case dc offset voltages in the dc-coupled loop filter circuits. For a net dc offset voltage V_1 at the loop filter input, the output (V_{SPE}) responds as follows:

$$\Delta V_{SPE}(t) = \frac{V_1 t}{\tau}$$

The worst case dc offset voltage is expected to be 20 mVdc, so

$$\Delta V_{SPE}(.040) = \frac{(20\text{mVdc})(.040)}{24.3} = .04 \text{ mVdc}$$

This ΔV_{SPE} will produce a frequency drift in the loop of (.04 mV)(66300 Hz/V) = 26 Hz. The loop will relock practically instantaneously for frequency offsets less than $2\zeta f_n$ = 22 Hz. The time for the PLL to relock is therefore much less than the lock detector time constant of two seconds and the receiver will not give an out-of-lock indication.

APPENDIX A.4

MOTOROLA VIEWGRAPHS

SHUTTLE/CENTAUR TDRSS USER TRANSPONDER RESPONSE TO ANTENNA-SWITCHING TRANSIENTS

- ANTENNA-SWITCHING TRANSIENTS (SIGNAL DROPOUTS) OF UP TO 40 MSEC DURATION SHALL BE ACCOMMODATED

- RECEIVER LOCK TELEMETRY SHALL NOT INDICATE LOSS OF LOCK

- INITIATION OF ACQUISITION SEQUENCE SHALL NOT BE REQUIRED

ANALYSIS

- TRACKING LOOP WILL DROP LOCK AND THEN WILL RELOCK WITHIN A FEW MSEC OF END OF TRANSIENT, EVEN UNDER WORST-CASE CONDITIONS (STDN OR TDRSS MODE)

- OUT-OF-LOCK SENSOR TIME CONSTANT IS APPROXIMATELY 2 SEC AND WILL NOT INDICATE OUT-OF-LOCK

- COMMAND DATA WILL BE LOST DURING TRANSIENT AND RELOCK TIME. CDU MAY OR MAY NOT INDICATE OUT-OF-LOCK. COMMAND BIT SYNC MUST BE RE-ESTABLISHED (132 BITS OF 1/0).

DATA (TDRSS MODE)

FORWARD LINK LEVEL	DATA RATE	TRANSIENT DURATION REQUIRED FOR OUT-OF-LOCK INDICATION
-120 dBm	LOW	2.2 SEC
-135 dBm	LOW	0.7 SEC
-138 dBm	LOW	0.2 SEC
-126 dBm	HIGH	1.6 SEC

NOTES:

1. TRACKING THRESHOLD WAS -139 dBm
2. FORWARD LINK SWEEPING ±700 Hz AT 70 Hz/Sec

APPENDIX A.5

ANTENNA-SWITCHING TRANSIENT TESTS ON THE NASA STANDARD TDRSS USER TRANSPONDER

27 OCTOBER 1981

PIA 3123-700

ANTENNA SWITCHING TRANSIENT TESTS ON THE NASA STANDARD TDRSS USER TRANSPONDER

Prepared for

GENERAL DYNAMICS/CONVAIR

Prepared by

John R. Nelson

MOTOROLA • Government Electronics Division • 8201 E. McDOWELL ROAD, SCOTTSDALE, ARIZ. 85252

Antenna Switching Transient Tests on the NASA Standard TDRSS User Transponder

Shuttle/Centaur antenna switching will cause level and phase transients in the received signal supplied to the transponder. These transients are estimated to be less than 5 msec in duration when "make-before-break" antenna switches are employed.

Previous test data and analysis have shown conclusively that these antenna switching transients will cause no loss-of-lock indication or reacquisition sequence for the TDRSS mode of operation. Motorola has now also conducted a series of tests wherein these transient conditions were simulated for the STDN mode of operation and the transponder behavior was characterized. The transponder under test was a flight model NASA Standard TDRSS User Transponder which was configured for a STDN mode command data rate of 2 kbps and a TDRSS mode command data rate of 1 kbps.

The tests described herein were performed under the worst-case conditions for the STDN-ONLY mode of operation. The forward link signal level was -112 dBm and the command data was alternate 1/0 at 2 kbps. Tests were conducted at various forward link frequencies, command modulation indices, and transient durations. At least 25 test trials were conducted for each test condition. The test conditions and test results are summarized in Table 1.

The test data shows that the transponder will accommodate antenna switching transients of more than 50 msec duration (10 times the specified duration) without indicating loss-of-lock and without requiring initiation of the receiver acquisition sequence.

TABLE 1

Antenna Swtiching Transient Test Results

TEST CONDITIONS [1]

Frequency	Command Mod. Index	Transient Duration	Results
f_c [2]	1.0 rad	50 msec	No out-of-lock or false lock.
		100 msec	No out-of-lock or false lock
		200 msec	Drop lock and relock to lower 16 kHz sideband.
f_c	1.3 rad	50 msec	No out-of-lock or false lock.
		100 msec	No out-of-lock or false lock
		200 msec	Drop lock and relock to lower 16 kHz sideband
f_c+150 kHz	1.0 rad	50 msec	No out-of-lock or false lock
		100 msec	Dropped lock and went to center rest frequency without reacquisition once out of 50 trials. No out-of-lock or false lock for 49 out of 50 trials.
		200 msec	Drop lock and relock to lower 16 kHz sideband
f_c+150 kHz	1.3 rad	50 msec	No out-of-lock or false lock
		100 msec	Dropped lock and went to center rest frequency without reacquisition for 12 out of 25 trials.
		200 msec	Drop lock and relock to lower 16 kHz sideband
f_c-150 kHz	1.0 rad	50 msec	No out-of-lock or false lock
		100 msec	No out-of-lock or false lock
		200 msec	Drop lock and relock to lower 16 kHz sideband
f_c-150 kHz	1.3 rad	50 msec	No out-of-lock or false lock
		100 msec	No out-of-lock or false lock
		200 msec	Drop lock and relock to lower 16 kHz sideband 1 out of 10 trials.

NOTES:

1. For all tests, forward link signal is -112 dBm with alternate 1/0 command data at 2 kbps.
2. f_c = design center frequency.

APPENDIX B

CENTAUR ANTENNA APPROACHES

APPENDIX B.1

SHUTTLE/CENTAUR TT&C LINK MARGIN TRADE STUDY

SHUTTLE/CENTAUR TT&C LINK MARGIN TRADE STUDY

GENERAL DYNAMICS
Convair Division

ANTENNAS	SWITCHING ANTENNA	STEERABLE ANTENNA	COMBINATION ANTENNA
TYPE	CIRCUMFERENTIAL ARRAY	HELICAL ANTENNA W/2 AXIS DRIVE	AUTONOMOUS OMNI-DIRECTIONAL ANTENNA
DESCRIPTION	SERIES OF RADIATORS AROUND CIRCUMFERENCE OF VEHICLE SWITCHED TO ESTABLISH AND MAINTAIN LINK.	HIGH GAIN HELIX POINTED BY MEANS OF TWO AXIS DRIVE CONTROLLED BY DCU.	30 MICROSTRIP RADIATORS USED WITH SWITCHING POWER DIVIDERS TO PRODUCE STEERABLE BEAM. MICROPROCESSOR CONTROLLED.
PARTS	SERIES OF CIRCUMFERENTIAL RADIATORS RF SWITCHES AS REQUIRED 1 SWITCHING INTERFACE BOX	2 HELICAL RADIATORS 2 TWO-AXIS MOTOR DRIVES 1 DRIVE INTERFACE BOX	2 TRUNCATED SPHERE RADIATOR ARRAYS 1 MICROPROCESSOR CONTROLLER
DEVELOPMENT STATUS	CONCEPT PROVEN. HARDWARE NOT YET DEVELOPED. SWITCHING ALGORITHM NOT DEVELOPED.	HARDWARE DESIGN PARTIALLY ACCOMPLISHED. INTERFACE BOX DESIGN REQUIRED.	HARDWARE DESIGN PRIMARILY ACCOMPLISHED. SOFTWARE DESIGN REQUIRED.
ADVANTAGES	LOW PROFILE. NO LARGE RF AMPLIFIER REQUIRED. SIMPLE HARDWARE.	+13 dBi GAIN OVER 27° BEAMWIDTH	+7 dBi GAIN OVER 47° BEAMWIDTH. MINIMAL PHASE DISTORTION WITH MOVING BEAM.
DISADVANTAGES	SPECIFIC HARDWARE UNDEVELOPED. DEVELOPMENT, QUALIFICATION AND SWITCHING ALGORITHM REQUIRED.	MECHANICAL STEERING UNIT MORE PRONE TO FAILURE THAN ELECTRONIC STEERING UNIT.	HEAVY (10#/ARRAY) ANTENNA WOULD REQUIRE STRONGER SUPPORT BOOM.
ESTIMATED DELIVERY DATE	LATE '83 TO EARLY '84	EARLY TO MID '83	MID '83 TO EARLY '84

GENERAL DYNAMICS
Convair Division

SHUTTLE/CENTAUR TT&C LINK MARGIN TRADE STUDY

AMPLIFIERS	SOLID-STATE AMPS		TWT AMPS
TYPE	DUAL 20 WATT AMPS	GANGED 20 WATT AMPS	130 WATT TWTA
DESCRIPTION	AN AMP AT THE BASE OF EACH ANTENNA BOOM. THIS MINIMIZES CABLE LOSS.	TWO OR MORE AMPLIFIERS WITH OUTPUTS PARALLELED TO INCREASE EFFECTIVE OUTPUT PWR	DERIVATIVE OF SHUTTLE/ ORBITER POWER AMPLIFIER
PARTS	2 - 20 WATT RF POWER AMPLIFIERS	2 OR MORE 20 WATT POWER AMPLIFIERS	1 - 130 WATT NON-REDUNDANT TWTA.
DEVELOPMENT STATUS	CURRENTLY AVAILABLE FROM SEVERAL VENDORS. FURTHER QUALIFICATION MAY BE REQUIRED.		RECONFIGURING AND REQUALIFICATION REQUIRED.
ADVANTAGES	DRASTICALLY REDUCES CABLE LOSSES.	INCREASE IN POWER LIMITED ONLY TO SPACE AVAILABLE.	MAKES LINK WITH POWER TO SPARE. POTENTIAL ABILITY TO INCREASE DATA RATE.
DISADVANTAGES	LINK STILL MARGINAL. ADDITIONAL GAIN REQUIRED.	INCREASE IN POWER NOT DIRECTLY ADDITIVE. (20 + 20 < 40) WEIGHT AND HEAT GO UP AS A PERFECT SUM.	WILL NEED HIGH POWER ANTENNA AND SWITCHES. LARGE HEAT DISSIPATION PROBLEM.
ESTIMATED DELIVERY DATE	LATE '83, EARLY '84	LATE '83, EARLY '84	LATE '83, EARLY '84

ANTENNA LINK MARGIN TRADE STUDY

PLACEMENT OF RADIATORS AND AMPLIFIERS
FOR DUAL 20-WATT CONFIGURATION.

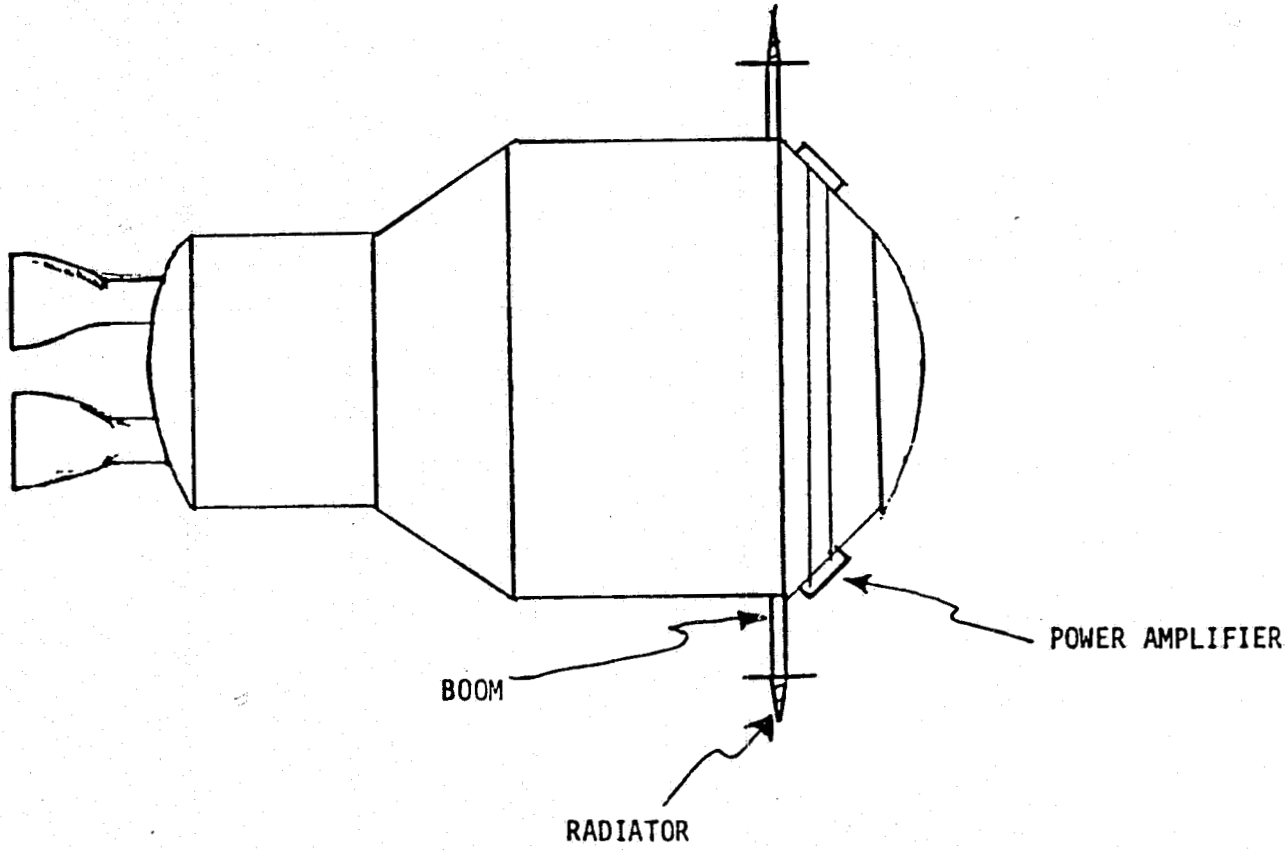

GENERAL DYNAMICS
Convair Division

ANTENNA LINK MARGIN TRADE STUDY

PLACEMENT OF RADIATOR BAND FOR
SWITCHING ANTENNA CONFIGURATION.

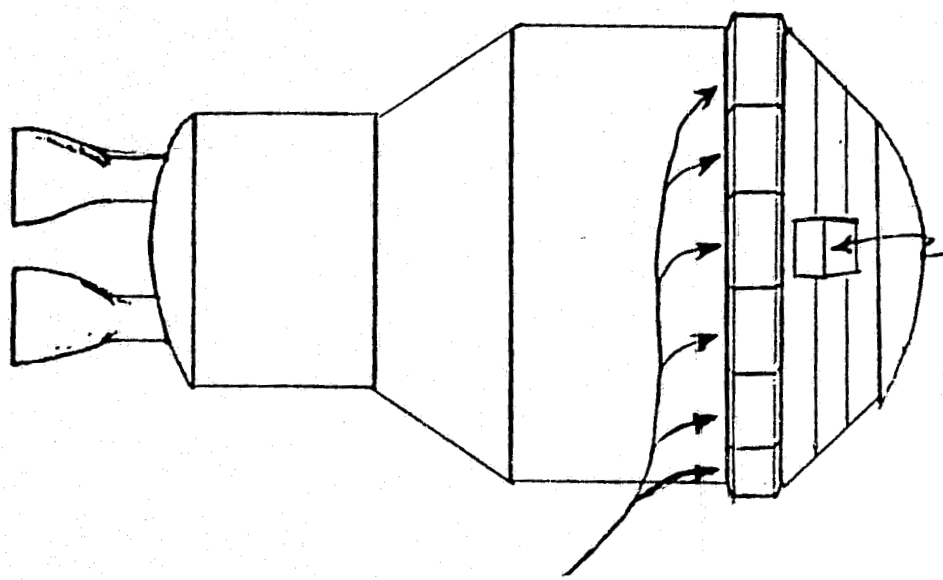

ANTENNA LINK MARGIN TRADE STUDY

PLACEMENT OF RADIATING AND MOTOR DRIVE ELEMENTS FOR STEERABLE ANTENNA CONFIGURATION.

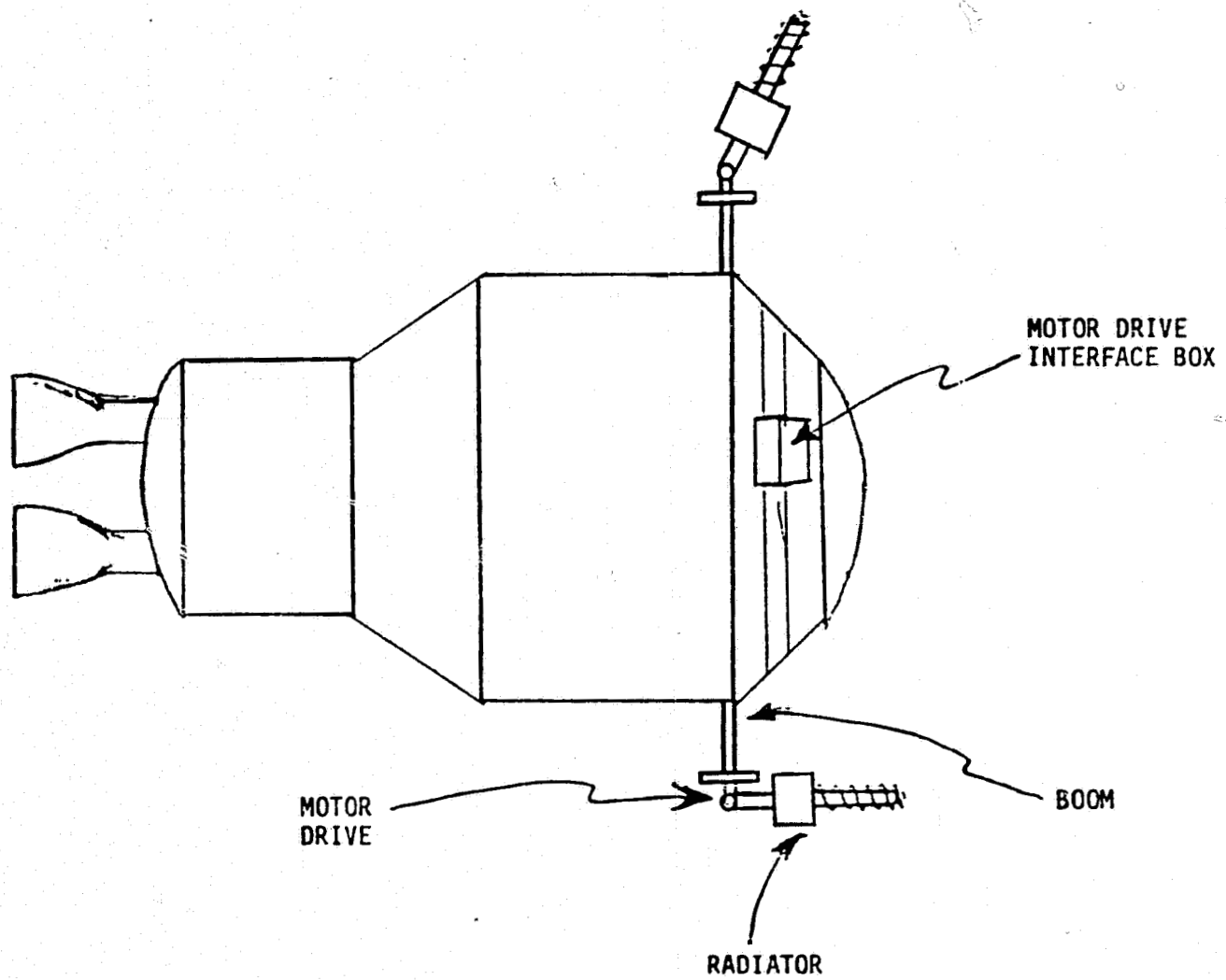

ANTENNA LINK MARGIN TRADE STUDY

PLACEMENT OF RADIATORS FOR COMBINATION ANTENNA CONFIGURATION

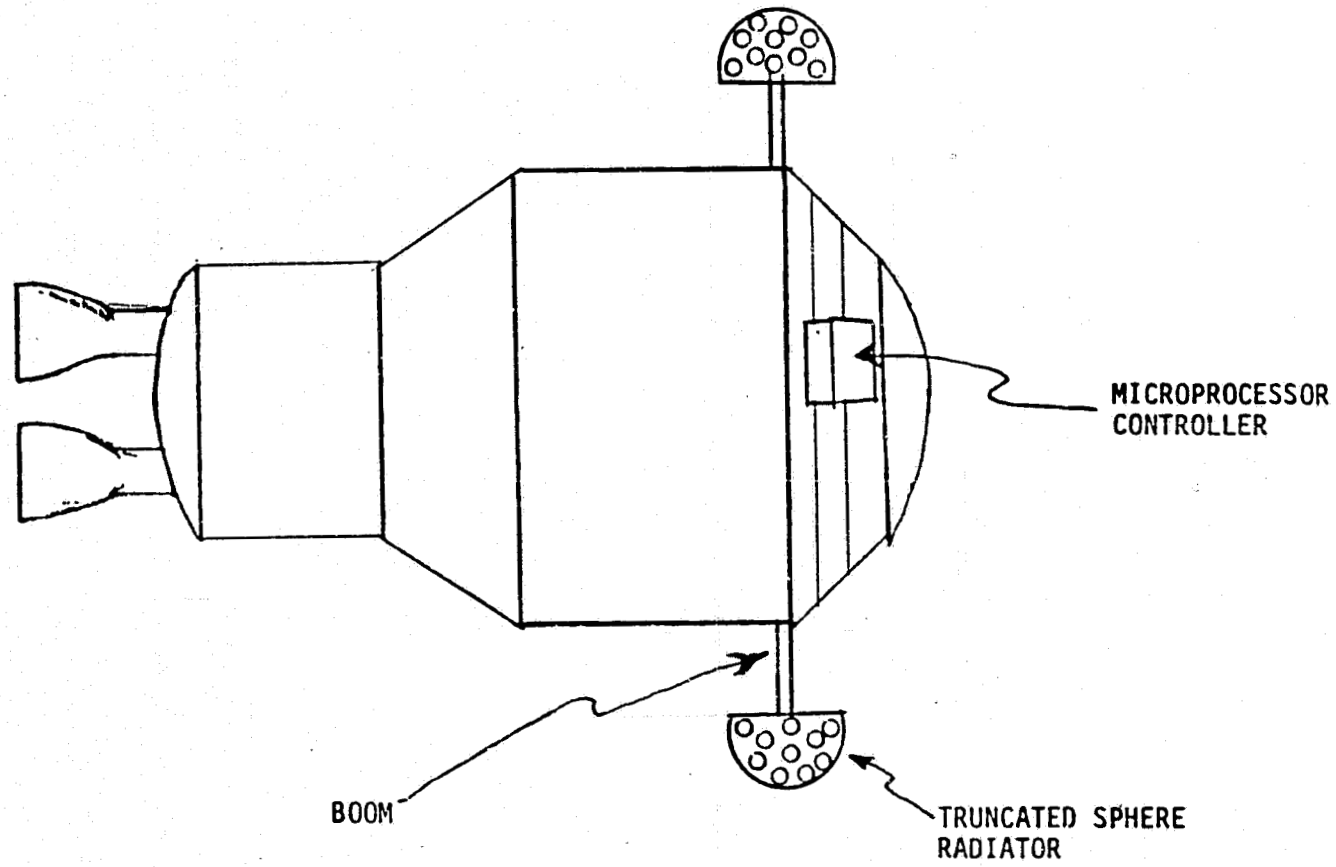

APPENDIX B.2

A CANDIDATE CENTAUR SWITCHED-BEAM HIGH-GAIN ANTENNA SYSTEM

A CANDIDATE CENTAUR SWITCHED-BEAM HIGH-GAIN ANTENNA SYSTEM

NAS 9-16067, EXHIBIT B

Interim Report

Technical Monitor
William Teasdale

Prepared for
NASA Lyndon B. Johnson Space Center
Houston, Texas 77058

Prepared by

Dr. Richard Iwasaki
Axiomatix
9841 Airport Blvd., Suite 912
Los Angeles, California 90045

Axiomatix Report No. R8109-1
September 10, 1981

1.0 INTRODUCTION

The selection of a suitable antenna configuration for a spacecraft is always a critical factor in achieving the communications systems requirements. Many conflicting design parameters must be considered to select a reasonable assortment of suitable antenna configuration candidates and then judiciously arrive at a final recommended choice.

The purpose of this study will be to first examine the existing IUS antenna system and the proposed Centaur antenna system and then gradually develop an alternate scheme which should be considered for possible implementation if the basis for the development appears warranted by the arguments introduced. Since some of the communication link margin budgets have not been firmly established, some flexibility in design exists and various alternatives are discussed.

In order to increase the acceptance of these proposed concepts, the study will concentrate heavily on existing spacecraft antenna systems which have been space-qualified by actual operation and then introduce a means for improving the antenna system performance by adapting a switched-beam concept which is currently being implemented on the Shuttle Orbiter S-band quad antenna system. Therefore, using the existing technology with little modification, a high-gain spherical-coverage switched-beam antenna system is developed for the particular system constraints of the Centaur vehicle.

2.0 GENERAL DYNAMICS CENTAUR ANTENNA CONFIGURATION

During the system formulation phase for the Centaur vehicle development, Axiomatix was asked to evaluate the antenna configuration tentatively proposed by General Dynamics. The design proposed is very basic, being two log conical spiral antennas extending outwardly on opposite sides of the Centaur vehicle on pods, as shown in Figure 1. Having hemispherical coverage, the two log conical spiral antennas would provide spherical coverage by appropriately switching while the Centaur vehicle was rotated for thermal equalization reasons.

There are two problem areas that must be directly addressed with the General Dynamics antenna approach because of the communications system constraints. First, it has been established by analysis that reacquiring a communications link is estimated to require a maximum time of 17 seconds

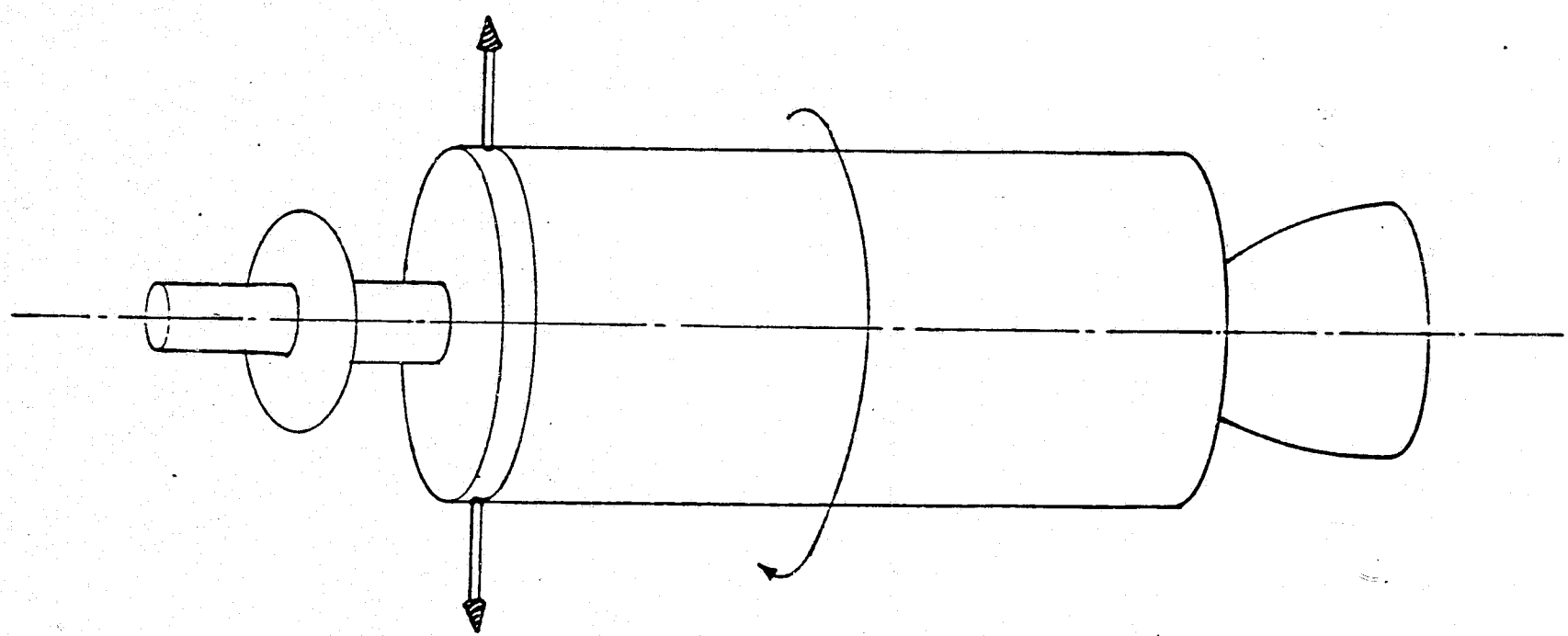

Figure 1a. Proposed General Dynamics Centaur Antenna System

DETACHED MODE S-BAND RF LINKS

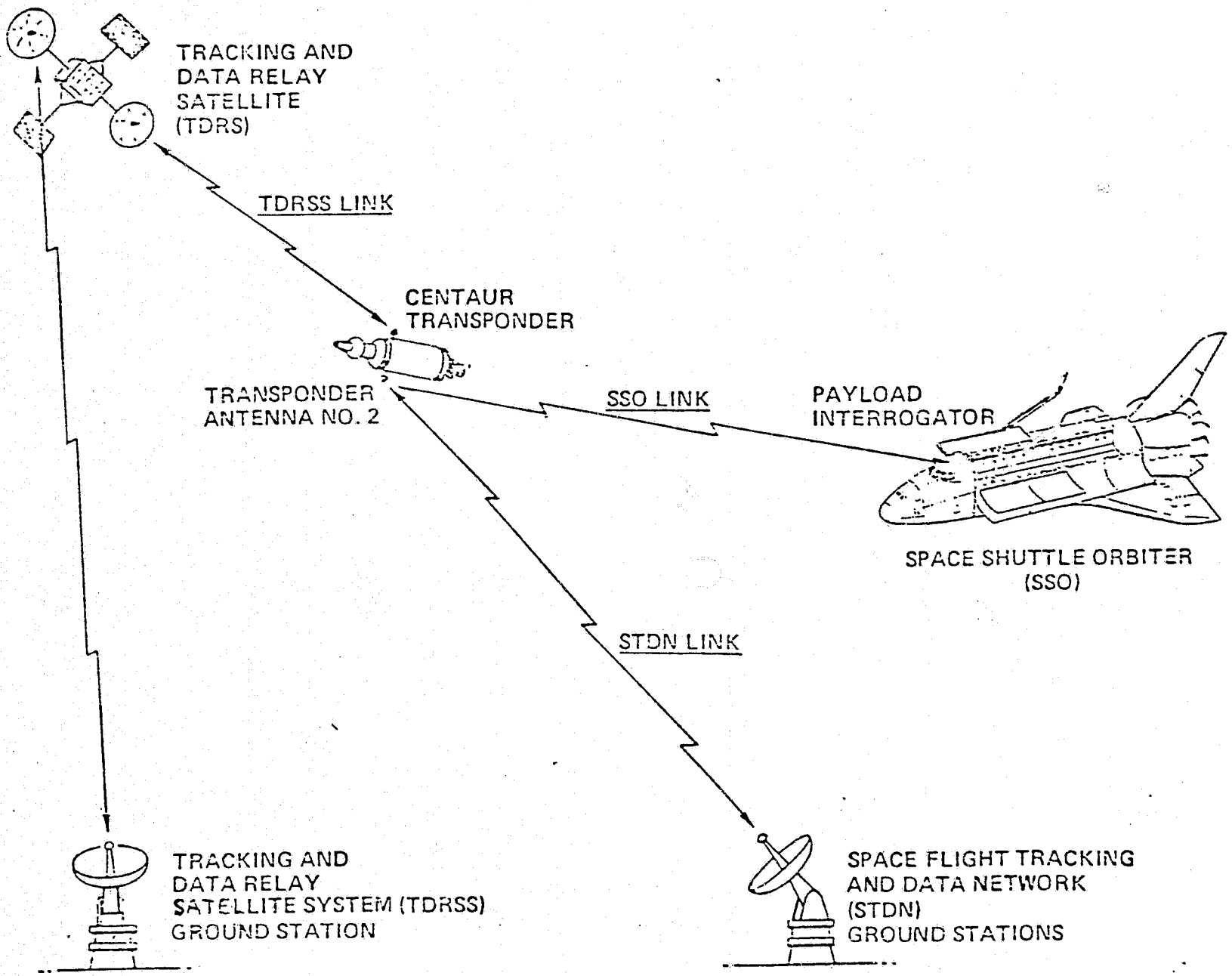

Figure 1b. Centaur Vehicle Communication Links

automatically and 30 seconds manually if a link is disrupted and the phase-locked loop synchronization is lost. In the case of the Shuttle Orbiter/Centaur link, an astronaut must be dedicated to maintaining this link since the manual reacquisition process of the NASA/Motorola transponder requires the switching off and on of the data and carrier channels. Since the Centaur vehicle rotates at one revolution per minute, if lock is indeed lost by either phase or amplitude transients, then the astronaut will be continuously trying to reacquire, and much essential data will be lost in the process during the constant interruptions.

The other problem that must be considered is the gain and orientation of the antenna patterns with respect to the Centaur vehicle itself. The proposed log conical spiral antennas could be reasonably expected to have a peak gain of 5 dB with broad coverage, with lower values of 0 dB or less at the extremes of the hemisphere. The antenna coverage along the longitudinal axis of the Centaur vehicle is therefore greatly restricted. In addition, since the two hemispherical coverages are on the opposite sides of the vehicle in the roll-plane, switching between antennas is necessary for continuous coverage, with the attendant phase transient difficulties. The preliminary link budgets indicate a negative margin of -4 to -5 dB in the critical Centaur/TDRS link, and, although these margins can theoretically be reduced by further refinements in the approximations used in determining the losses attributed to link performance, it might be prudent to consider long range goals of having sufficient gain to provide positive link margins, especially during the initial system design rather than as an expensive retrofit which cannot be later considered because of the cost and schedule impacts.

3.0 BOEING INERTIAL UPPER STAGE (IUS) ANTENNA CONFIGURATION

The Boeing ISU system has been retained for military operations and still might be considered for NASA applications. Basically, the IUS antenna configuration utilizes clusters of five log conical spirals, as sketched in Figure 2, mounted on pods to extend the clusters outwardly from the vehicle. Four clusters are used, as shown in Figure 3, to obtain full spherical coverage about the vehicle, as indicated in Figure 4. The main purpose in having so many log conical spiral antennas is that each optimizes the gain obtainable for a specific coverage region so that, by multiplicity, optimum high-gain percentage coverage is achieved at the expense of complexity.

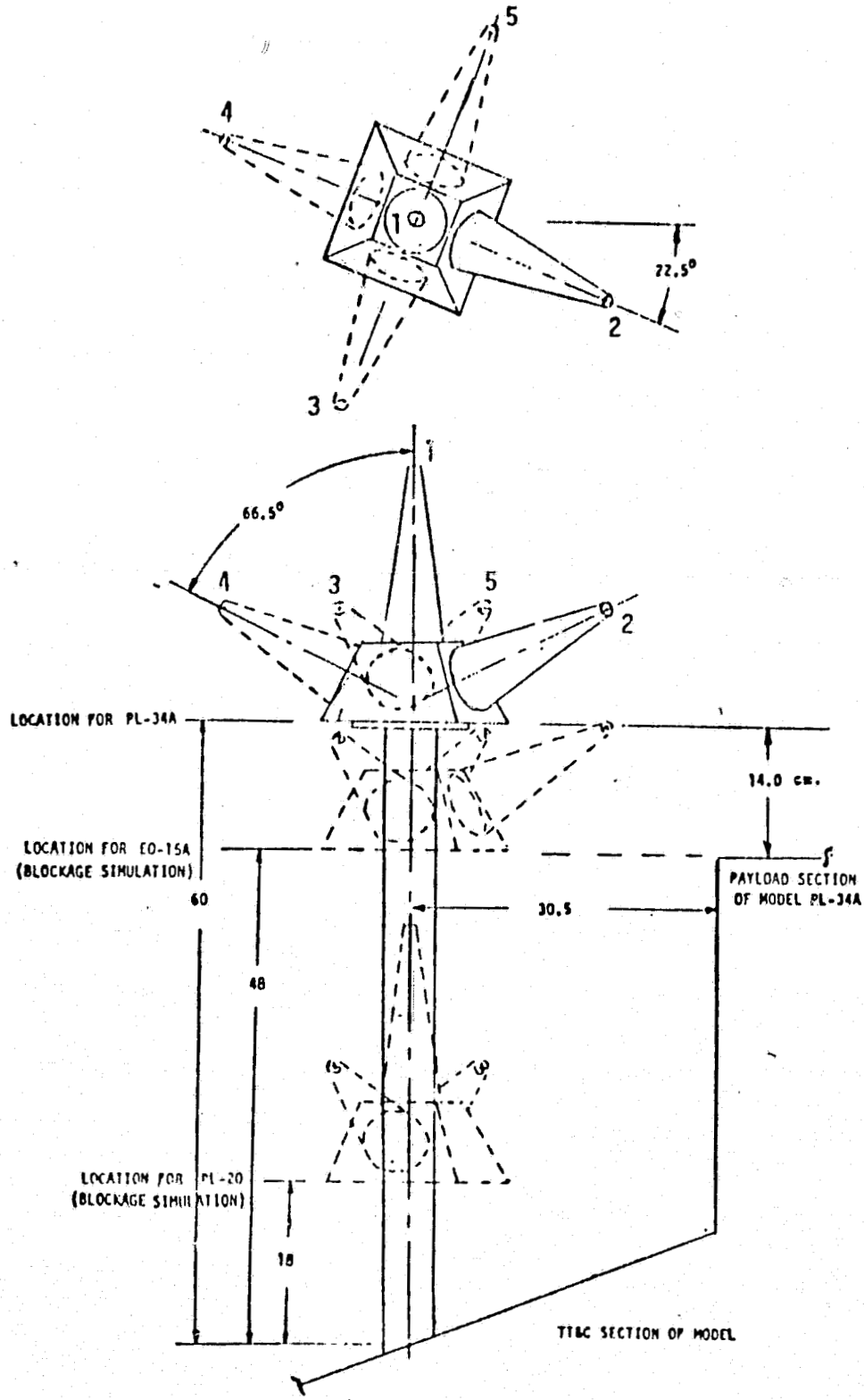

Figure 2. Antenna Assembly Positions

Figure 3. Five-Element Antenna Assembly Positions

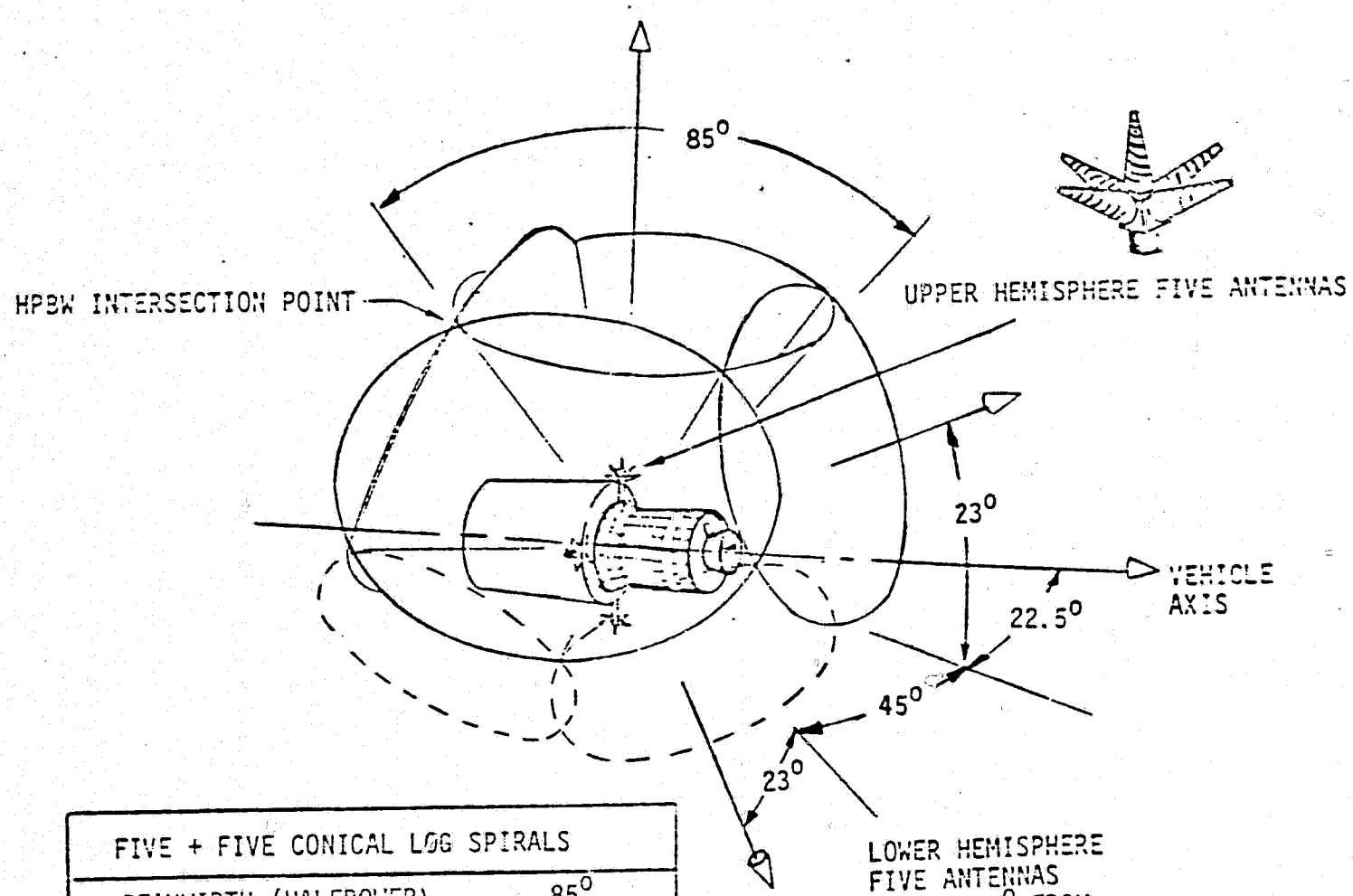

FIVE + FIVE CONICAL LOG SPIRALS	
BEAMWIDTH (HALFPOWER)	85°
GAIN	6.8 dB
REDUNDANT COVERAGE	31.4%

Figure 4. NASA IUS TT&C Antenna Assembly Meets TDRSS Requirements

Although the IUS antenna system satisfies the gain requirements of the Centaur/IUS vehicles, there is a definite phase transient problem which arises from two sources from the IUS configuration since it also rotates about its longitudinal axis and, therefore, requires switching between antennas and clusters to maintain proper antenna pointing. As Boeing noted in its phase transient analysis, the switching of patterns from one antenna to another can result in a phase discontinuity of up to 90°. This phase shift is caused by the abrupt change in effective phase centers which cannot be physically collocated in the cluster of five log conical spiral antennas. This physical phase center displacement can be geometrically described, as shown in Figure 5, and is a potential source of the loss of lock of synchronization of the link.

An even more drastic phase shift can arise from the switching between antenna clusters as the vehicle rotates. It is obvious that the phase centers of the two antennas on the extending pods, as in the presently proposed Centaur configuration, will be physically separated by many meters since they are located on opposite sides of the Centaur vehicle, as was depicted earlier in Figure 1. As the vehicle rotates, these phase centers also rotate. The major concern is then the phase relationship between these two phase centers during switching. Ideally, they would be identical so that phase continuity exists. The best position for antenna switching might be when the two antennas are equidistant from the target antenna. Other positions are located at specific orientations of the vehicle during rotation wherever the differential distances to the target antenna are an integral number of wavelengths apart. In summary, it is possible to switch between antennas without causing phase transients that would create loss of lock of the communications link, but the switching must be precisely temporally controlled by a computer. Identical conditions apply to the Boeing IUS configuration, which is even more complicated because it has four asymmetrically located antennas.

Rather than pursuing this approach, which is susceptible to error, Axiomatix proposes another approach which will not rely on antenna switching, yet will provide high gain to increase the link margin.

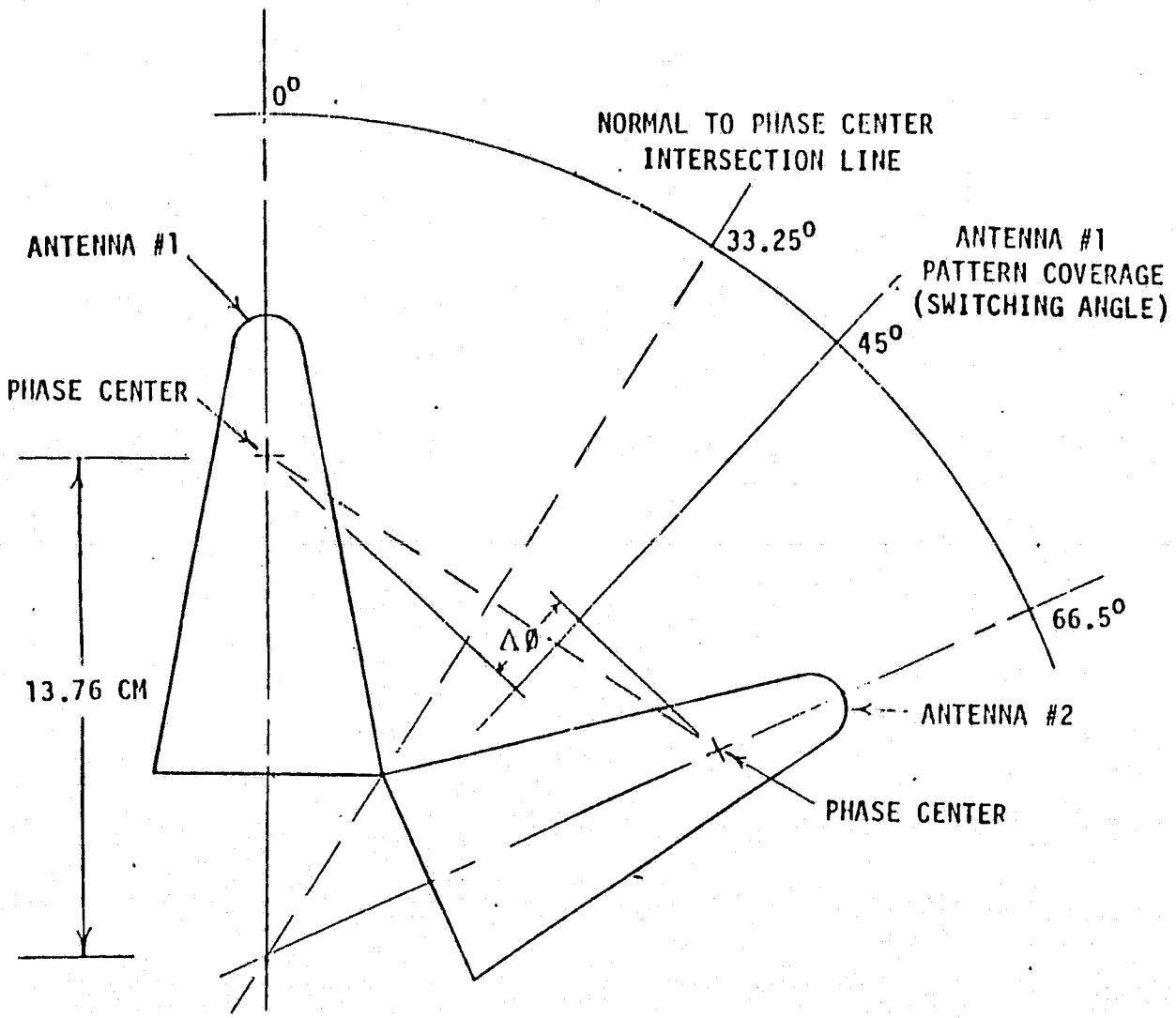

Figure 5. Phase Shift due to NASA Antenna Switching

4.0 AXIOMATIX CENTAUR ANTENNA CONFIGURATION PROPOSAL

Axiomatix proposes a switched-beam system which is compatible with the operational requirements of the Centaur vehicle. The primary concern is the presence of phase discontinuity when antennas are switched, thereby causing a loss of lock of synchronization in the communications link. As discussed earlier, the Centaur vehicle rotates at a rate between 1 and 3 RPM to more uniformly distribute solar irradiance. This requires that antennas be switched to avoid vehicle blockage if the antennas are radially extended, as in the case of both present IUS and Centaur configurations.

The Axiomatix approach attempts to avoid this switching requirement by utilizing a toroidal antenna pattern in the roll plane. Using this configuration allows continuous coverage in the roll plane to a target without the need for switching, thereby eliminating phase transients. The circular symmetry of the Centaur vehicle rotation is ideally suited to this toroidal pattern, which can also be tilted to accommodate targets which are not exactly perpendicular to the longitudinal roll axis. This tilting will be accomplished by a switched-beam technique similar to that being employed by the Shuttle Orbiter switched-beam quad antenna system, as will be discussed in more detail later.

Fore and aft coverage will be provided by log conical spiral antennas which have been used extensively in the other proposed configurations. Figure 6 shows such a log conical spiral antenna configured with a biconical antenna, which will provide the toroidal pattern discussed earlier. This dual-antenna configuration has been used previously on other space programs, e.g., the Global-Positioning Satellite (GPS) shown in Figure 7.

The main problem with the biconical antenna toroidal coverage is that very little gain is achievable in the roll plane, being of the order of 0 - 1 dBci. Although this can be used for broad coverage in the roll plane, it is not suitable for high-gain requirements which may arise from a realistic assessment of the communication link budgets presently being evaluated, especially concerning the Centaur/TDRS link. The Axiomatix adaptation to this concept is to develop a collinear array of three biconical antennas, as sketched in Figure 8. These three biconical antennas now constitute a three-element array similar to the switched-beam antennas

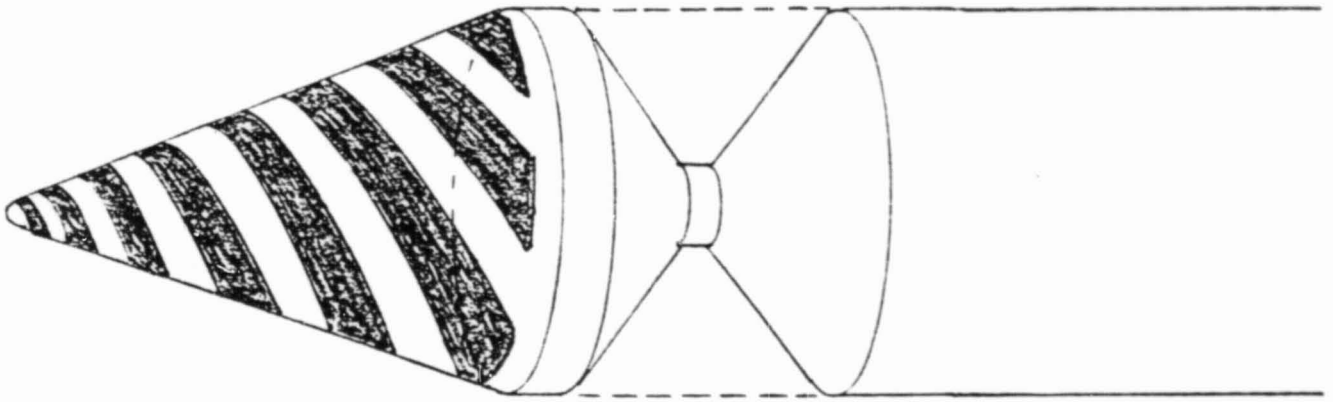

Figure 6. Log Conical Spiral/Biconical Antenna Combination

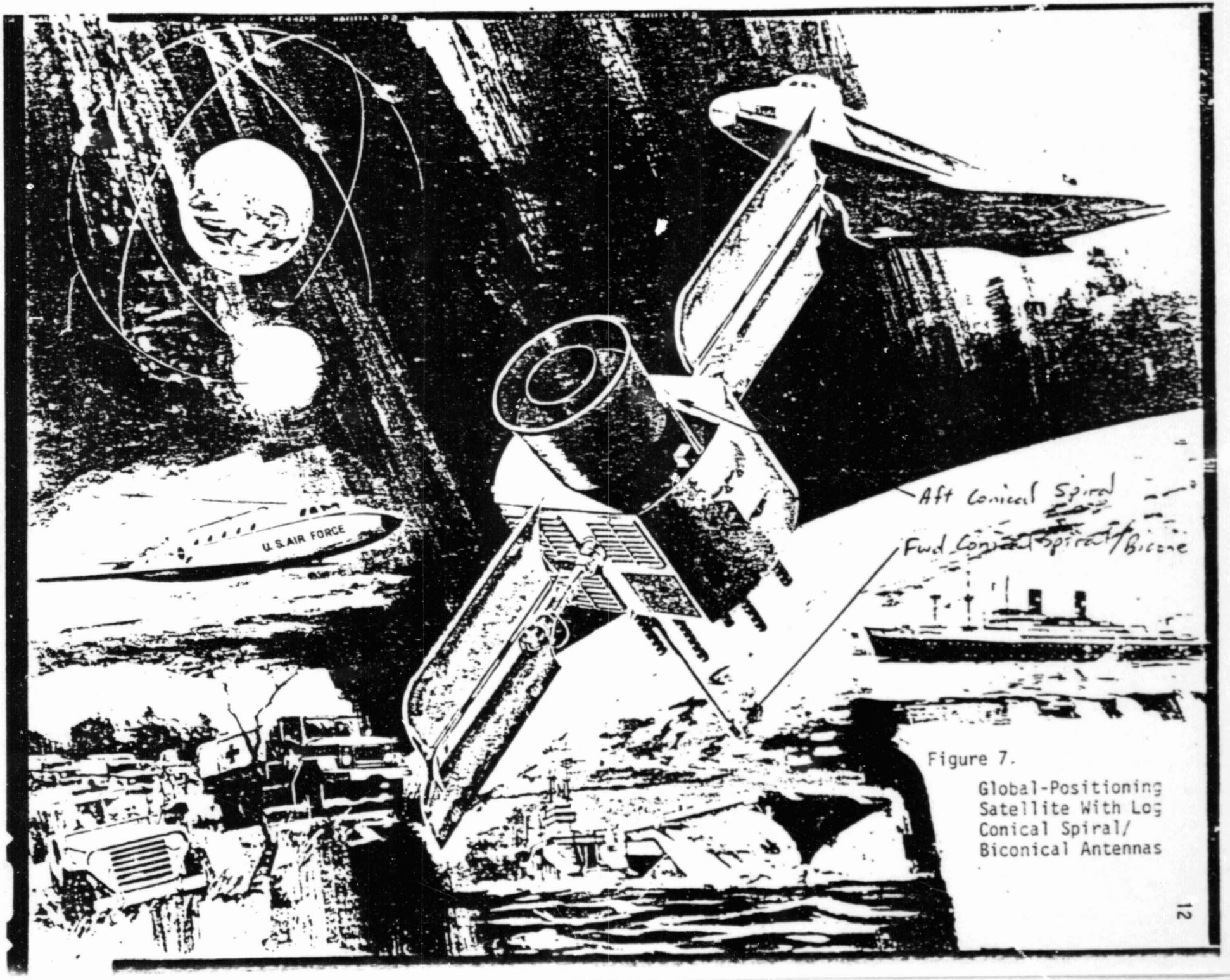

Figure 7.

Global-Positioning Satellite With Log Conical Spiral/ Biconical Antennas

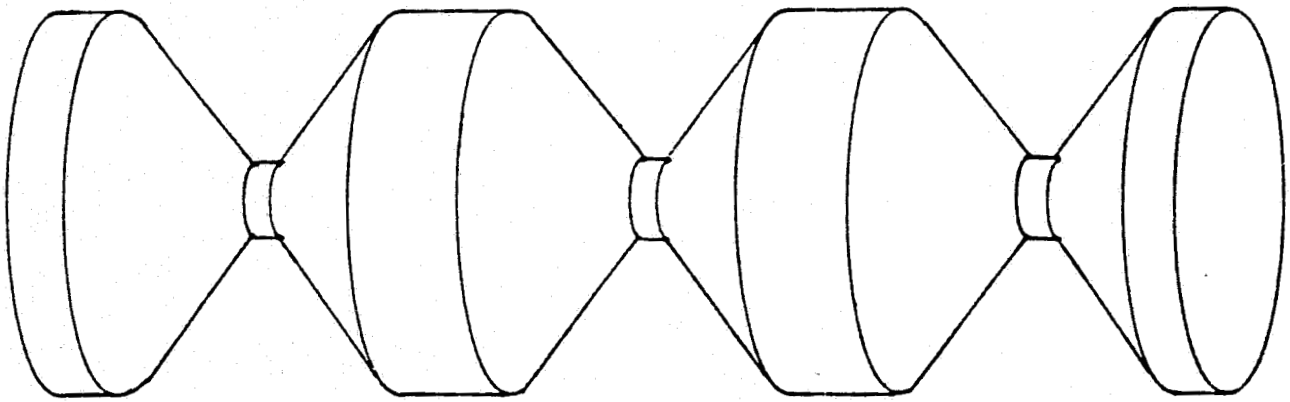

Figure 8. Collinear Array of Three Biconical Antennas

of the Shuttle Orbiter switched-beam quad antenna system. The center element is directly fed with a voltage amplitude ratio of 1.0, and the two outer biconical antennas have a relative voltage amplitude ratio of 0.6. Beam-orientation switching is attained by mechanically switching discrete phase shifts. The three-element array achieves higher gain, "guesstimated" in the range of 4 - 5 dBci, in the roll plane.

The log conical spiral antenna/biconical antenna array combination now looks like the configuration shown in Figure 9. Note that the two antenna systems are independently operated in that, with one setting the log conical spiral antenna is employed and, with the other, the high-gain biconical antenna array is operational.

The other major obstacle to the antenna design is vehicle obscuration effects on the pattern. This difficulty has been surmounted in the past by extending long pods (or booms) past the vehicle and its payload. In this particular case, the antenna configuration might take the appearance shown in Figure 10, where pods fore and aft position the antennas clear of the obstructing vehicle. Note that the roll plane clearance is essential for proper operation of this biconical antenna and array concept since this is the only means to avoid antenna switching. If only one roll plane antenna is necessary (i.e., low-gain biconical or high-gain biconical array), then only one long pod is required since the fore and aft log conical spirals do not need the extension. As for the antennas located adjacent to the nozzle of the Centaur vehicle, high-temperature quartz radomes have been successfully implemented in previous programs to avoid the thermal problems associated with the rocket plume.

And finally, the main justification for considering the biconical antenna array is the multiple high-gain switched-beam patterns available in the roll plane, as shown in Figures 11 and 12. For simplicity, consider the two-switched-beam case, forward (Figure 11) and aft (Figure 12). The switching concept is identical to that used in the Shuttle Orbiter S-band quad antenna except that higher gain and less effective loss is attained by using a directly fed center element in a three-element array rather than the quad two-element array. Further, the number of possible switched beams is related to the number of switches n used in series in the feed line, with the appropriate phase shifts. The number of possible switched beams is determined by 2^n so that, if one switch is used, two switched beams are possible, and four beams arise from two switches. The

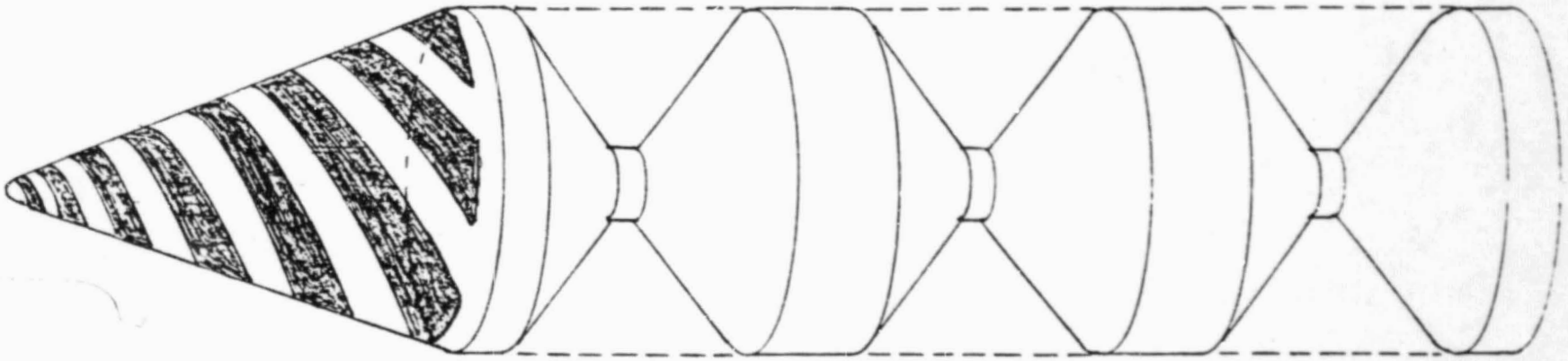

Figure 9. Log Conical Spiral/Biconical Array Combination

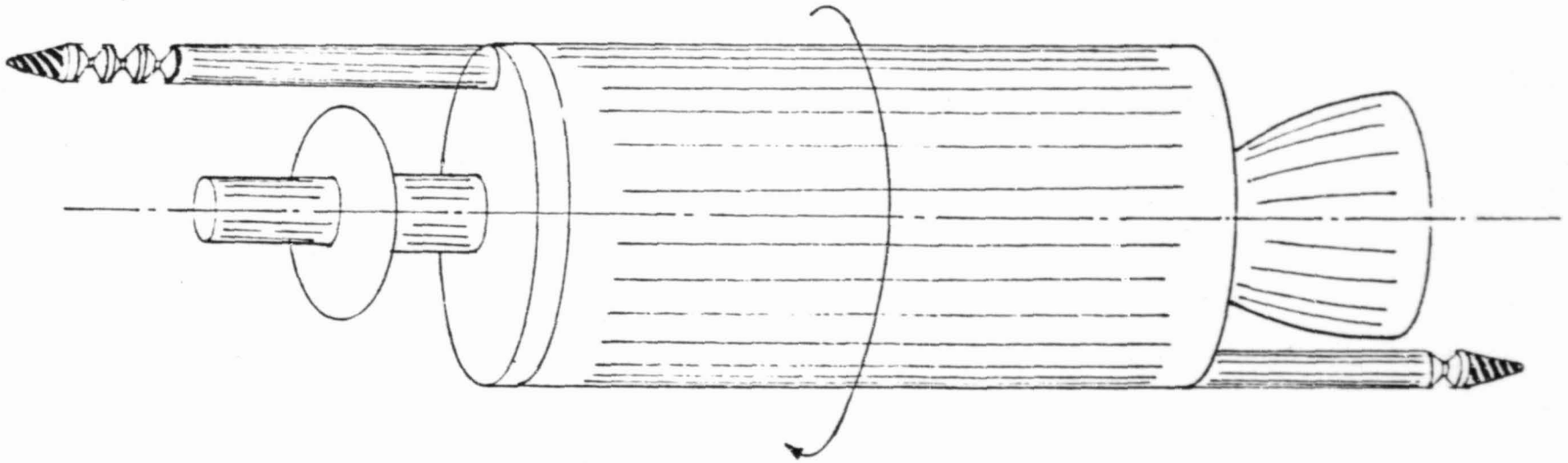

Figure 10. Proposed Axiomatix Log Conical Spiral/Biconical Array Antenna Configuration

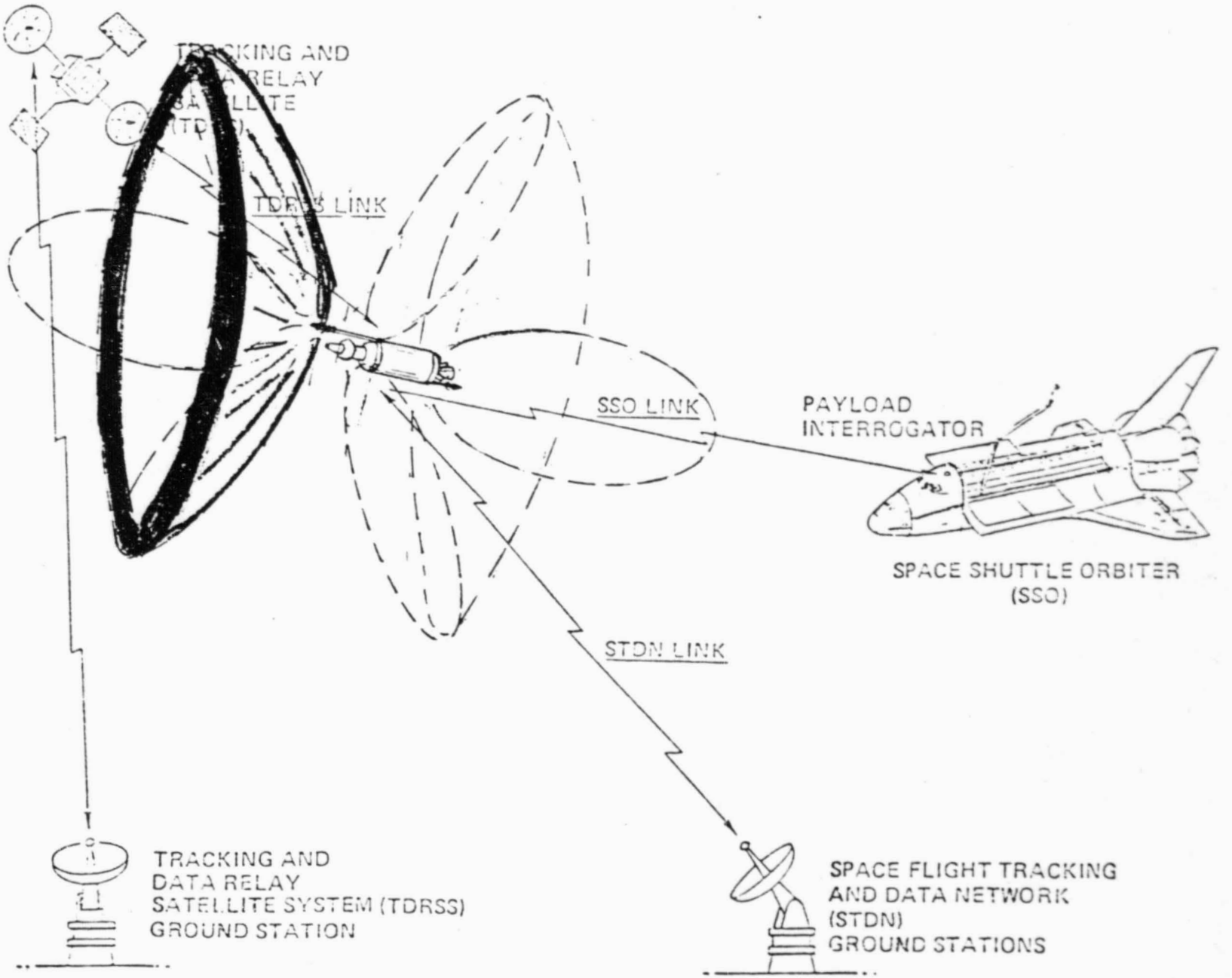

Figure 11. Forward-Looking Switched High-Gain Biconical Array Antenna Pattern

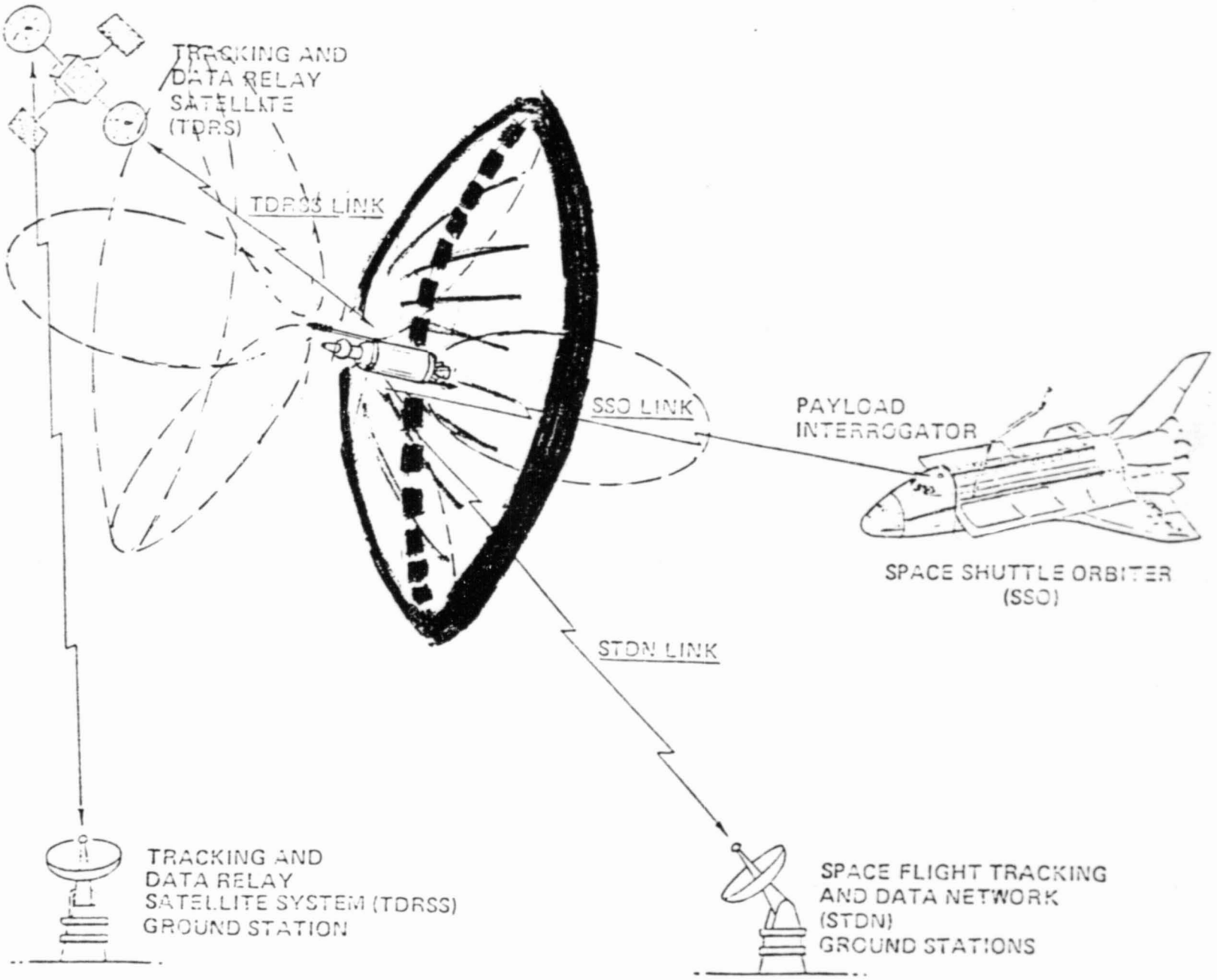

Figure 12. Aft-Looking Switched High-Gain Biconical Array Antenna Pattern

use of three switches enables the antenna system to have eight beam positions, which greatly enhances the antenna capabilities because the high gain of the three-element array can be selectively positioned for optimal performance. These mechanical latching switches require no electrical holding power and add, with the discrete phase-shift circuit, only 0.2 dB per switch. The center element, which is directly fed, carries the majority of the radiated power so that the effective antenna loss is less than that of the additive switch losses.

The final proposed Centaur antenna configuration then consists of either a forward-looking or aft-looking log conical spiral or, in the roll plane, any of the multiple biconical antenna array switched beams. It is anticipated that full +4 dBci gain coverage is achievable about the Centaur vehicle with no antenna switching phase or power transients since, once the proper mode of operation is selected, no further switching is required.

APPENDIX B.3

CONFIGURATION MODIFICATION
OF THE
PRELIMINARY BICONICAL/CONICAL LOG SPIRAL ANTENNAS
AND PHASE SYNCHRONIZATION TECHNIQUE
FOR THE CENTAUR VEHICLE

CONFIGURATION MODIFICATION OF THE PRELIMINARY BICONICAL/CONICAL LOG SPIRAL ANTENNAS AND PHASE SYNCHRONICATION TECHNIQUE FOR THE CENTAUR VEHICLE

Interim Report

Contract No. NAS9-16067, Exhibit B

Technical Monitor: William Teasdale

Prepared for

NASA Lyndon B. Johnson Space Center
Houston, Texas 77058

Prepared by

Dr. Richard Iwasaki

Axiomatix
9841 Airport Blvd., Suite 912
Los Angeles, California 90045

Axiomatix Report No. R8111-6
November 20, 1981

1.0 INTRODUCTION

The two primary objections to the initial antenna design concept involved the extended protrusion of the forward antenna past the payload and the protrusion of the aft-looking conical log spiral antenna adjacent to the Centaur rocket nozzle which would be affected by the thermal and RF blockage effects of the plume during transfer. The objections were well taken if, indeed, the envelope restrictions do not allow antennas extended in such a manner although, ideally, a biconical array is most suitable along the longitudinal axis in front of the payload, where it would have an unobstructed view of a large portion of space. But, if the payload envelope does not allow this configuration, modifications are obviously required.

The biconical-array configuration has been modified to change its proposed location to deploy radially outward from the Centaur vehicle similar to the other boom-mounted antenna configurations proposed by General Dynamics (GD). Two biconical arrays are now required because of pattern blockage by the body of the vehicle itself, and the switching requirements have been reduced to switching between the two sides of the vehicle only.

To avoid the loss of data during this unavoidable switching between arrays, a simple detection scheme has been developed to switch during a period of phase synchronization using the constructive interference pattern of the overlap region between the two arrays. Even though the onboard computer knows the geometric relationship of the communicator with respect to the Centaur, the technique electronically determines the optimum switching time to maintain phase coherence by actually sampling the received signals using the dual-antenna scheme.

2.0 PRESENT GENERAL DYNAMICS CENTAUR ANTENNA CONSIDERATIONS

Two design criteria were changed substantially. One was the roll about the longitudinal axis for thermal equalization reasons which was reduced to 0.1 RPM versus the earlier 1-RPM roll rate. The maximum roll rate prior to payload separation was also reduced from the earlier 2.9 RPM to 0.67 RPM. Therefore, the loss-of-lock conditions on which the earlier design was based was minimized significantly. Similarly, it was

noted that the Motorola transponder does not initiate frequency sweep immediately upon loss of synchronization; rather, it simply "holds" momentarily until the signal is reacquired if there is an abrupt loss of received power. Synchronization is then automatically reacquired; however, data loss occurs during this procedure until the phase-locked-loop is again synchronized. Thus, this condition is to avoided if possible. Under this new operating environment, the candidate antenna configuration will then be modified to attempt to alleviate objectionable features of the initial preliminary baseline design and, hopefully, thus exploit the advantageous features of the earlier configuration which will then add the alternatives being proposed by GD to the antenna system.

It should be reemphasized that the stated purpose of this study is to explore other possible approaches to the antenna problem besides the IUS approach and those being proposed by GD. This report is then an attempt to develop some new ideas for the Centaur antennas in addition to evaluating the existing candidate configurations by outlining inherent advantages and disadvantages independently from the GD system engineers. By using this process, which is, by definition, an iterative procedure that is continuously refined, some insight into an optimal antenna configuration for this application will arise. This antenna configuration evaluation is especially critical for the Centaur vehicle since it is not obvious that any of the existing proposed systems is suitable for the operational requirements of the mission; therefore, the problem should be approached openly in a constructive manner so that no possible satisfactory solution is overlooked.

Before continuing a more detailed description of the biconical array, it would be worthwhile to quickly reexamine the other alternative antenna candidates proposed by General Dynamics and describe specific features for comparison purposes. First, the two conical log spirals extending out radially on booms, as illustrated in Figure 1, does not provide adequate gain in all directions, especially along the longitudinal axis of the Centaur vehicle. This low-gain fore-and-aft coverage deficiency also exists for the circumferential array, shown in Figure 2, which consists of flush-mounted radiators around the Centaur vehicle, with the appropriate hemispherical coverage array facing the target switched into operation as the vehicle rotates. Another candidate antenna system

ANTENNA LINK MARGIN TRADE STUDY

PLACEMENT OF RADIATORS AND AMPLIFIERS FOR DUAL 20-WATT CONFIGURATION

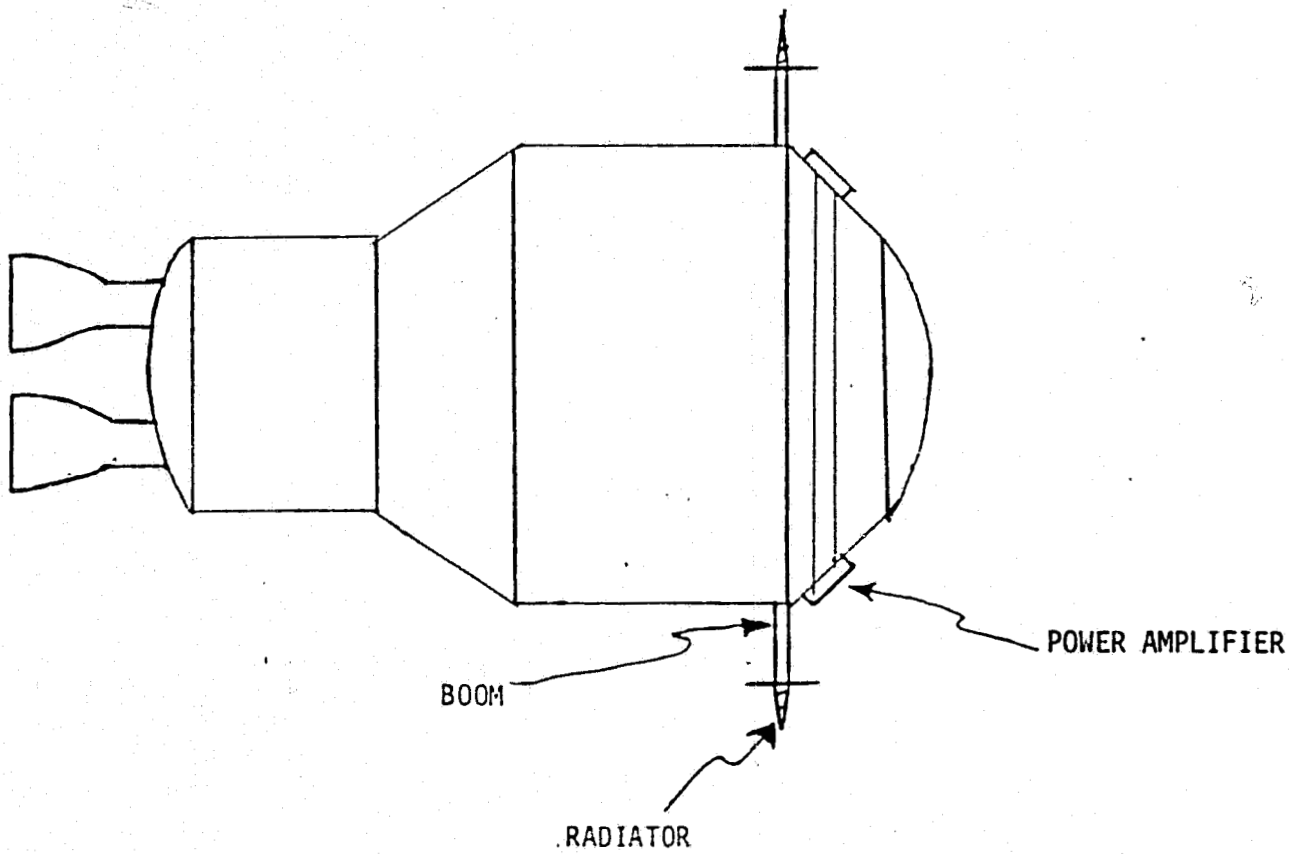

Figure 1. General Dynamics Log Conical Spiral Antenna Configuration

ANTENNA LINK MARGIN TRADE STUDY

PLACEMENT OF RADIATOR BAND FOR ANTENNA-SWITCHING CONFIGURATION

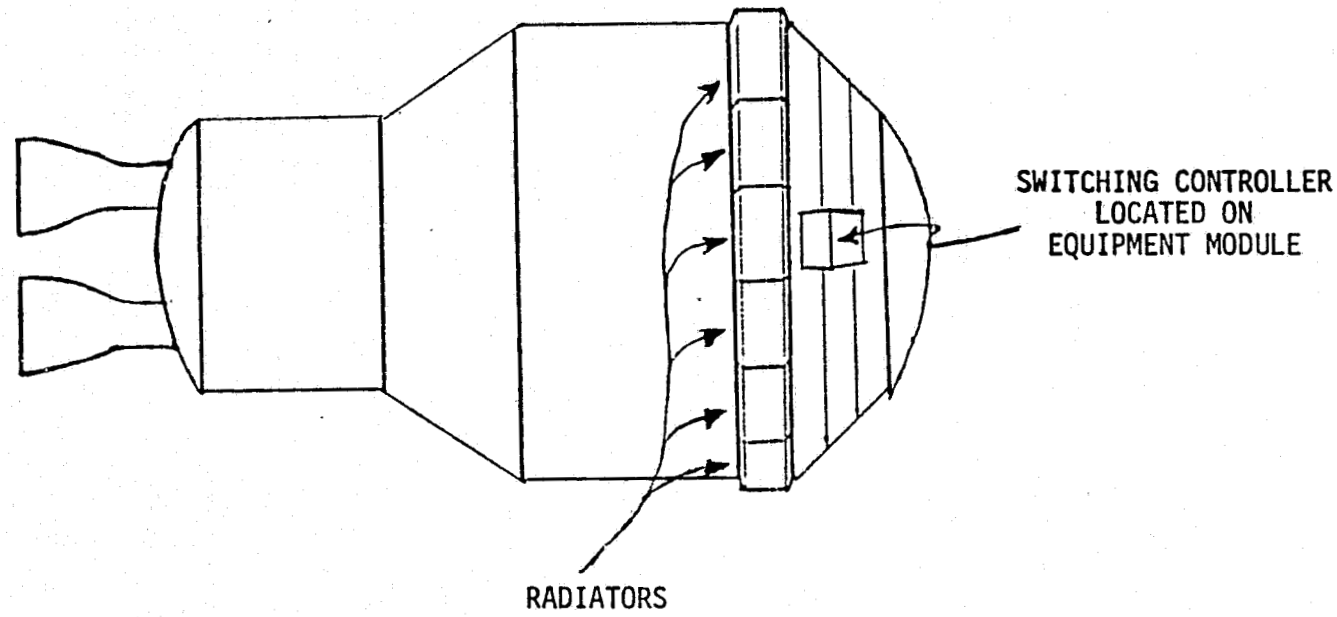

Figure 2. General Dynamics Circumferential Array

recently discussed was two motor-driven two-axis steerable helical antennas located on booms, as sketched in Figure 3, which are pointed at the target by a computer since it would not have tracking capabilities. The obvious problem with this approach is the uncertainty in the reliability of the motor-driven platform, which is greatly complicated by the revolution rate of the vehicle. The difficulties encountered by the scanning Ku-band rendezvous radar/communication antenna preclude ready acceptance of a similar configuration. Another attempt to solve the spherical high-gain coverage problem uses two truncated sphere radiators extended radially out on booms, as depicted in Figure 4. This novel concept most closely satisfies the antenna system requirements, so it will be described in more detail and compared to the biconical array.

2.1 Truncated Sphere Antenna

The truncated sphere radiator is a clever means of obtaining spot-beam coverage over a hemisphere with good axial ratios for circularly polarized radiation. This coverage is achieved by using many circular radiating discs mounted on a hemispherical ground plane for proper pointing attitudes for hemispherical coverage. The circular polarization is obtained by proper positioning of the RF cable connection such that the proper radiation mode is set up. Individually, these circular discs have a relatively wide beam, so a cluster array of four adjacent discs is used as a three-dimensional array to create a high-gain narrow spot beam. The selection of the appropriate cluster of four elements is determined by a computer which, for the smaller 15-inch-diameter model, can select one of 128 separate beams with 8-dB gain and 47° beamwidth. Electronic switching of the radiating discs is achieved by PIN diode switches placed at the hub of a centralized distributing network not unlike the spokes of a wheel. The PIN diode, which can be switched from "off" to "on" in less than 1 μs, is reverse biased for the "off" condition and forward biased for the "on" condition. Since only four diodes are "on" at any time, the electrical holding power requirements are small because the reversed-biased diode state requires very little power. The virtual phase centers of these radiating discs on the hemisphere are relatively close together, so switching adjacent beams on the same truncated sphere causes very little phase shift (estimated at 4° to 10°). However, the differential phase shift

ANTENNA LINK MARGIN TRADE STUDY

PLACEMENT OF RADIATING AND MOTOR DRIVE ELEMENTS FOR STEERABLE ANTENNA CONFIGURATION

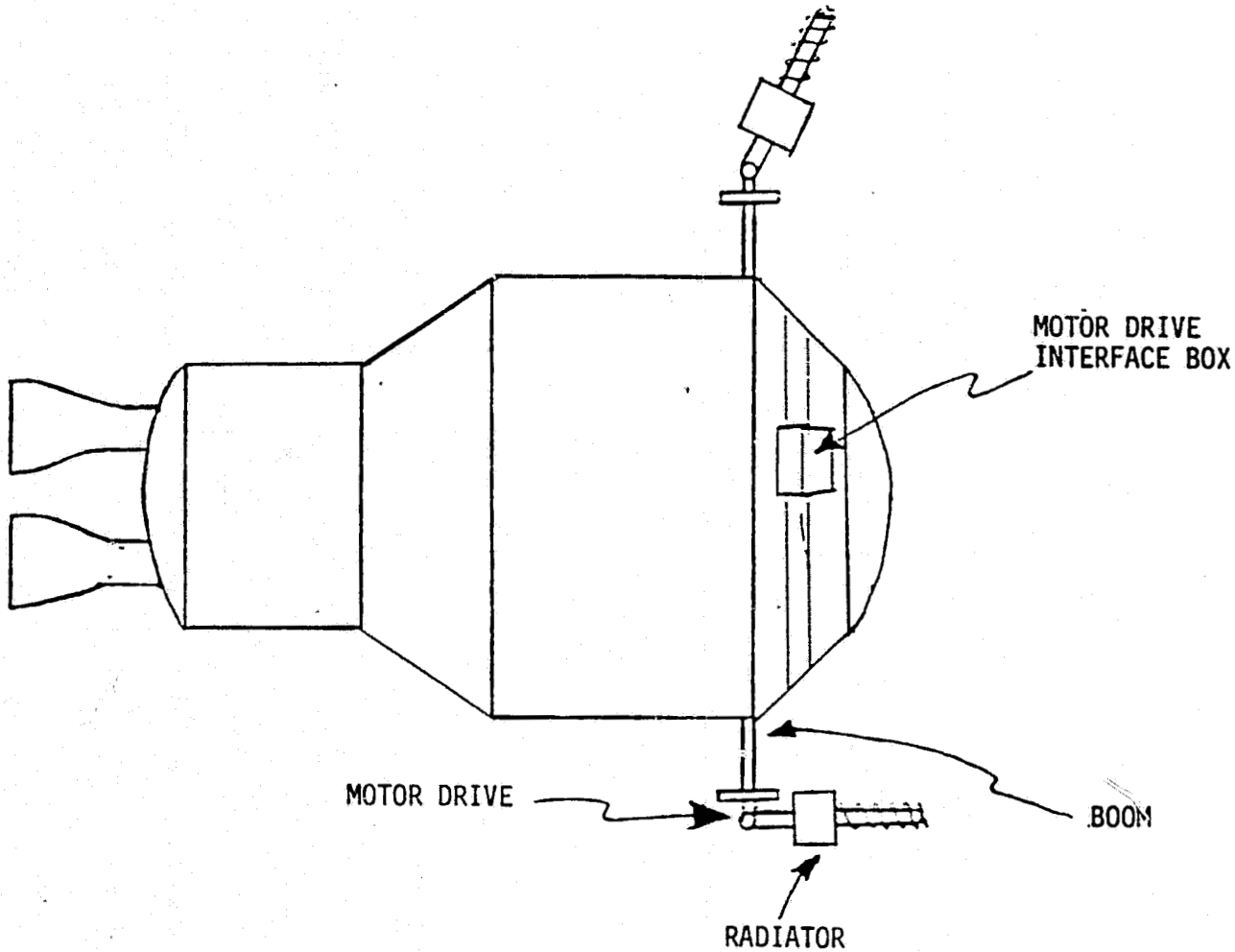

Figure 3. General Dynamics Steerable Helical Antennas

ANTENNA LINK MARGIN TRADE STUDY

PLACEMENT OF RADIATORS FOR COMBINATION ANTENNA CONFIGURATION

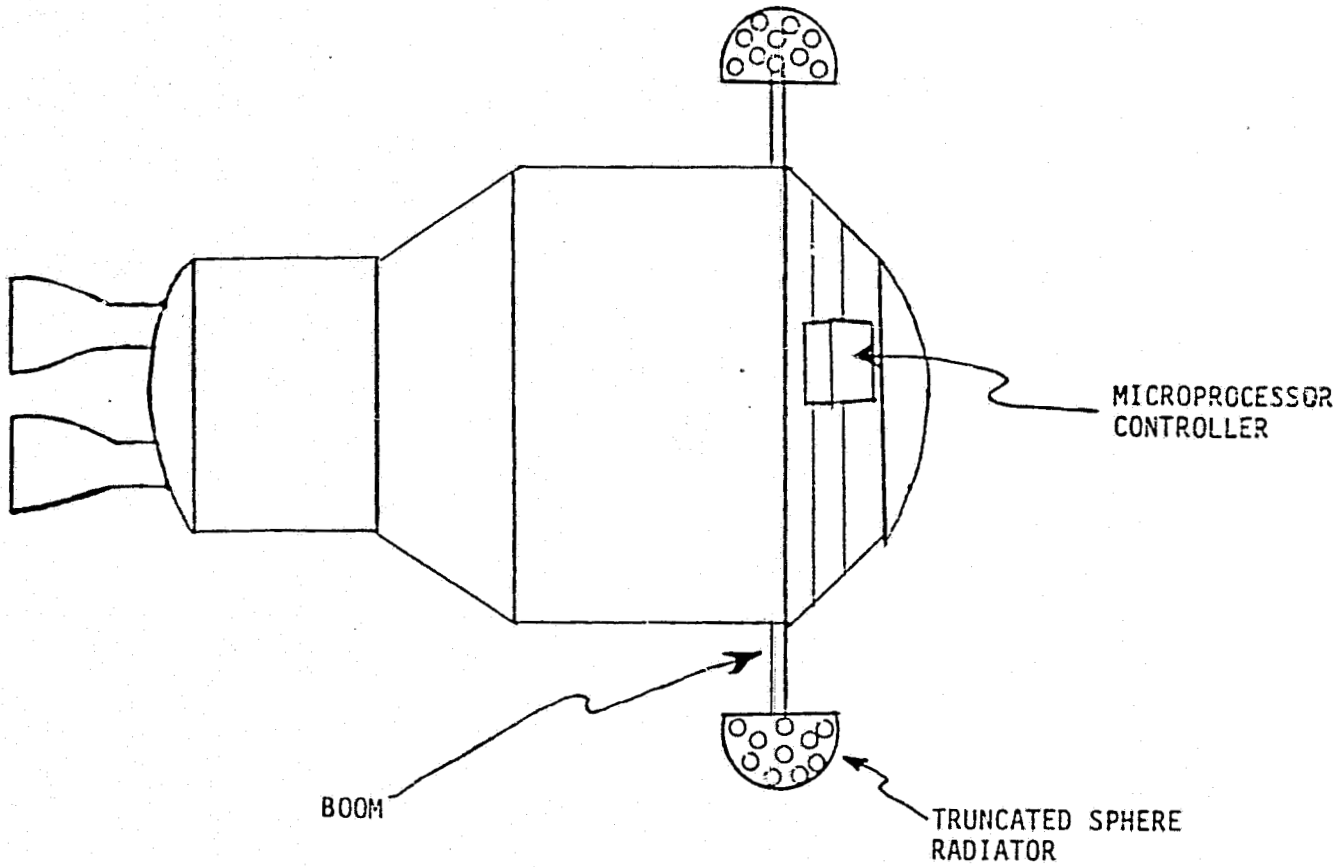

Figure 4. Truncated-Sphere Antennas

between the two truncated sphere antennas on opposite sides of the vehicle suffer the same problem as all other similar configurations since the virtual phase centers are located a substantial distance apart. The fore-and-aft coverage is adequately satisfied, however, with the same limitations as any of the extended-boom configurations.

Ideally, this truncated sphere antenna is suited for a stable platform since the spot-beam orientation for a stationary target is a simple problem. The rotation of the Centaur vehicle, however, creates a degree of complexity since the spot beam must now be continuously switched to follow the target about the axis of rotation, which is equivalent to electronic conical scanning. By viewing the photograph of the prototype model and assuming that only two elements are switched in a serially progressive manner, it is estimated that there would be eight switched spot beams per hemisphere in the broadside case, for a total of 16 switched spot beams per revolution in the worst case. This necessity to continuously switch is one of the disadvantages of this system, but it is shared in the similar arrangement used for the IUS cluster approach using five conical log spiral antennas.

3.0 MODIFIED BICONICAL-ARRAY CONFIGURATION

The objections voiced at the Centaur meeting are readily corrected by simply repositioning the placement of the boom and slightly modifying the configuration to accommodate the new requirements. Instead of forward-and-aft booms, if two booms are extended radially outward from the vehicle, as proposed by IUS/Boeing and Centaur/General Dynamics, the configuration then becomes compatible with the current system plan for deployed antennas. Two separate antenna systems are now required on opposite sides of the vehicle rather than the main one extending past the payload, as originally proposed. The proposed modified configuration is sketched in Figure 5. It should be noted that this sketch is not to scale. Dimensionally, the actual cylindrical antennas themselves should be approximately six inches in diameter and less than two feet long. The deployment feature, as in the case of the other candidate configurations, is to physically separate the antennas from the spacecraft body for improved performance by minimizing blockage and ground plane effects.

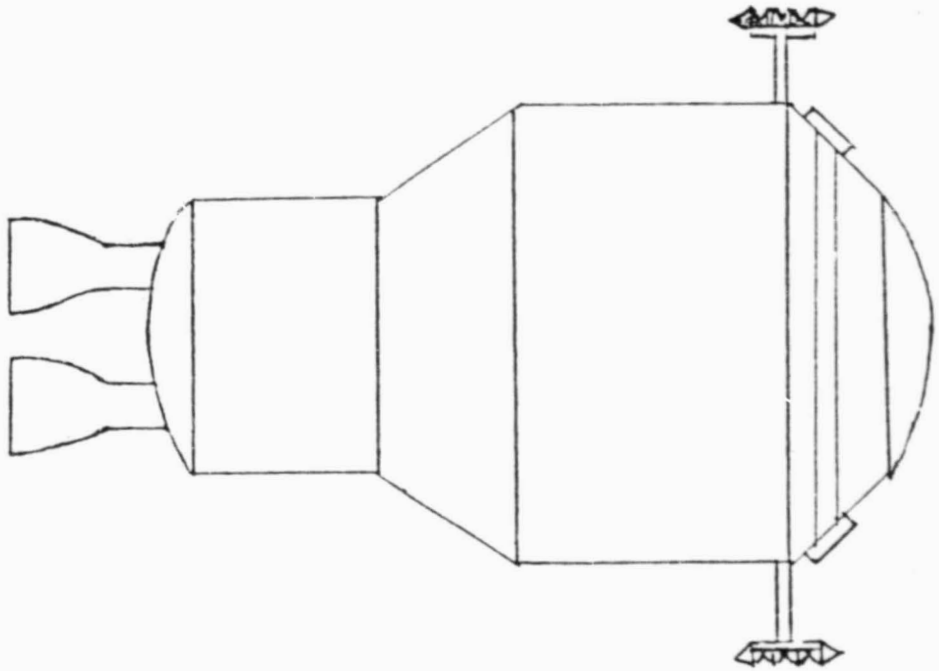

Figure 5. Modified Compound Log-Conical-Spiral/Biconical-Array Antenna

3.1 Circular Symmetry

The primary advantage of the biconical array is that the antenna pattern is a conical toroid which, since the target remains at a constant conical angle, would not normally be switched at all. The restriction that longitudinally extended booms are not permitted, however, has compromised this concept but, by using the same radially extended boom concept, it is possible to recreate this pattern using two truncated biconical arrays, each radiating half the required toroid since the vehicle blockage effects cannot be avoided. Only two antenna switches per revolution are now necessary, which is a definite advantage, depending on the final rate of revolution of the vehicle, which seems somewhat uncertain.

Each compound antenna consists of a forward-looking and an aft-looking log conical spiral antenna which are separated by the biconical array described earlier, as shown in Figure 6. But, since the Centaur vehicle now obstructs the circularly symmetric biconical antenna pattern, the biconical element is truncated so that the sector facing the Centaur vehicle is removed and serves instead as a supporting structure which also houses the electromechanical switches that select the operational modes of the antenna. Therefore, two biconical arrays on opposite sides of the vehicle provide broadside coverage about the Centaur vehicle, and the conical log spiral antennas cover the region in front of and behind the vehicle, as sketched in Figure 7. Basically, the IUS system uses the same concept for fore-and-aft coverage; however, the biconical array provides flexibility for multiple switched-beam performance with high gain and circular symmetry, which is important when accounting for the Centaur revolving slowly about its longitudinal axis. The obvious advantage of the circular symmetry is, of course, to reduce pointing and tracking requirements since a target remains relatively stationary with respect to the conical angle to the rolling Centaur vehicle. Since two compound antennas exist on opposite sides of the vehicle, each revolution requires only two switching procedures, greatly reducing the possibility of losing data. Since the two opposite semicircular beams overlap and make-before-break electromechanical switches are recommended, the signal dropout will momentarily occur only if lobing of the antenna pattern exists from the two widely separated radiating elements during the period of transition, i.e., 40 ms. The amount of phase shift during the compound antenna switching may be

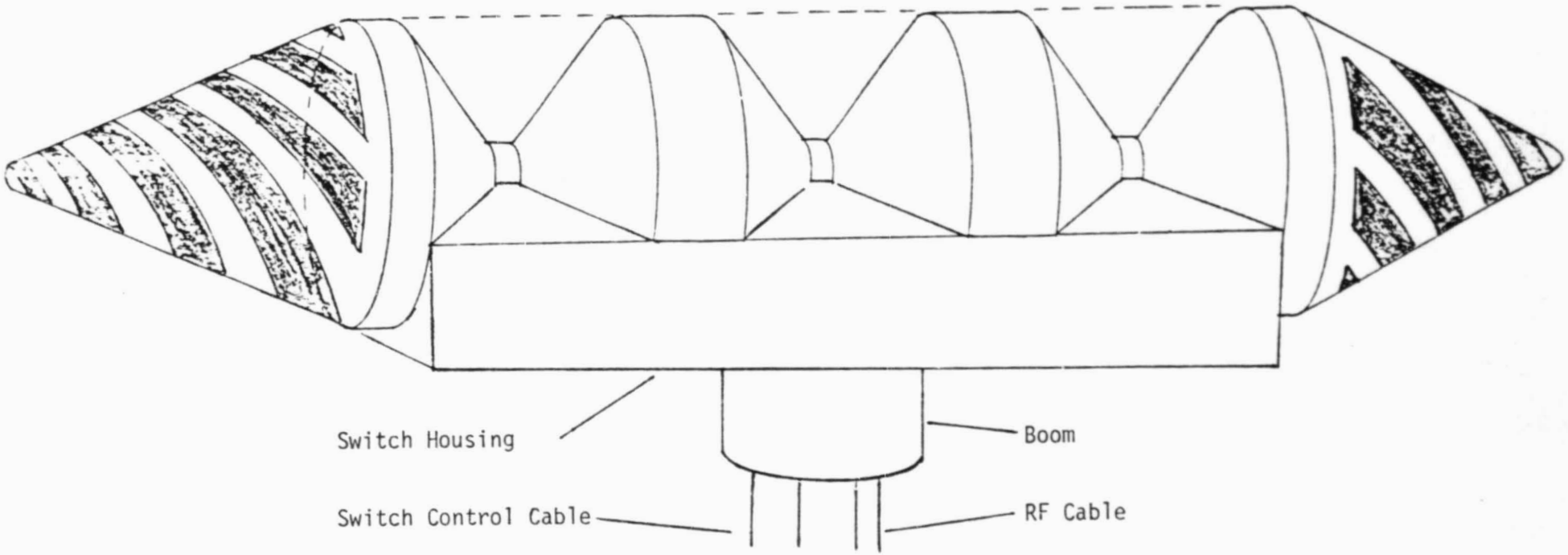

Figure 6. Compound Log-Conical-Spiral/Biconical-Array Antenna

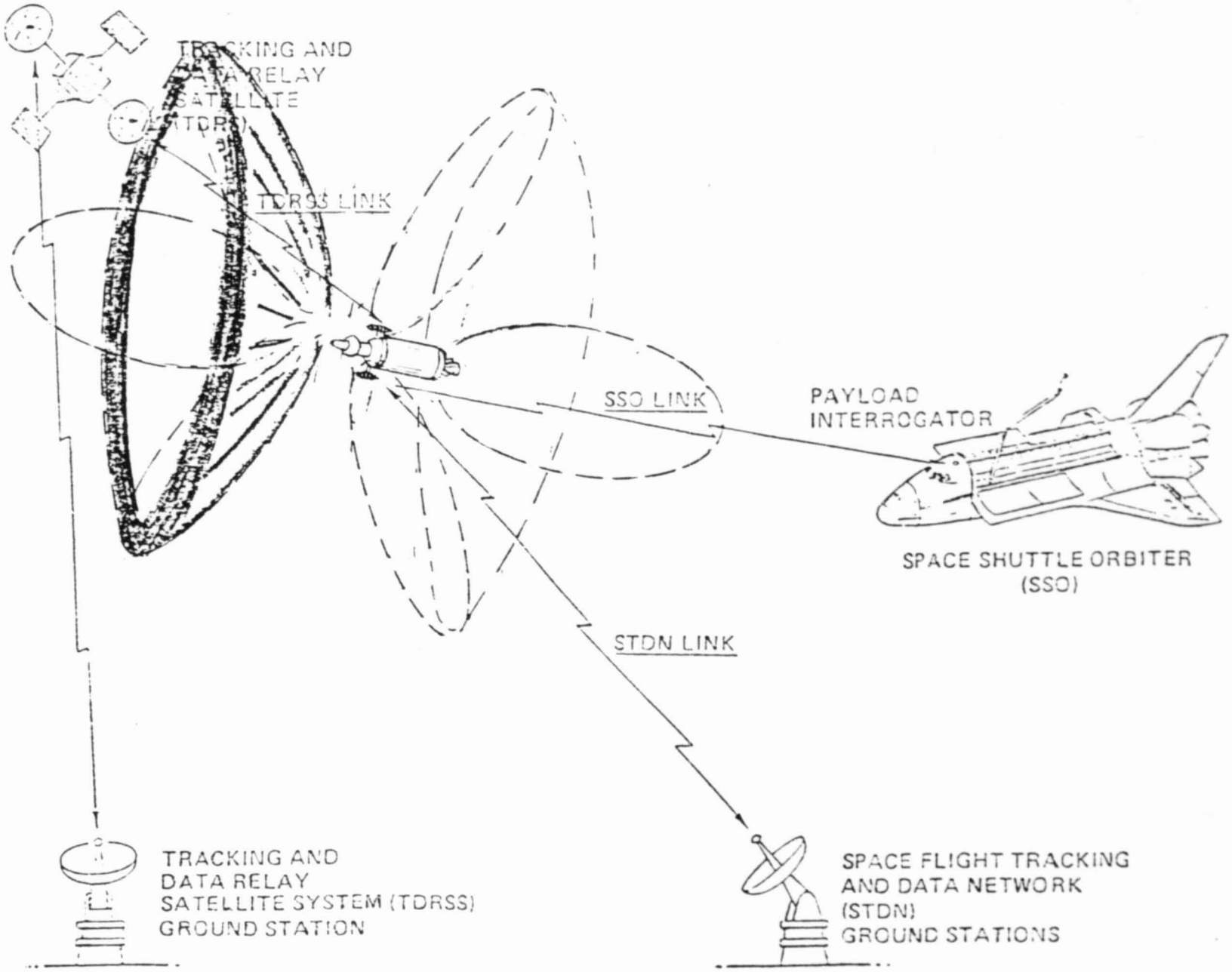

Figure 7. Toroidal Coverage Provided by the Switched-Beam Biconical Array

substantial since the phase centers are widely separated, but all the candidate antenna systems proposed to date suffer from this possible problem. The only real solution is to have only one biconical array which, as has been determined, is not feasible because of payload envelope requirement limitations.

The operation of the biconical array needs further explanation since it is a relatively new idea for this type of application. First, the idea is to create a conical toroidal pattern which has the desirable characteristics of circular symmetry, since the Centaur vehicle revolves and the target, therefore, is always at a constant conical angle with respect to the Centaur, except for the fore-and-aft coverage case which is obviously accommodated by the conical log spiral antennas pointed in those directions. An array of three individual biconical antennas is used to achieve higher gain, which is one of the essential requirements of the Centaur antenna system since the Centaur/TDRS link is marginal, at best. The choice of only three biconical antennas for the array is based on simplicity since electromechanical switching is envisioned. Of course, this method is not absolutely necessary, and situations may arise where PIN diode phase shifters and more than three biconical elements are needed to provide higher gain but, for the moment, this baseline configuration can be used to justify the feasibility of this approach. The PIN diode phase shifters require costly electrical holding power and are lossy, but the use of more biconical elements with PIN diode phase shifters should be studied if this configuration is seriously considered since higher gain might be a critical mission requirement.

3.2 Switched-Beam Concept

The Shuttle Orbiter S-band quad-antenna program uses a two-element switched two-beam configuration with one electromechanical switch to transpose discrete phase shifts of the two radiating elements, thereby creating two selectable switched beams. Since there are four quad antennas composed of two switched beams about the Orbiter, a total of eight switched beams are possible. This Centaur biconical-array configuration, on the other hand, would have two clusters of three biconical elements which can have, for example, 32 "half"-toroidal beam positions (for a total of 16 toroidal beam positions), which covers most of the surrounding space except for the

fore-and-aft coverage provided by the conical log spiral antennas. Once the particular toroidal beam is selected and concurrently set by the switch position of both clusters, only one switch is activated to direct power to the appropriate side of the vehicle, which greatly simplifies acquisition, tracking and reliability considerations.

3.3 Power-Handling Capability

Electromechanical latching switches on the Orbiter S-band quad antennas were used primarily because of the high power of the transmitter, which is of the order to 50 watts. Since the Centaur vehicle TWTA might be similar to the Hughes 40-W version, this high-power switch requirement must also be evaluated seriously for this application because PIN diode switches cannot handle much power. This consideration must also be taken into account, for example, when studying the feasibility of the truncated sphere antenna concept since the four activated PIN diode switches must be capable of handling 40 W of power. The high switching rate of PIN diodes is desirable, of course, but, for the Centaur application, it does not appear to be a critical design parameter since, once the beam position is selected, the switches do not have to be activated. The only switch to be activated during operation is that which directs power alternately from one side of the vehicle to the other. High-power PIN diode SPDT switches have recently been developed, but their insertion loss of 0.7 dB is substantially higher than the 0.1-dB loss of the electromechanical switches.

3.4 Multiple-Beam Switching Configurations

The beam-pointing mechanism of a linear phased array is used to point the toroidal beam. Three biconical elements were chosen for the array because this is the most basic phased array for the electromechanical high-power switches. The center element is directly fed with a voltage ratio of 1.0; the two outer elements are then fed with a voltage ratio of 0.6 to provide illumination taper. Introducing discrete phase shifts to the two outer elements then causes the beam position to shift, thereby creating the necessary pointing capability. For example, Figure 8 shows the tilting of the radiated phase front by adjusting the phase at the two outer elements. Figure 9 shows the two-beam configuration, Figure 10

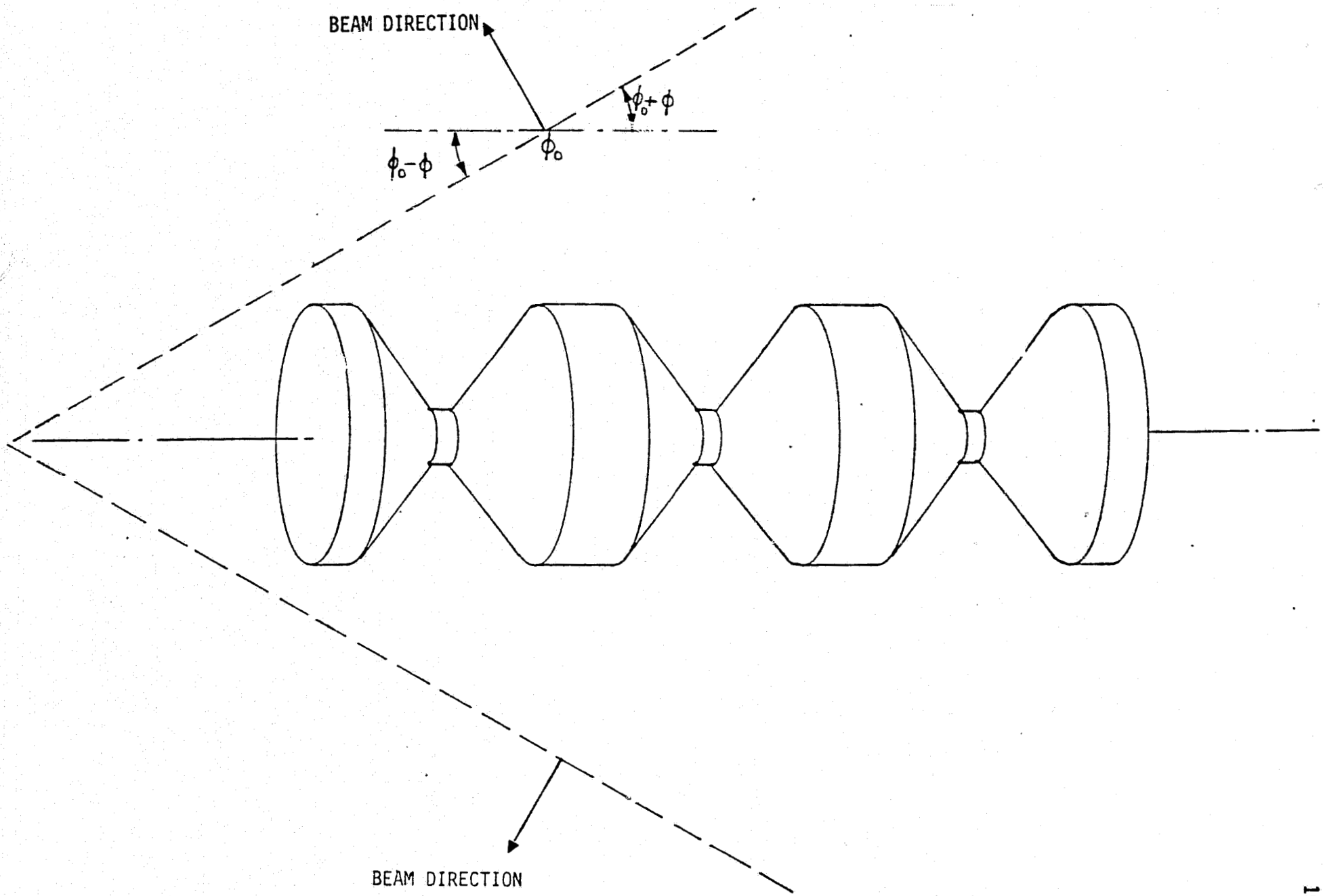

Figure 8. Beam Tilting by Phase Shifting

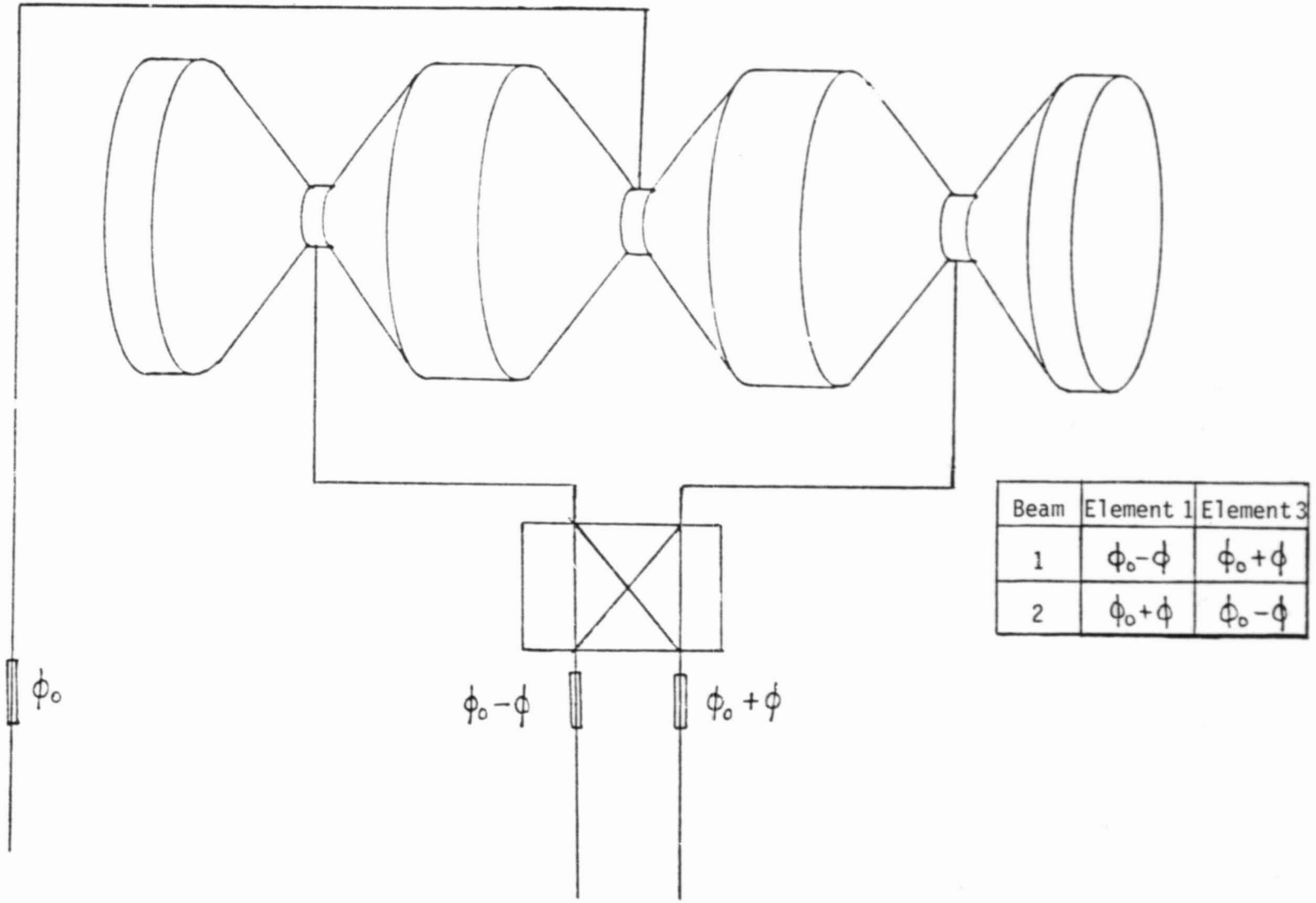

Beam	Element 1	Element 3
1	$\phi_o - \phi$	$\phi_o + \phi$
2	$\phi_o + \phi$	$\phi_o - \phi$

Figure 9. Two-Beam Switching Scheme

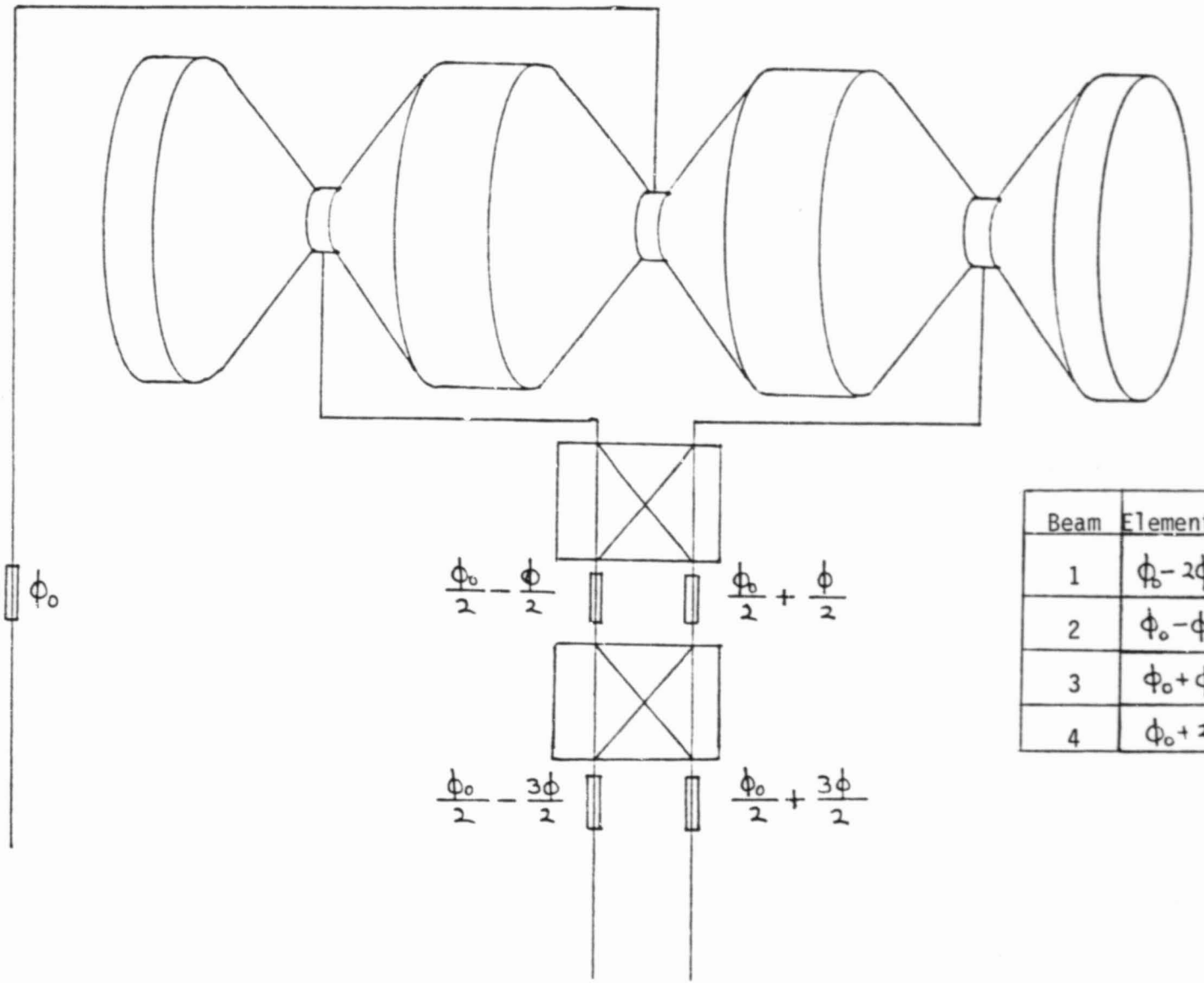

Beam	Element 1	Element3
1	$\phi_0 - 2\phi$	$\phi_0 + 2\phi$
2	$\phi_0 - \phi$	$\phi_0 + \phi$
3	$\phi_0 + \phi$	$\phi_0 - \phi$
4	$\phi_0 + 2\phi$	$\phi_0 - 2\phi$

Figure 10. Four-Beam Switching Scheme

depicts the four-beam configuration, Figure 11 illustrates the eight-beam configuration and, finally, Figure 12 gives the 16-beam configuration. Note that the addition of each switch and discrete phase shift adds only 0.2 dB of additional loss so that four electromechanical switches in a series is not unreasonable. Also, since the center element* which carries most of the power is directly fed, the use of multiple switches does not significantly degrade performance in the normal additive manner. These switches can readily be housed in the base of the truncated biconical array so that only one RF cable is required to carry the power along the boom to the compound antenna. The switching arrangement might appear as shown in Figure 13, where switch A determines which side of the Centaur is activated, switch B determines if the biconical array or conical log spiral antennas are used, and switch C determines the fore-or-aft conical log spiral antenna. For the sake of illustration, the beam-switching switches are not emphasized here. Note that these electromechanical latching switches can be characterized by binary numbers to describe the switch state. For example, if the "straight-through" state is defined as "0," the "cross-over" state is then "1." Thus, a given beam position can be adequately described by a series of binary numbers. If switch A is "1," switch B is "0," etc., then a specific beam position has a uniquely defined code. Thus, each beam position can be obtained by switch drivers being controlled by this code, and switching between the two opposite sides of the Centaur requires the switch A position to switch alternately from "1" to "0" and back cyclically, depending only on the roll rate of the vehicle. Since the beam position code on both compound antennas can be made identical, the specific beam position code remains the same and only switch A operates, greatly minimizing the software requirements. Similarly, an electromechanical switch (not included here) can switch functions from the transmitter and receiver modes. Although the electromechanical switch provides a high degree (>40 dB) of isolation, a duplexer might be required to further protect the receiver, especially since the "half"-toroidal patterns overlap.

3.5 Broadside-Beam Coverage

At this time, it would be approrpiate to discuss the problem associated with beam symmetry, which may be apparent by close examination of Figure 10, where the broadside beams are separated by 2Ø (i.e., $Ø_0 + Ø$

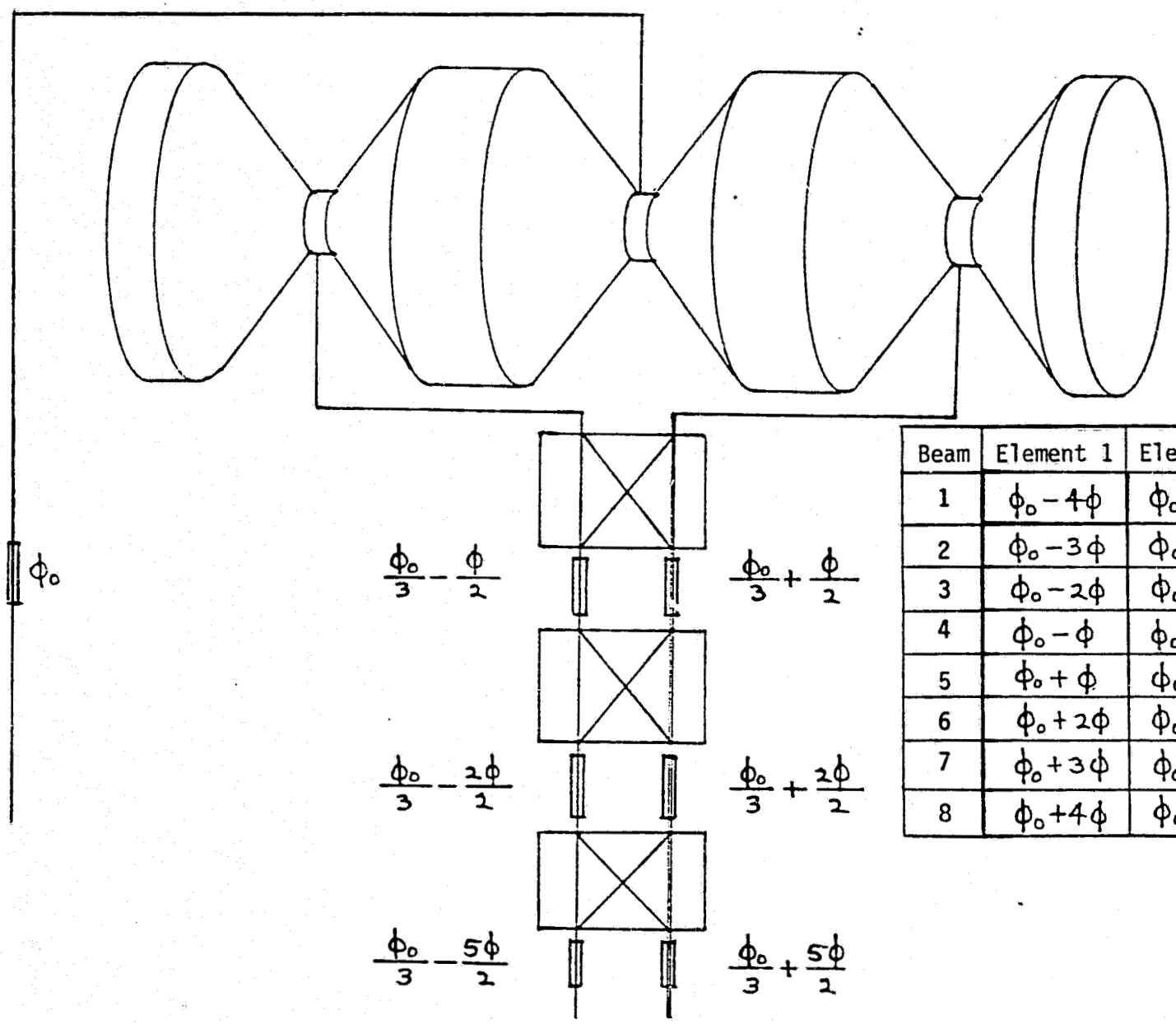

Beam	Element 1	Element 3
1	$\phi_0 - 4\phi$	$\phi_0 + 4\phi$
2	$\phi_0 - 3\phi$	$\phi_0 + 3\phi$
3	$\phi_0 - 2\phi$	$\phi_0 + 2\phi$
4	$\phi_0 - \phi$	$\phi_0 + \phi$
5	$\phi_0 + \phi$	$\phi_0 - \phi$
6	$\phi_0 + 2\phi$	$\phi_0 - 2\phi$
7	$\phi_0 + 3\phi$	$\phi_0 - 3\phi$
8	$\phi_0 + 4\phi$	$\phi_0 - 4\phi$

Figure 11. Eight-Beam Switching Scheme

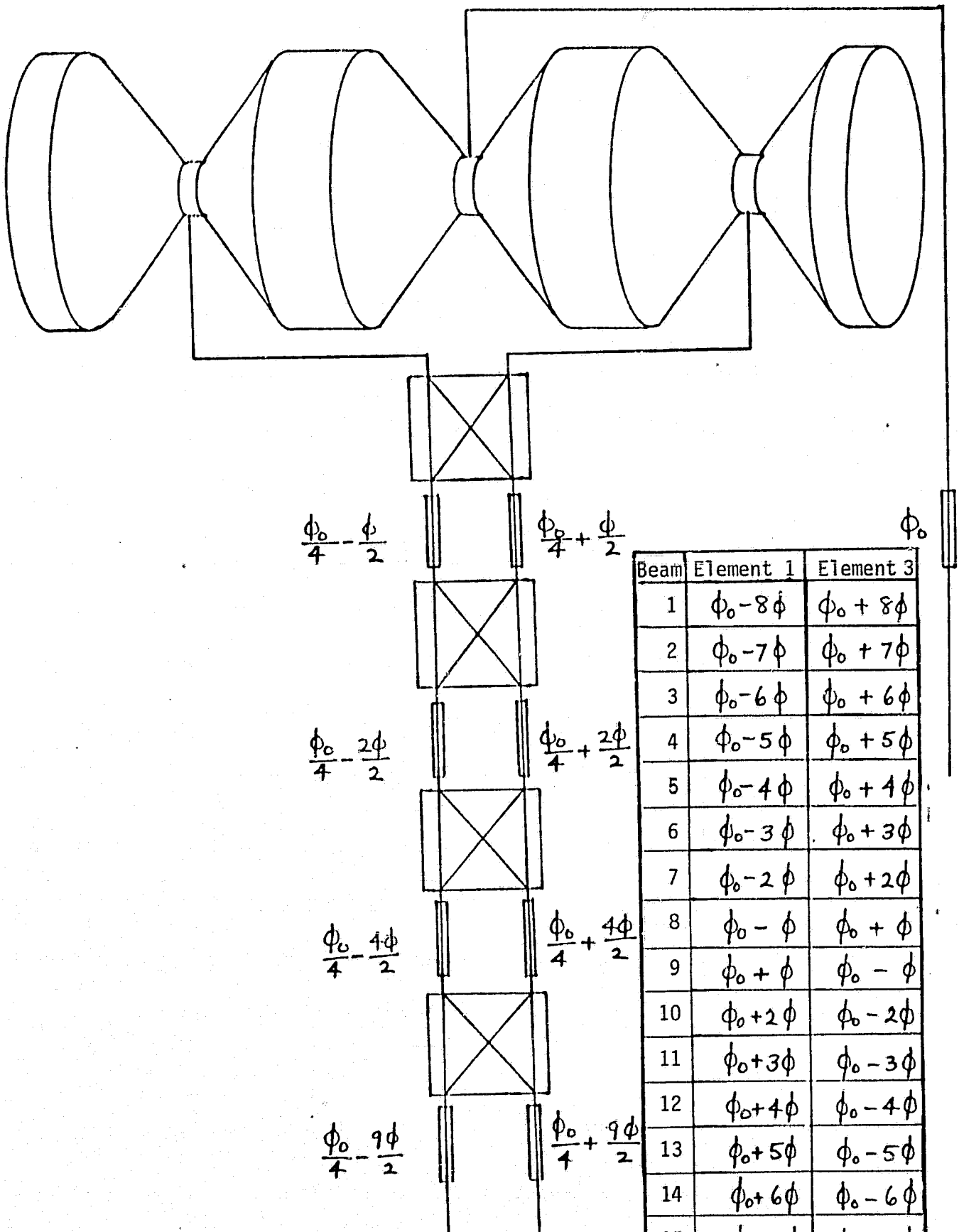

Beam	Element 1	Element 3
1	$\phi_o - 8\phi$	$\phi_o + 8\phi$
2	$\phi_o - 7\phi$	$\phi_o + 7\phi$
3	$\phi_o - 6\phi$	$\phi_o + 6\phi$
4	$\phi_o - 5\phi$	$\phi_o + 5\phi$
5	$\phi_o - 4\phi$	$\phi_o + 4\phi$
6	$\phi_o - 3\phi$	$\phi_o + 3\phi$
7	$\phi_o - 2\phi$	$\phi_o + 2\phi$
8	$\phi_o - \phi$	$\phi_o + \phi$
9	$\phi_o + \phi$	$\phi_o - \phi$
10	$\phi_o + 2\phi$	$\phi_o - 2\phi$
11	$\phi_o + 3\phi$	$\phi_o - 3\phi$
12	$\phi_o + 4\phi$	$\phi_o - 4\phi$
13	$\phi_o + 5\phi$	$\phi_o - 5\phi$
14	$\phi_o + 6\phi$	$\phi_o - 6\phi$
15	$\phi_o + 7\phi$	$\phi_o - 7\phi$
16	$\phi_o + 8\phi$	$\phi_o - 8\phi$

Figure 12. 16-Beam Switching Scheme

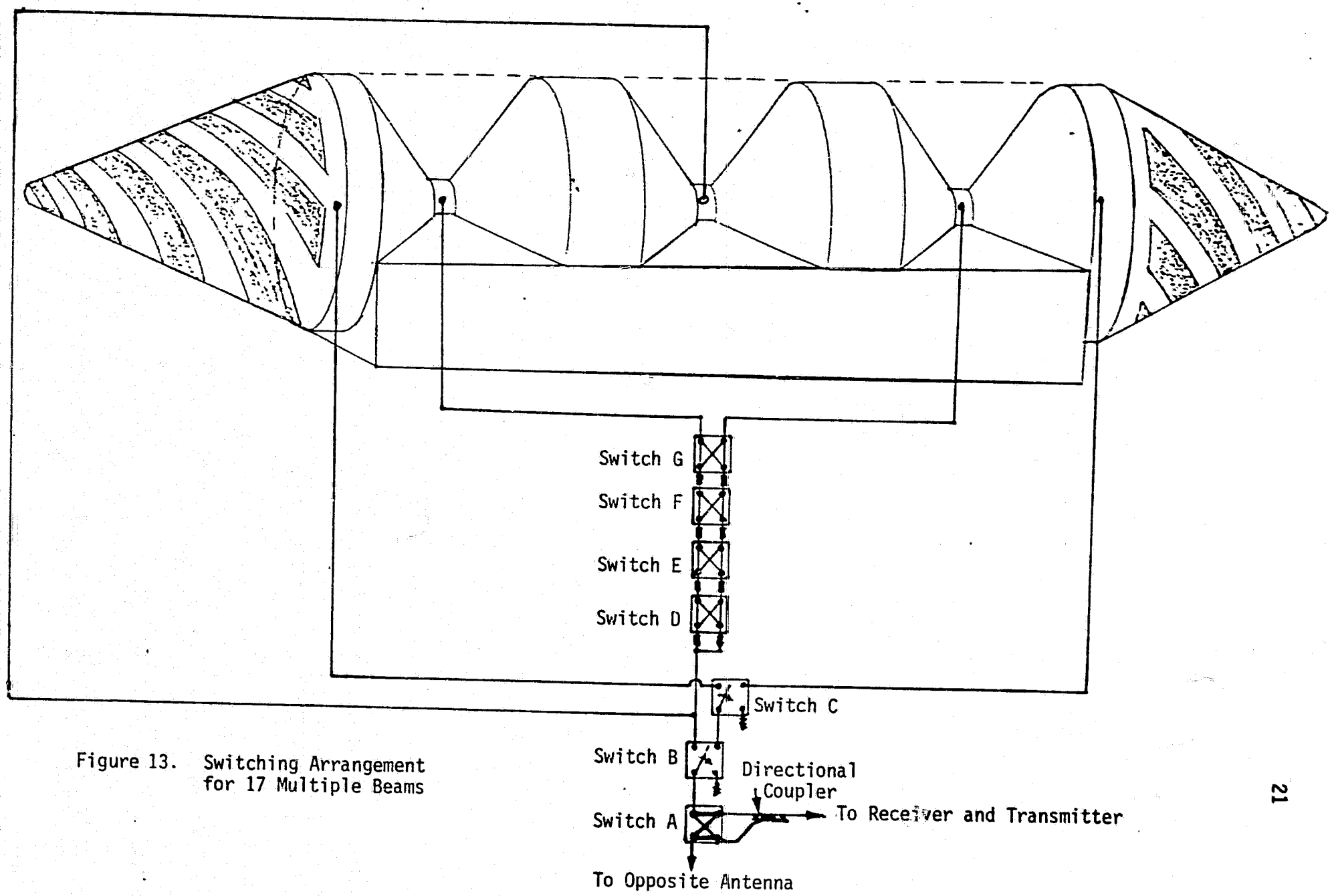

Figure 13. Switching Arrangement for 17 Multiple Beams

and $\phi_0 - \phi$). The exact broadside beam requires equal phase angles at all three elements (ϕ_0). This condition is attainable, but only at the expense of one beam position since the broadside beam is double redundant; therefore, two switch settings comprise the broadside case. For a large number of beam positions, this consideration is not important. For example instead of 16 beams, 15 beam positions are used. The necessary phase shift changes to effect this change are listed in Figures 14 through 16 for the three-, seven- and 15-beam configurations, respectively. Incidentally, a 31-beam configuration should at least be evaluated since the additional pointing flexibility justifies the additional switch if obtaining the peak biconical array gain is important.

3.6 Circular Polarization

The biconical antenna is usually associated with linear polarization since it is readily envisioned with a radiating probe feed at the intersecting apex of the two conical sections comprising the impedance-matching taper of the antenna. However, a number of methods may be employed to generate circular polarization and these different techniques must be evaluated further to determine their feasibility for this particular application. The intent of this discussion is to indicate that circular polarization is readily achievable, although the best type of transducer is not specified. The simplest and probably most efficient transducer would consist of the probe feed used for linear polarization, combined with an orthogonal probe with the appropriate phase-shifting network to create circular polarization. This orthogonal probe would not necessarily be located at the apex of the cones, but might be located at a position that is radially outward from the conical axis, as sketched in Figure 17, such that the orthogonal mode can readily propagate outward. Because of the conical tapering effect, this probe would be reactively terminated and the radial distance can be usefully employed to contribute to the necessary phase shift needed to generate circular polarization. The phase relationship of this orthogonal probe (with respect to the original probe at the apex of the conical antenna) then determines whether the transducer is right-hand circularly polarized (RHCP) or left-hand circularly polarized (LHCP). Since the biconical element is truncated, the orthogonal probe feed is only a section of the circular loop, and the gain is accordingly higher.

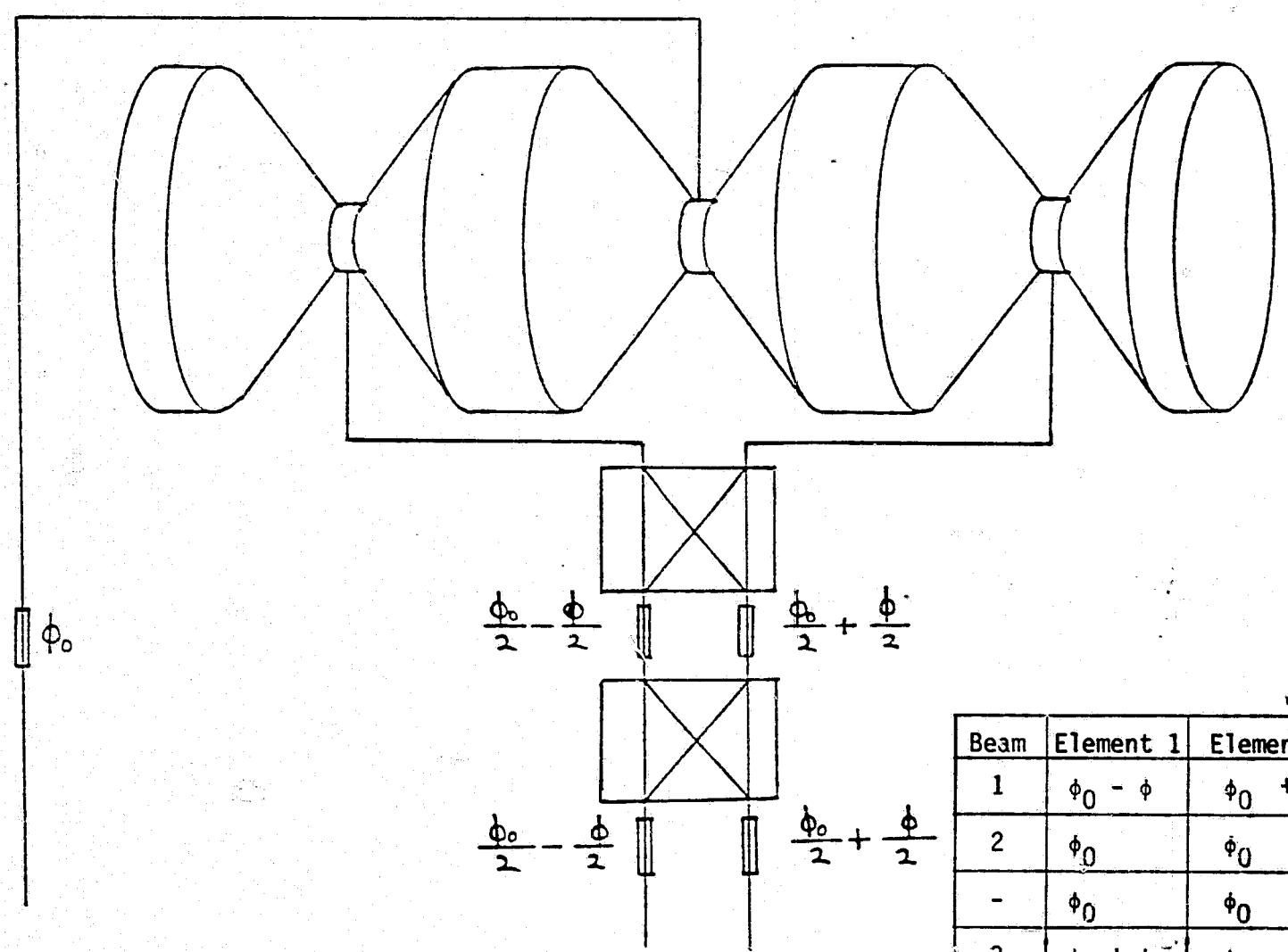

Beam	Element 1	Element 3
1	$\phi_0 - \phi$	$\phi_0 + \phi$
2	ϕ_0	ϕ_0
-	ϕ_0	ϕ_0
3	$\phi_0 + \phi$	$\phi_0 - \phi$

Figure 14. Three-Beam Switching Scheme

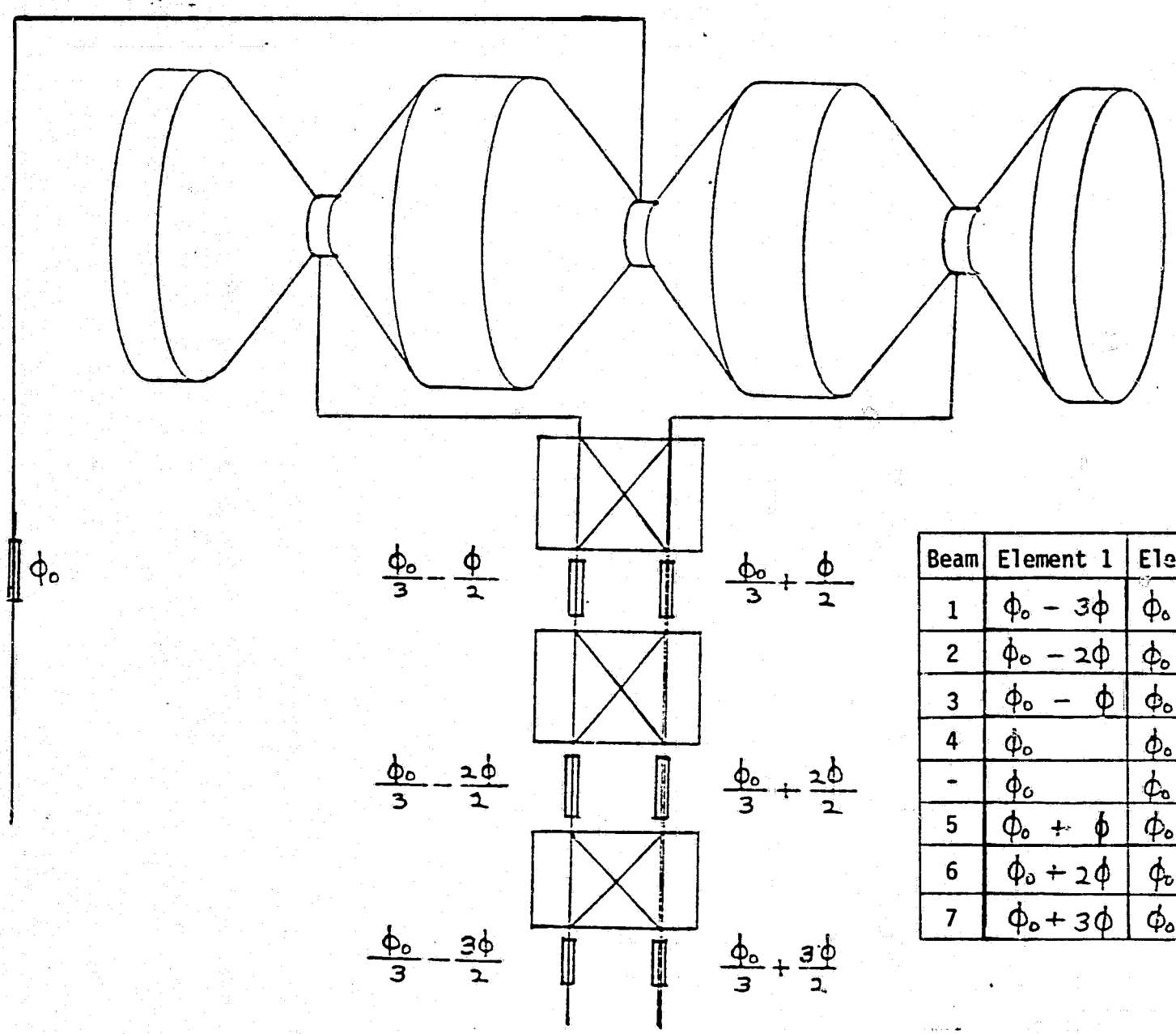

Beam	Element 1	Element 3
1	$\phi_o - 3\phi$	$\phi_o + 3\phi$
2	$\phi_o - 2\phi$	$\phi_o + 2\phi$
3	$\phi_o - \phi$	$\phi_o + \phi$
4	ϕ_o	ϕ_o
-	ϕ_o	ϕ_o
5	$\phi_o + \phi$	$\phi_o - \phi$
6	$\phi_o + 2\phi$	$\phi_o - 2\phi$
7	$\phi_o + 3\phi$	$\phi_o - 3\phi$

Figure 15. Seven-Beam Switching Scheme

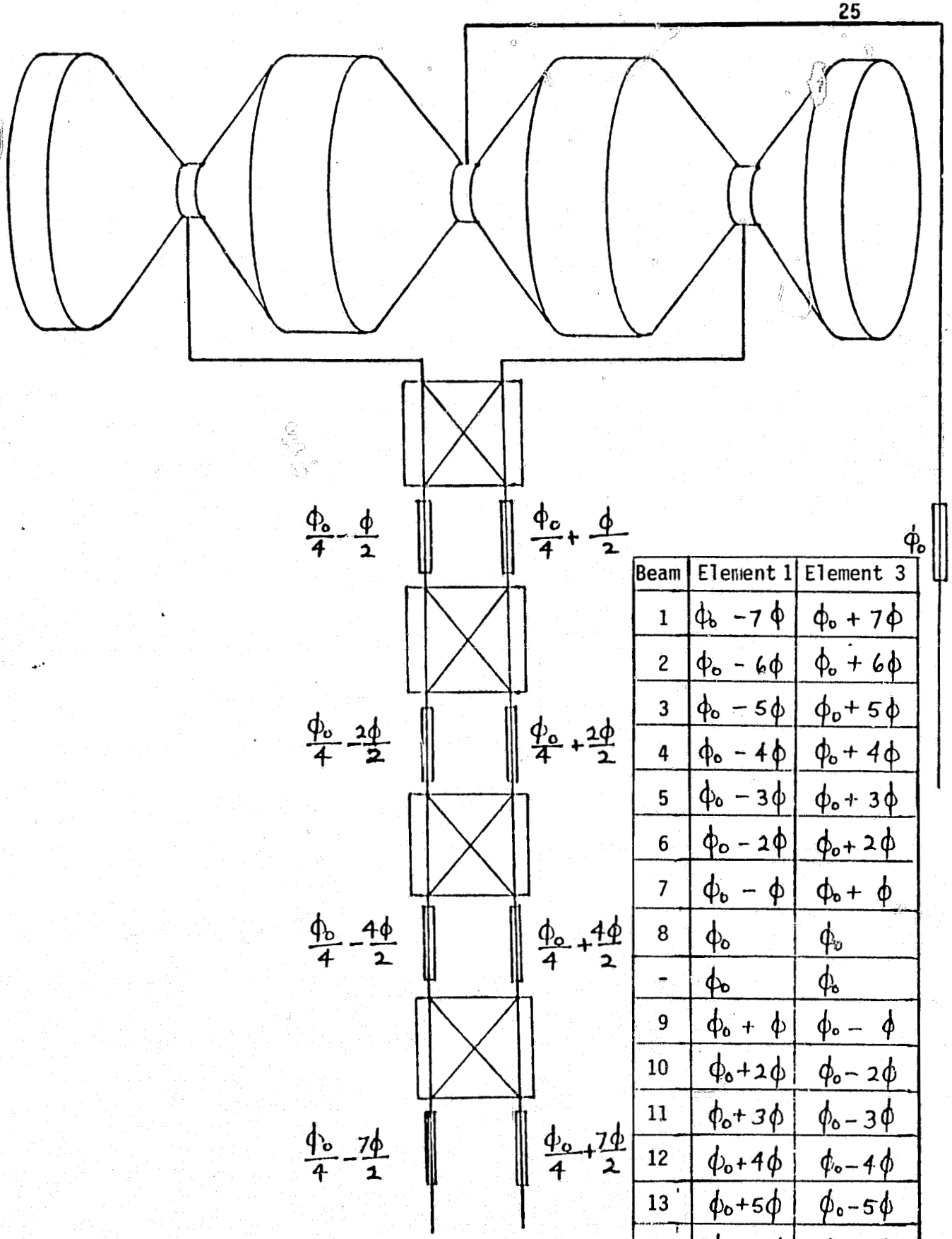

Beam	Element 1	Element 3
1	$\phi_o - 7\phi$	$\phi_o + 7\phi$
2	$\phi_o - 6\phi$	$\phi_o + 6\phi$
3	$\phi_o - 5\phi$	$\phi_o + 5\phi$
4	$\phi_o - 4\phi$	$\phi_o + 4\phi$
5	$\phi_o - 3\phi$	$\phi_o + 3\phi$
6	$\phi_o - 2\phi$	$\phi_o + 2\phi$
7	$\phi_o - \phi$	$\phi_o + \phi$
8	ϕ_o	ϕ_o
-	ϕ_o	ϕ_o
9	$\phi_o + \phi$	$\phi_o - \phi$
10	$\phi_o + 2\phi$	$\phi_o - 2\phi$
11	$\phi_o + 3\phi$	$\phi_o - 3\phi$
12	$\phi_o + 4\phi$	$\phi_o - 4\phi$
13	$\phi_o + 5\phi$	$\phi_o - 5\phi$
14	$\phi_o + 6\phi$	$\phi_o - 6\phi$
15	$\phi_o + 7\phi$	$\phi_o - 7\phi$

Figure 16. 15-Beam Switching Scheme (With Redundant Broadside Beams)

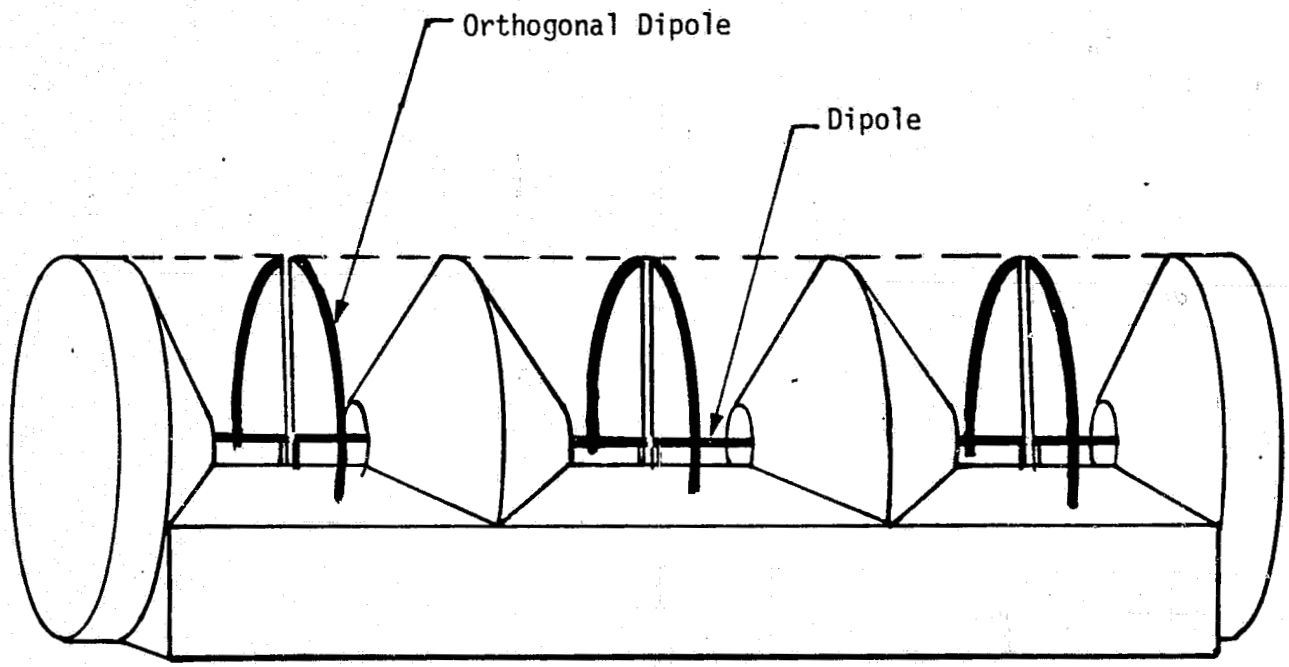

Figure 17. Circular Polarization Transducers for Biconical Antennas

Mounting of the orthogonal probe feed can be on a dielectric circular wedge for mechanical stability and increasing the effective taper of the biconical element. Since the biconical elements will be spaced so that their phase centers are less than a half wavelength apart, the effective taper of the bicone is increased by the factor $\sqrt{\varepsilon_r}$, where ε_r is the relative permittivity of the dielectric. Use of the dielectric thus effectively shortens the physical wavelength and gives greater flexibility in design considerations.

The design criteria for these orthogonal probes are basically those of two crossed half-wavelength dipoles (or monopoles), separated by $\pi/2$ to provide the quadrature phase relationship. This phase shift can also be achieved by phase shifters, but an intrinsic physical design relationship exists with the biconical element which can be readily exploited. Since the biconical element is circularly symmetric and the orthogonal dipole is curved accordingly, the off-axis axial ratio degradation is decreased substantially.

Other techniques used to obtain circular polarization from a biconical element are more complex and therefore require more study. However, the basic operating principles can be discussed. Jasik [1] discusses the use of inclined slots as a feed for a biconical element which utilizes the differential propagation delay of the horizontal and vertical polarization modes to create the phase quadrature relationship, where the slant length of the biconical horn is experimentally adjusted to achieve the $\pi/2$ phase shift at the aperture. The inclined-slot arrangement simply provides both polarizations with equal amplitudes and the horn slant length then creates the differential delay.

4.0 ANTENNA SWITCHING WITH PHASE CONTINUITY

The phase discontinuity arising from switching between the two antennas on opposite sides of the vehicle appears to be an insurmountable problem unless very sophisticated phase detection circuitry is incorporated into the system, thereby increasing complexity and cost. Even the conceptual development of such a system is difficult. Although this time period may be very short (of the order of the switching time of 40 ms), the importance of this data must be weighed in terms of the difficulties required to attempt to rectify the problem.

The IUS system for minimizing phase and amplitude transients appears to be based on an onboard computer which switches at the 45° position of the 85° HPBW. The computer knows the direction of the appropriate TDRSS and the center of the earth and can therefore switch when the theoretical pattern overlap occurs. The computer algorithm is said to be developed and system is therefore operational. A close examination of this antenna switching is warranted, however, since there may be another solution to the problem.

First, minimization of the phase transient relies on maintaining the phase centers of each antenna on the two clusters close together. Ideally, these phase centers are coincident and the phase shifts due to the feed lines have to be matched. These conditions can be accomplished, especially since the apparent phase centers of the log conical spiral antenna can be adjusted. Note that the actual phase center is difficult to determine without very accurate phase pattern measurements, but it is possible. The only real problem then is switching between clusters since, by definition, the phase centers cannot be coincident on opposite sides of the vehicle. It is this aspect of the problem that should be studied in a little more detail and, using the biconical-array configuration, a possible approach is outlined.

First, recall that the biconical array has higher gain and a circularly symmetric pattern with overlap, and requires only two switching procedures per revolution. The main consideration now is to minimize the phase transient problem switching from one antenna to the other on the opposite side of the vehicle. The easiest solution is to switch when the phase centers are exactly equidistant from the target (i.e., when the antennas form an isosceles triangle with the target). This is probably the condition employed by the IUS antenna switch scheme but, because of the large physical leverage arms of the antennas extended out on booms, the exact switching position is difficult to ascertain. The antenna-switching scheme to be discussed here is an attempt to solve this problem by using a modified monopulse sum pattern technique to determine the optimum switching position.

The optimum switching position occurs when the phases of two simultaneous signals from both antennas on opposite sides of the Centaur vehicle are identical. This condition can be described as a constructive interference pattern when the phases of the two signals reinforce each

other to create a higher gain sidelobe, which is the mechanism by which phased arrays and monopulse tracking circuits operate. Therefore, if this constructive interference pattern exists at the point where the antennas are switched, phase continuity is maintained. Again, although this condition exists cyclically since it causes lobing phenomena, the optimum switching position is where the antennas are equidistant to the target; the onboard computer should know this approximately. This position must be known exactly, however, if it is determined that no data loss is acceptable. A phase synchronization scheme has therefore been devised to determine the optimum switching point.

If a double-pole/double-throw (DPDT) electromechanical switch is used to switch power between the two arrays, the introduction of a directional coupler to split the power unequally will create a modified phased array situation where an asymmetrical toroidal pattern exists. The region of concern is then the beam overlap region where pattern interference occurs. This pattern interference is characterized by lobing, where both constructive and destructive interference exists. If both biconical arrays received equal power, serious lobing with deep nulls develop in the main antenna pattern when destructive interference conditions are satisfied and undesirable amplitude signal loss would occur. However, if unequal power distribution is employed, the effects of constructive and destructive interferences are reduced accordingly. For example, if a 10-dB coupler is used, 10% of the power is diverted to the other (secondary) antenna, with the operational or primary antenna receiving 90% of the power. This power division ratio is somewhat arbitrary now for explanatory purposes and can be determined later by system analysis if such a scheme is considered seriously. Also, it is emphasized that the only reason that power division is feasible is that the higher gain of the biconical array compensates for the apparent power loss.

As a result of the power division, the beam overlap region now develops sidelobes by constructive and destructive interference in the main antenna pattern, as shown in Figure 18. The cyclical fluctuations arise from the additional radiation from the secondary antenna. The condition for phase concurrence is constructive interference, where the newly developed sidelobe is at its peak and, if the antenna can be switched at this position, phase continuity is maintained. In essence, this is a modified monopulse-tracking scheme where the sum pattern is used to detect a relative maximum whose amplitude is related to the power division ratio.

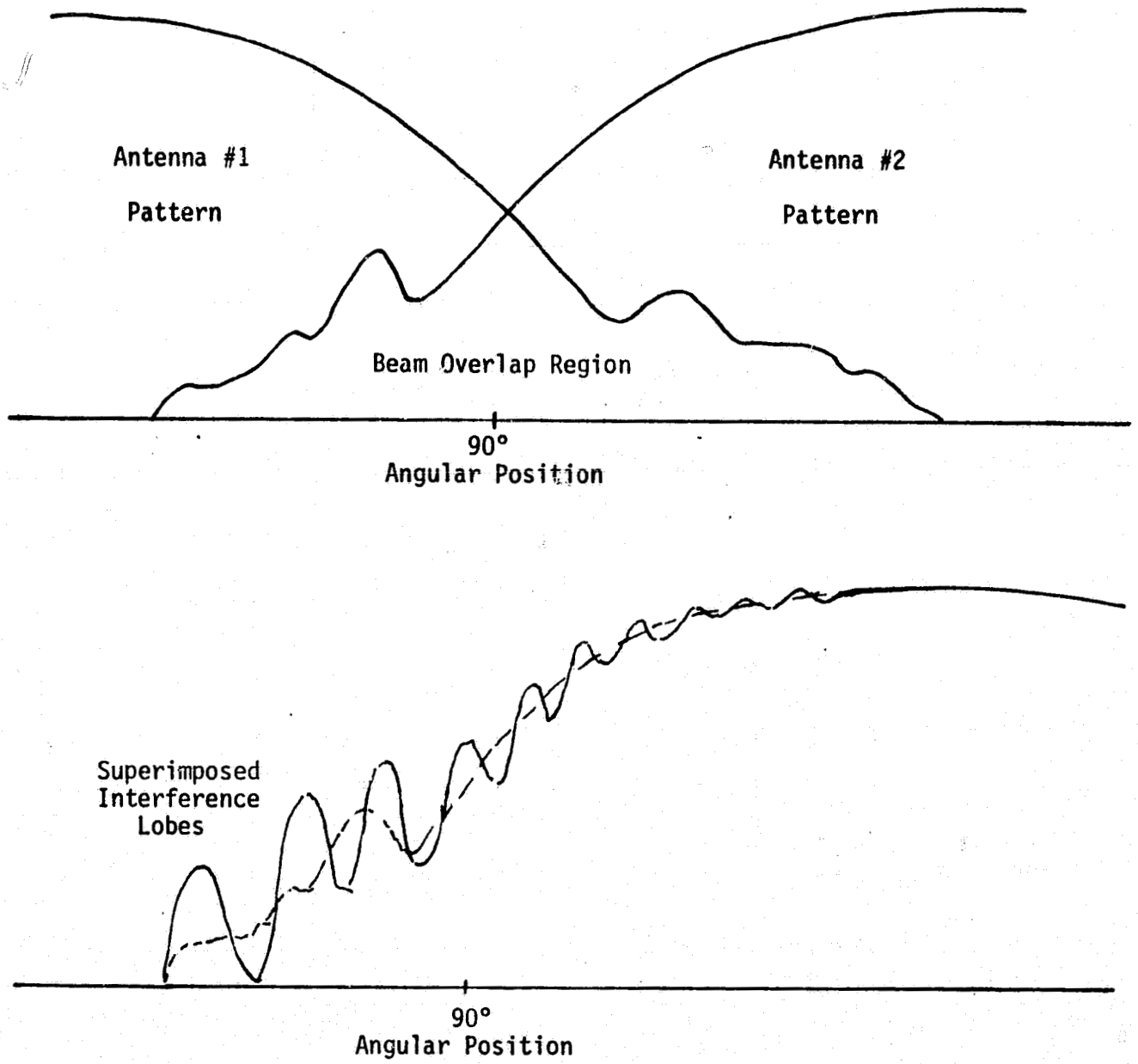

Figure 18. Interference Lobes Superimposed on Primary Antenna Patterns

The simplest method of implementing this phase continuity switching scheme is to use the automatic gain control (AGC) voltage as a basic power-level detector. This power-level detector then monitors the receiving antenna pattern in the beam overlap position and actually measures the antenna-switching position, which can then be stored for use during the transmission mode also. At the present time, determination of the optimum switching points can be made in the receive mode only when a distant source, such as the TDRSS, transmits.

The detected power-level voltage at the transition point should consist of a periodic series of lobes varying ±10% if a 10-dB directional coupler is used as a power divider. The phase concurrence position will be at the peak voltage, where the maximum lobe exists, since constructive phase interference occurs there. It is desirable to have some beam overlap between antennas so that approximately equal signal levels exist when the antennas are switched to the opposite side. Although the optimum switching point on a system basis has not been established, this phase synchronization concept can be used as a basis for further development of a scheme to maintain a continuous communication link for rotating space vehicles.

5.0 SWITCHABLE PREAMPLIFER

It is obviously advantageous to operate in a mode where the signal-to-noise ratio (SNR) is high. One possible means of improving this condition in the "receive" mode is to employ preamplifiers close to the antennas, especially since very low noise figure FET preamplifiers exist at S-band. This can be feasible if, during the "transmit" mode, the preamplifiers can be switched out of the circuit. One means that might be considered is to again use the double-pole/double-throw (DPDT) electromechanial switch in a novel manner and turn the preamplifier off during transmission. Figure 19 shows a possible scheme which, in the "0" state, allows transmission by bypassing the preamplifier and incorporatin the preamplifier in the "1" state. The isolation between connectors is critical, but 30 dB should not be unreasonable. If the preamplifier is de-energized during transmission, no damage due to leakage currents shoul occur. Since the preamplifier is located at the antenna, the noise figure of the receiver is greatly enhanced and the link margin is substantially improved.

The preamplifier also serves to simplify the phase synchronization scheme since it permits the equalization of received signal amplitude levels by amplifying the signal from the secondary antenna to the receiver to compensate for the loss imposed by the directional coupler. Since the contributions from both the primary and secondary antennas would then be equal, the constructive and destructive interference patterns will consist of lobes with well-defined peaks and nulls. Therefore, determination of the optimum switching-level detection circuitry problem might be reduced to a basic threshold detection problem. The preamplifier can remain on after the antenna-switching procedure, thereby substantially lowering the receiver system noise temperature.

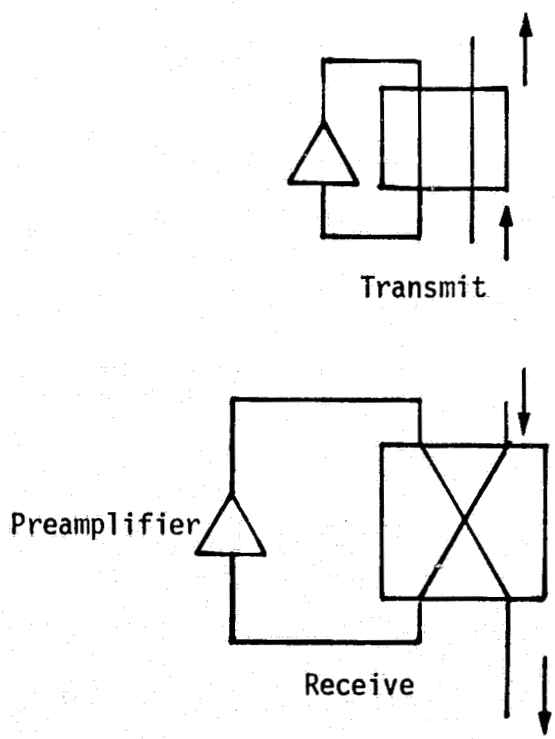

Figure 19. Candidate Switchable Preamplifier

APPENDIX C

CENTAUR HARDLINE ICD

8.4 Instrumentation & Command Data Links.

8.4.1 Instrumentation Data Links. The Orbiter shall provide the capability to transmit selected data from four PCM digital data streams (CISS, Centaur, and two S/C) from the CCE to the ground.

During prelaunch checkout, the only two PCM streams (CISS and Centaur) will be hardwired from the CCE, through the Orbiter, to the Ground Computer Controlled Launch Set (CCLS). CCLS access will be required until T-0 (Note: at SRB ignition) in the countdown.

During the final countdown and ascent mission phases the CCE will provide the four data streams (max. 64 Kbps each) to the Orbiter and the Orbiter will select and interleave 6.4 Kbps (max) of data from the four PCM streams and transmit this information to the ground for real-time systems evaluation. In addition, two of the four CCE data streams shall be recorded by the Orbiter for transmission to the ground after achieving orbit. Each data stream to recorder and orbiter telemetry system shall be isolated from each other at the orbiter interface.

During on-orbit operations, prior to Centaur stage deployment, the Orbiter will select, interleave, and transmit a maximum of 34.4 Kbps of the CCE data. The Orbiter shall continue to record one of the CCE data streams for delayed transmission to the ground. After Centaur stage deployment, only one PCM stream (CISS) will continue to be supplied directly to the Orbiter via an RF link. This data will be interleaved with the orbiter operational PCM data for transmission to the ground.

8.4.1.1 Payload Data Interleaves Interface. The Orbiter shall provide for the acquisition of asynchronous PCM data via the Payload Data Interleaver (PDI) from the four (1 CISS, 1 Centaur stage, and 2 spacecraft) CCE channels and from the Payload Signal Processor for the deployed Centaur. The PDI has a maximum composite throughput on-orbit of 64 kbps, See Figure 1 for Payload Data Interleaver data flow. However, ascent downlink CCE data shall be limited to that specified in paragraph 8.3.1.1.3.1.

8.4.1.1.1 PDI Input Data Format Characteristics.

8.4.1.1.1.1 CISS Data Format Characteristics. The PDI shall accept one data stream from the CISS. The CISS Data Format is defined as a format containing master frames and minor frames. Refer to Figure 2. Every minor frame shall be identified by a minor frame sync pattern which occurs once each minor frame, and shall be the same for all minor frames. A master frame shall contain TBD minor frames. Additionally, every minor frame shall contain an eight bit minor frame count word. The start of the master frame shall be identified as the minor frame which contains the initial value of the minor frame count word. The CISS data format characteristics shall be as shown in Table 1.

8.4.1.1.1.2 Centaur Data Format Characteristics. The PDI shall accept one data stream from the centaur. The Centaur Data Format is defined as a format containing master frames and minor frames. Refer to Figure 2.

Every minor frame shall be identified by a minor frame sync pattern which occurs once each minor frame, and shall be the same for all minor frames. A master frame shall contain TBD minor frames. Additionally, every minor frame shall contain an eight bit minor frame count word. The start of the master frame shall be identified as the minor frame which contains the initial value of the minor frame count word. The Centaur data format characteristics shall be as shown in Table 2.

8.4.1.1.1.3 Centaur Payload Data Format Characteristics. The PDI shall accept two redundant NRZ-L data streams and associated clock with each stream from the Centaur Payload. The data format is identical for both data streams and each is defined as a format containing master frames and minor frames. Refer to Figure 2.

Every minor frame shall be identified by a minor frame sync pattern which occurs once each minor frame, and shall be the same for all minor frames. A master frame shall contain TBD minor frames. Additionally, every minor frame shall contain an eight bit minor frame count word. The start of the master frame shall be identified as the minor frame which contains the initial value of the minor frame count word. The Centaur Payload data format characteristics shall be as shown in Table 3.

8.4.1.1.1.4 Detached Centaur Data Format Characteristics. In the detached mode, the Centaur will transmit a data stream via an RF link to the Orbiter Payload Signal Processor (PSP) via the Payload Interrogator. The PDI shall accept the data stream from the PSP. The detached Centaur data format is defined as a format containing master frames and minor frames. Refer to Figure 2.

Every minor frame shall be identified by a minor frame sync pattern which occurs once each minor frame, and shall be the same for all minor frames. A master frame shall contain TBD minor frames. Additionally, every minor frame shall contain an eight bit minor frame count word. The start of the master frame shall be identified as the minor frame which contains the initial value of the minor frame count word. The Detached Centaur data format characteristics shall be as shown in Table 4.

8.4.1.1.2 PDI Electrical Interface Characteristics.

8.4.1.1.2.1 CCE/PDI Data Electrical Interface Characteristics. The electrical interface characteristics of each of the CCE data streams interfacing with the orbiter PDI shall be as shown in Table 5.

8.4.1.1.2.2 CCE/PDI Clock Electrical Interface Characteristics. The electrical interface characteristics of each of the Centaur Payload clocks interfacing with the Orbiter PDI shall be as shown in Table 6.

8.4.1.1.2.3 Grounding and Shielding. Grounding and shielding for the PDI Data and clock interfaces shall be as shown in Figure 6.

8.4.1.1.3 Orbiter PCM TLM Downlink Service. Throughputting CCE data to the ground via the Orbiter's PCM downlink is implemented via the PDI's data RAM. Before individual measurements within the minor frame can be transferred to the PDI's data RAM, valid recognition of two successive minor frame sync patterns and their corresponding minor frame count patterns must first occur. When this has happened, Data RAM storage for each CCE measurement shall proceed as follows:

a. Within each minor frame word column of a master frame, those eight bit words containing data samples for a payload measurement, which are to be accessed by the PCM Master Unit (PCMMU) shall be stored within a unique PDI data RAM address. Each word stored in the PDI data RAM is accessed by the PCMMU at a uniform rate of 5 times per second and placed into a unique location in the PCMMU data RAM. Those words required for PCM downlink are formatted by the PCMMU into unique locations within the PCM downlink format.

b. A multisyllable CCE measurement shall have its constituent eight bit bytes independently stored within a separate PDI data RAM byte address whenever its word position within the appropriate minor frame is processed.

c. Maintaining the time homogenity for both individual and multisyllable CCE measurements and CCE measurement word sets cannot be guaranteed.

8.4.1.1.3.1 CCE and Detached Centaur PCM Downlink Measurements. Measurements and their format locations for CISS, attached Centaur, detached Centaur and Centaur Payload, required for PCM downlink are identified in Appendix A.

8.4.1.1.3.1.1 CCE Ascent Downlink Data. Total combined CISS, Centaur and Centaur Payload downlink data shall be limited to 6.4 KBPS during the ascent phase.

8.4.1.1.3.1.2 CCE On Orbit Downlink Data. Total combined CISS, Centaur and Centaur Payload downlink PCM data shall be limited to 34.4 KBPS during on orbit prelaunch checkout.

8.4.1.1.3.1.3 Detached Centaur PCM Downlink Data. The Payload Signal Processor (PSP) receives Centaur telemetry data via the Payload Interrogator and routes the telemetry data to the PDI. Total data on this link is limited to 16 KBPS.

8.4.1.1.4 Orbiter GPC Software Service. Transferring individual CCE or detached Centaur measurements to the GPC Software Services is implemented via the PCMMU data RAM. Individual measurements are accessed by the PCMMU as specified in paragraph 8.4.1.1.3.

Measurements and their format locations for CISS, attached Centaur, Detached Centaur and Centaur Payload required for GPC software service are identified in Appendix A.

8.4.1.2 Detached Centaur/Payload Interrogator Interface. The characteristics for the telemetry link from the detached centaur to Shuttle Orbiter are defined in ICD 2-TBD.

8.4.1.3 CCE PCM Recording. The orbiter shall provide the capability to record biphase-level digital data from two sources. Additionally the orbiter operational recorders will record all data included in the PCM downlink data stream. Payload recorder data flow is shown in Figure 12.

8.4.1.3.1 CISS PCM Recording. The orbiter shall provide the capability to record biphase-level digital data from the CISS for a period of 64 minutes. The electrical interface characteristics at the orbiter /CISS interface shall be as shown in Table 7.

8.4.1.3.2 Centaur PCM Recording. The orbiter shall provide the capability to record biphase-level digital data from the centaur for a period of 13 hours, 52 minutes. The electrical interface characteristics at the orbiter/Centaur interface shall be as shown in Table 7.

8.4.1.3.3 Grounding and Shielding. Grounding and shielding for the CCE data recording shall be as shown in Figure 7.

8.4.1.3.4 Centaur Payload PCM Recording. No direct recording capability will be provided for the recording of Centaur Payload PCM data. However, those parameters in the PCM data downlink will be recorded on the operational recorder.

8.4.1.3.5 Recorder Playback. In flight playback of CCE digital data is via the orbiter KU-Band transmitter to ground. Playback of data to GSE is via the orbiter T-0 umbilical.

8.4.1.4 Multiplexer/Demultiplexer (MDM) Signal Acquisition Interface. The orbiter shall provide data channels for the acquisition of data parameters through MDM's which are under control of the on-board computers. MDM signal transfer capabilities at the orbiter/CCE interface are TBD.

Processing requirements to activate these interfaces are specified in Section 9.0 of this ICD.

8.4.1.4.1 MDM/CCE Electrical Interfaces. TBD.

8.4.2 Command Data Link.

8.4.2.1 Payload Signal Processor (PSP). The PSP receives command data from the GPC via the payload MDM. The PSP rate buffers the data and sends it to the Payload Interrogator (detached Centaur), payload umbilical (attached CCE) or GSE. A functional block diagram of the PSP command portion is shown in Figure 3. PSP command data flow is shown in Figure 11.

Configuration Message Control - The PSP receives a configuration message from the GPC (via the payload MDM) consisting of five 16-bit words and configures the PSP to the proper command and telemetry rates. The bit assignment of the PSP configuration message is shown in Figure 4.

Message Validation Logic - The message validation logic performs data validation on each word in the configuration and command messages from the MDM. When one of the words of the configuration message fails to conform to the data validation criteria, the word shall be considered invalid and shall be rejected. If any word is rejected by the validation logic, the entire configuration and command message shall be rejected. The PSP shall then reconfigure according to the instructions in a new configuration message within one millisecond after receipt of the message. If the configuration message is different from the previous configuration message while the command data is being transmitted, the validation logic shall reject both the configuration message and the command data message.

Status Message Assembler - Provide five 16-bit status messages to the GPC (via payload MDM up to once every 80 milliseconds) for verification of the PSP configuration. The bit assignment of the PSP status message is shown in Figure 5.

Initial Configuration and Status - The PSP shall assume a known initial configuration within 30 seconds after the application of prime power and shall remain in the initial configuration until the reception and execution of the first configuration message. The PSP shall also assume the initial configuration within 1 msec when power interruption from 24 vdc to 0 back to 24 vdc is experienced and/or when the "Re-Initialize bit of configuration message is at logic 1". The following is the initial configuration:

a.	Command Rate	2 kbps
b.	Command Data Type	NRZ-L
c.	Command Data Subcarrier	16 khz sine wave with no modulation
d.	Idle Pattern	off
e.	Telemetry Rate	16 kbps
f.	Telemetry Type	Bi-Phase-L
g.	Telemetry Frame Length	Sixty-four 8-bit words
h.	Telemetry Frame Sync Word Length	32 bits
i.	Telemetry Frame Sync Word	All "one's"

j.	Subcarrier Output	Output to P/L umbilical, P/I, or GSE umbilical is inhibited
k.	Subcarrier Input	Input from PLI or GSE umbilical is inhibited.

Idle Pattern Generation - PSP can output an unmodulated or modulated 16 khz subcarrier to allow a payload to maintain command receiver lock. The idle pattern modulation consist of alternating "ones" and "zeros". The rate of the idle pattern is the same as the last "real" command data transmission, and always begins with a logic "one." The idle pattern begins in the first bit period following the last bit of the last "real' command data word transmission if the idle pattern enable bit in the previous PSP configuration word has been set. Likewise, the idle pattern will end with the last bit period prior to transmission of the first bit of the next "real" command message.

8.4.2.1.1 PSP/CCE Command Interface. The PSP shall provide command data on two redundant paths to the CCE while operating in the attached Centaur mode, and on an RF link via the Payload Interrogator while operating in the detached Centaur mode. Only one of the redundant paths shall be active at one time when operating in the attached mode. The CCE shall select the active path for receiving the command data. The PSP data output characteristics at the PSP/CCE interface shall be as shown in Table 8. The Centaur command format is shown in Figure 10.

8.4.2.1.2 Grounding and Shielding. Grounding and shielding for the PSP/CCE interfaces shall be as shown in Figure 7.

8.4.2.2 MDM/CCE Command Interface. TBD.

8.4.2.3 Detached Centaur Command Data Link. The characteristics for the command link from the orbiter to the detached Centaur are defined in ICD 2 - TBD.

TABLE 1

Payload Data Interleaver Input Data Format Characteristics-CISS

Parameter	Dimension	PDI Tolerance	Payload Characteristic	Notes
Bit rate	KPBS	64	64	
Code		BiØ-L	BiØ-L	
Word Length	Bits	8 or multiples of 8	TBD	
Minor Frame Length	Words	8 to 1024	TBD	
Minor Frame Rate	Frames/Sec	200 Max	TBD	
Master Frame Length	Minor Frames	1-256	TBD	
Minor Frame Sync		8, 16, 24 or 32 bits any pattern Contiguous locations at start of minor frame	TBD	
Master Frame Sync		8, 16, 24 or 32 bits any pattern Contiguous locations at start of minor frame	TBD	
Master Frame Sync		8 bit minor frame counter	TBD	
Format Sample Rates		One equal to minor frame rate. Five equal to interger submultiple of Minor Frame Rate.	TBD	

TABLE 2

Payload Data Interleaver Input Data Format Characteristics-CENTAUR

Parameter	Dimension	PDI Tolerance	Payload Characteristic	Notes
Bit rate	KPBS	64	64	
Code		BiØ-L	BiØ-L	
Word Length	Bits	8 or multiples of 8	TBD	
Minor Frame Length	Words	8 to 1024	TBD	
Minor Frame Rate	Frames/Sec	200 Max	TBD	
Master Frame Length	Minor Frames	1-256	TBD	
Minor Frame Sync		8, 16, 24 or 32 bits any pattern Contiguous locations at start of minor frame	TBD	
Master Frame Sync		8, 16, 24 or 32 bits any pattern Contiguous locations at start of minor frame	TBD	
Master Frame Sync		8 bit minor frame counter	TBD	
Format Sample Rates		One equal to minor frame rate. Five equal to interger submultiple of Minor Frame Rate.	TBD	

TABLE 3

Payload Data Interleaver Input Data Format Characteristics-
CENTAUR Payload

Parameter	Dimension	PDI Tolerance	Payload Characteristic	Notes
Bit rate	KPBS	9.6	9.6	
Code		NRZ-L	NRZ-L	
Word Length	Bits	8 or multiples of 8	TBD	
Minor Frame Length	Words	8 to 1024	TBD	
Minor Frame Rate	Frames/Sec	200 Max	TBD	
Master Frame Length	Minor Frames	1-256	TBD	
Minor Frame Sync		8, 16, 24 or 32 bits any pattern Contiguous locations at start of minor frame	TBD	
Master Frame Sync		8, 16, 24 or 32 bits any pattern Contiguous locations at start of minor frame	TBD	
Master Frame Sync		8 bit minor frame counter	TBD	
Format Sample Rates		One equal to minor frame rate. Five equal to interger submultiple of Minor Frame Rate.	TBD	

TABLE 4

Payload Data Interleaver Input Data Format Characteristics
Detached CENTAUR

Parameter	Dimension	PDI Tolerance	Payload Characteristic	Notes
Bit rate	KPBS	16	16	
Code		NRZ-L	NRZ-L	
Word Length	Bits	8 or multiples of 8	TBD	
Minor Frame Length	Words	8 to 1024	TBD	
Minor Frame Rate	Frames/Sec	200 Max	TBD	
Master Frame Length	Minor Frames	1-256	TBD	
Minor Frame Sync		8, 16, 24 or 32 bits any pattern Contiguous locations at start of minor frame	TBD	
Master Frame Sync		8, 16, 24 or 32 bits any pattern Contiguous locations at start of minor frame	TBD	
Master Frame Sync		8 bit minor frame counter	TBD	
Format Sample Rates		One equal to minor frame rate. Five equal to interger submultiple of Minor Frame Rate.	TBD	

TABLE 5

PDI DATA INPUT/CCE TO ORBITER ELECTRICAL INTERFACE CHARACTERISTICS
ALL PARAMETERS REFERENCED TO CISS INTERFACE

Parameter	Dimension	Characteristics Orbiter/CCE Interface	Notes
Signal Type		Differential-Balanced	Refer to Figures 5-1 and 5-2
Amplitute	Volts pk-pk	Min: 2.5 Max: 9.0	Measured line-to-line AT CISS interface
Duty Cycle	Percent	50 $\pm$ 1	(1) (2)
Bit-Rate Accuracy	Percent	$\pm$ 3.25	(3)
Stability		< 1 part in 10^5 over 60 sec period	
Waveform Distortion		Overshoot and undershoot less than 20% of peak amplitude level	
Noise	Milivolts	100 pk-pk, differential line-to-line, DC to 100 KHz	CCE transmitting, not transmitting, or failed
Cable		2 conductor twisted, shielded, jacketed, controlled impedance	Rockwell design standard MP572-0328-0102
Cable Impedance	Ohm	75 $\pm$ 5	Characteristic Impedance
Cable Capacitance	Picofarads	2900 max	Capacitance across differential line pair from CISS interface to PDI (18 to 23 pf/ft)
Load Impedance	Ohm	74 min 91 max	DC resistance line-to-line at interface includes cable resistance

TABLE 5

PDI DATA INPUT CCE TO ORBITER ELECTRICAL INTERFACE CHARACTERISTICS
ALL PARAMETERS REFERENCED TO CISS INTERFACE (Continued)

Parameter	Dimension	Characteristics Orbiter/CCE Interface	Notes
Cable Resistance	Ohm	4.4 per conductor max	Based on 126 foot cable length from CISS interface to PDI input
Cable Length	Feet	126 (max)	From CISS interface to PDI input
Rise/Fall Time		Max: Refer to Differential Phase Skew	(4) RT/FT are independent of bit rate and data code type (BiØ or NRZ)
Skew-Differential Phase	Nanosecond to Millisecond depending on PL bit rate		(5) (7)
For BiØ data:		Max: $0.159\ Tp - 1x10^{-6} - 2NTp - (R/(R+1))\ Tp -$ $Tlr\ (Loge(Vlpk-100mv)/(Vlpk-300mv)) -$ $Ttr(Loge(Vtpk+300mv)/(Vtpk+100mv))$ Where: N = Payload Duty Cycle Offset $0 \leq N \leq 0.05$ R = PDI Programmed Bit Rate Offset with respect to Payload Bit Rate (Refer to Figures 5-4 and 5-5.	

TABLE 5

PDI DATA INPUT CCE TO ORBITER ELECTRICAL INTERFACE CHARACTERISTICS
ALL PARAMETERS REFERENCED TO CISS INTERFACE (Continued)

Parameter	Dimension	Characteristics Orbiter/CCE Interface	Notes
		Vlpk = Peak amplitude level of BiØ waveform leading edge. Vtpk = Peak amplitude level of BiØ waveform trailing edge. Tp - Reciprocal of CCE bit rate (center frequency) Tlr = Max. rise time of BiØ waveform leading edge measured between 10% & 90% points. Ttr = Max. fall time of BiØ waveform trailing edge measured between 10% and 90% points	
Skew-Differential Phase (Cont.) For NRZ data:		Max: 0.309 Tp - NTp - Tcr(LOGe(Vcpk-100mv)/(Vcpk-300mv)) - Tdr(LOGe(Vdpk + 300mv)/(Vdpk + 100mv)) Where: N = Clock Duty Cycle Offset $0 \leq N \leq 0.05$ Vcpk = Peak amplitude level of CCE Clock signal.	

TABLE 5

PDI DATA INPUT/CCE TO ORBITER ELECTRICAL INTERFACE CHARACTERISTICS
ALL PARAMETERS REFERENCED TO CISS INTERFACE (Continued)

Parameter	Dimension	Characteristics Orbiter/CCE Interface	Notes
		Vdpk = Peak amplitude level of CCE NRZ Data signal. Tp - Reciprocal of CCE bit rate (center frequency) Tcr = Max. transition time (rise or fall time) of CCE Clock signal measured between 10% and 90% points. Tdr = Maximum transition time (rise or fall time) of CCE NRZ DATA signal measured between 10% and 90% points.	
Common Mode	Volt	±3 pk-pk continuous or -60 pk-pk for 10 μ sec for damage level	(6) ± 3 volts from EMI, negligible from CCE or PDI. (6)

(1) Relative position of BiØ-L mid bit transition at interface

(2) Any bit or clock transition point occurs in time at the 50% pk-pk amplitude point.

(3) The PDI shall set an error flag within its BITE Status Register whenever the Payload bit rate exceeds ± 3.25% of its specified center frequency.

(4) The maximum limit for CCE signal Rise/Fall time is not to be determined independently, but instead is to be determined as part of a tradeoff with other related offsets. In order to make that tradeoff, the appropriate general case equation for Differential Phase Skew shall be utilized.

(5) These two general case equations for BiØ data and NRZ data are an expression of how the CCE bit period is partitioned between the PDI's Bit Lock Range, CCE Duty Cycle Offset, PDI Programmed Bit Rate Offset (for BiØ data only), and CCE maximum Rise and

TABLE 5

PDI DATA INPUT/CCE TO ORBITER ELECTRICAL INTERFACE CHARACTERISTICS
ALL PARAMETERS REFERENCED TO CISS INTERFACE (Continued)

Parameter	Dimension	Characteristics Orbiter/CCE Interface	Notes

Fall time. The solution for each of these two general case equations indicates that amount of the CCE bit period which remains (CCE bit period minus PDI Bit Lock Range minus appropriate Offsets) for partitioning between the CCE signal Differential Phase Skew and/or Phase Shift. A solution for either of these two general case equations which produces a negative result indicates that the appropriate offset themselves have utilized all the remaining CCE bit period such that none is available for Differential Phase Skew and/or Phase Shift. PDI Bit Lock Range identifies the absolute minimum amount of the CCE bit period required for the PDI's Bit Synchronizer to achieve and maintain bit lock.

Date Type	Bit Lock Range
BiØ	$0.159\ T_p - 1 \times 10^{-6}$
NRZ	$0.309\ T_p$

CCE Signal Differential Phase Skew, as defined here, shall consist of the absolute value of the difference between the Leading Edge Phase Shift and the Trailing Edge Phase Shift (refer to Figure 5-3 and is independent of Payload amplitude level.

CCE Signal Phase Shift is the time differential between the 50% points of associated amplitude transitions of the two CCE differential inputs.

(6) Volts over frequency spectrum from DC to 100 KHz.

(7) This examle illustrates how the BiØ Data general case equation for Differential Phase Skew shall be utilized by the CCE. The following interface characteristics are utilized as part of the first tradeoff for determining the upper limit for each of the Offsets applicable to the CCE.

Bit Rate (Center Frequency):	64 KBPS
BiØ Data Duty Cycle:	50 + 1%
BiØ Data Peak Amplitude	1.25 volts
Maximum Transition Time: (Rise and Fall Time)	1 μ sec

TABLE 5

PDI DATA INPUT/CCE TO ORBITER ELECTRICAL INTERFACE CHARACTERISTICS
ALL PARAMETERS REFERENCED TO CISS INTERFACE (Continued)

Parameter	Dimension	Characteristics Orbiter/CCE Interface	Notes

For the specified center frequency of 64 KBPS, the corresponding amout of time for one bit period is: T_p = 1/64 KBPS = 15.6 μ seconds.

Within each CCE bit period (Tp), the general case equation for BiØ Data Differential Phase Skew provides for the following amounts of T_p time to be dedicated to:

1) PDI's Bit Lock Range:

$0.159\ T_p - 1 \times 10^{-6} = 0.159\ (15.6\ \mu\text{ sec}) - 1\ \mu\text{ sec} = 1.48\ \mu\text{ sec}$
PDI'sBit Synchronizer to achieve and maintain bit lock.

2) Payload BiØ Data Duty Cycle Offset:
$2\ N\ T_p = 2\ (0.01)\ (15.6)\ \mu\text{ sec}) = 0.31\ \mu\text{ sec}$ with

N = 0.01 corresponding to a 1% Duty Cycle Shift.

3) PDI Programmed Bit Rate Offset: -

$(R/(R+1))Tp = (0.008/(0.008+1))(15.6\ \mu\text{ sec}) = 0.123\ \mu\text{ sec}$

with R = 0.8 % as obtained from Figure 5-5 for a Payload bit rate of 64 KBPS.

4) Ambiguity in Change of PDI Receiver Output Due to Slow Transition Time of CCE Data Differential Inputs:

$Tlr(LOGe(Vlpk-100mv)/(Vlpk-300mv)) + Ttr(LOGe(Vtpk+300mv)/(Vtpk+100mv)) = 1\mu\text{ sec}(LOGe(1.25-0.10)/(1.25-0.30)) + 1\mu\text{ sec}(LOGe(1.25+0.30)/(1.25+0.10)) = 1\mu\text{ sec}(LOGe\ 1.21) + 1\mu\text{ sec}\ (LOGe\ 1.15) = 0.3\ \mu\text{ sec}$

The remaining amount of T_p time which is available to the CCE user for partitioning between CCE BiØ Data Differential Phase Skew and/or Phase Shift is:

TABLE 5

PDI DATA INPUT/CCE TO ORBITER ELECTRICAL INTERFACE CHARACTERISTICS
ALL PARAMETERS REFERENCED TO CISS INTERFACE (Continued)

Parameter	Dimension	Characteristics Orbiter/CCE Interface	Notes
Diff. Phase Skew/Phase Shift = 1.48 μ sec - 0.31 μ sec - 0.123 μ sec - 0.3 μ sec = 0.747 μ sec This completes the first tradeoff such that the general case equation for BiØ Data Differential Phase Skew has enabled the user to dedicate the following amounts of time as upper limits for: 0 ≤ Duty Cycle Offset ≤ 0.31 μ seconds 0 ≤ Transition Time Ambiguity ≤ 0.30 μ seconds 0 ≤ Diff. Phase Skew/Phase Shift ≤ 0.747 μ seconds If these upper limits are acceptable, then the CCE user shall determine the actual amounts of time to be allocated to each appropriate Offset. These "Actual Values" shall be specified within this ICD so as to characterize the Payload-to-PDI interface. If these upper limits are not acceptable, then the Payload user shall have to develop a second tradeoff with an appropriate change in either the Duty Cycle Shift, Maximum Transition Time, or Peak Amplitude. It should be noted that a Payload user can only change PDI Bit Lock Range and PDI Programmed Bit Lock Range and PDI Programmed Bit Rate Offset by choosing a different Payload Bit Rate. The general case equation for NRZ Data Differential Phase Skew is utilized in a manner identical to its BiØ Data counterpart with the exception that PDI Programmed Bit Rate Offset is not included.			

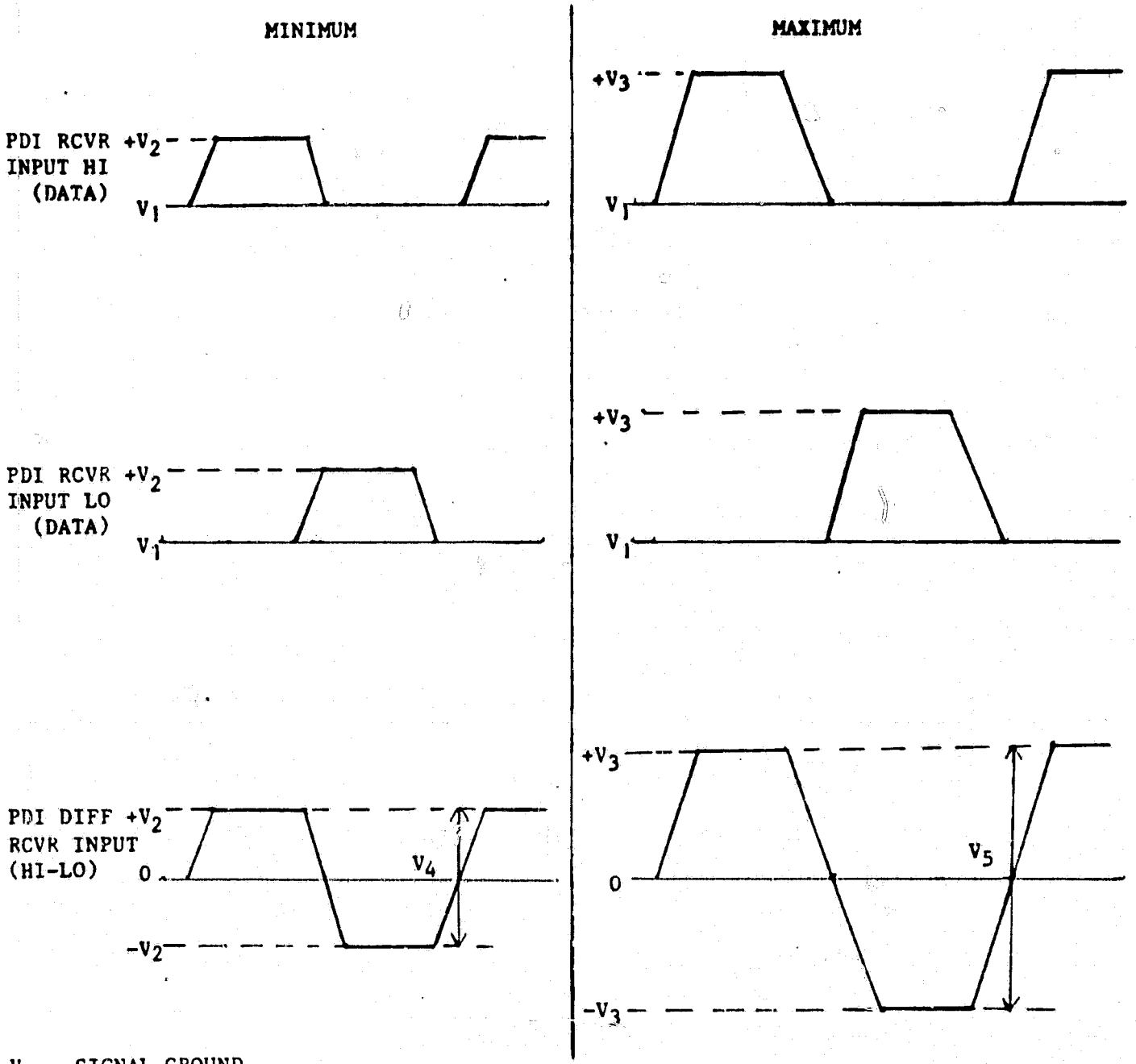

V_1 = SIGNAL GROUND
V_2 = 1.25 VOLTS LINE TO SIG. GND.
V_3 = 4.5 VOLTS LINE TO SIG. GND.
V_4 = 2.5 VOLTS P -P LINE TO LINE DIFFERENTIAL BALANCED
V_5 = 9.0 VOLTS P -P LINE TO LINE DIFFERENTIAL BALANCED

FIGURE 5-1 Data/Data - Differential Transmission

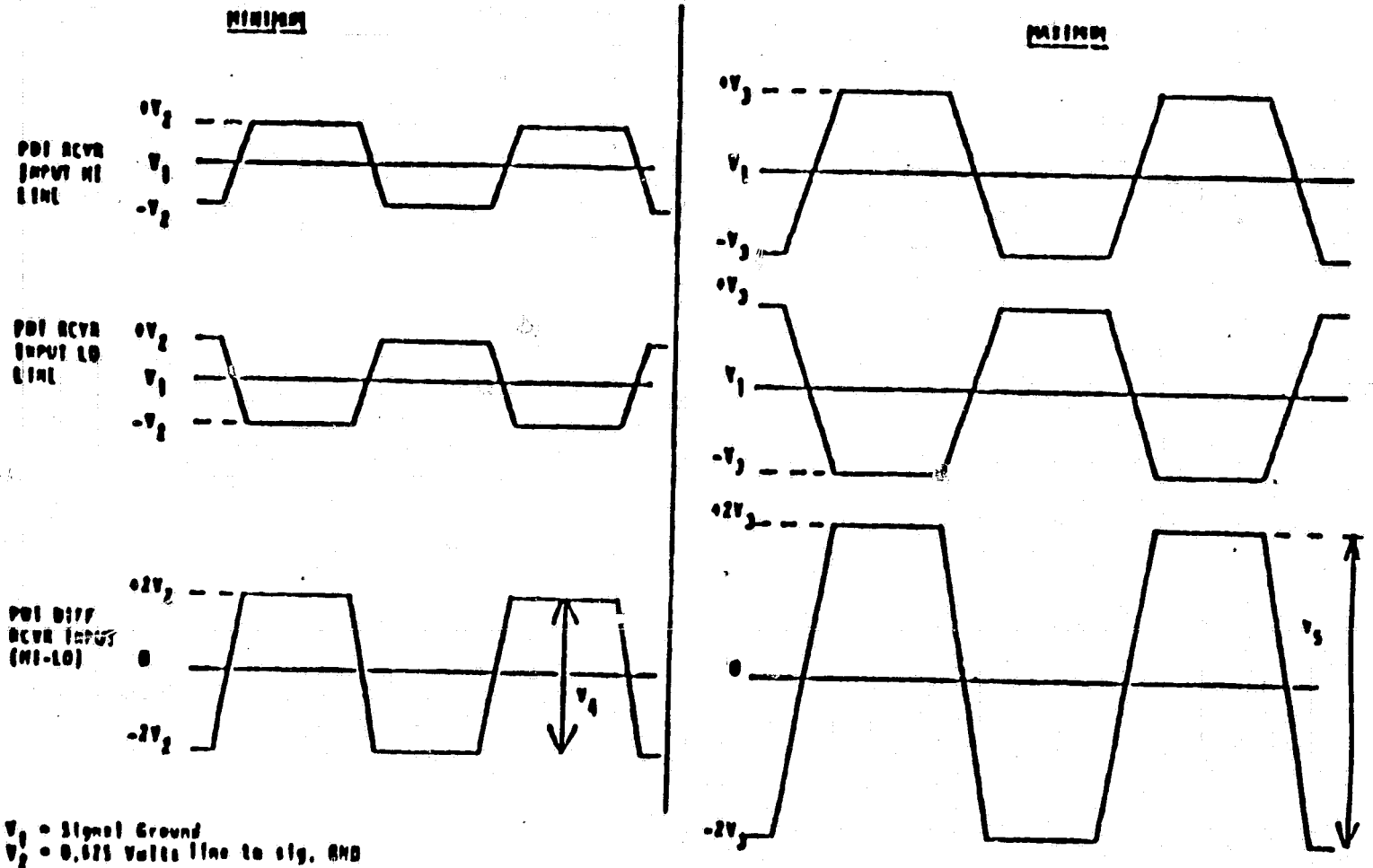

V_1 = Signal Ground
V_2 = 0.575 Volts line to sig. GND
V_3 = 2.28 Volts line to sig. GND
V_4 = 2.5 Volts P-P Differential Line-to-Line Balanced
V_5 = 9.0 Volts P-P Differential Line-to-Line Balanced

FIGURE 5-2 Bi-Polar Lines - Differential Transmission

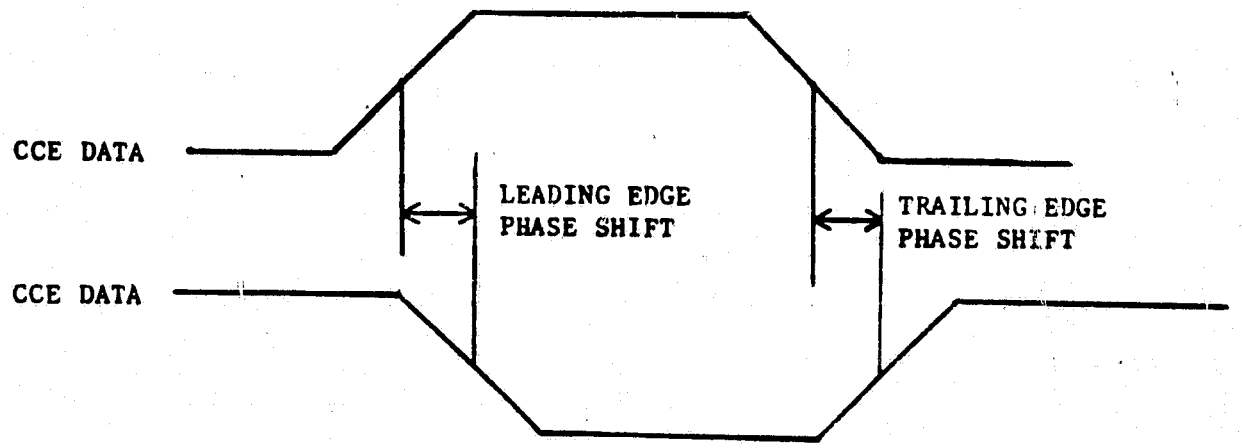

Differential Phase Skew = | Leading Edge Phase Shift - Trailing Edge Phase Shift |

Shere:

Leading/Trailing Edge Phase Shift is the time differential between the 50% points of associated amplitude transitions of the two differential inputs.

FIGURE 5-3 Differential Phase Skew

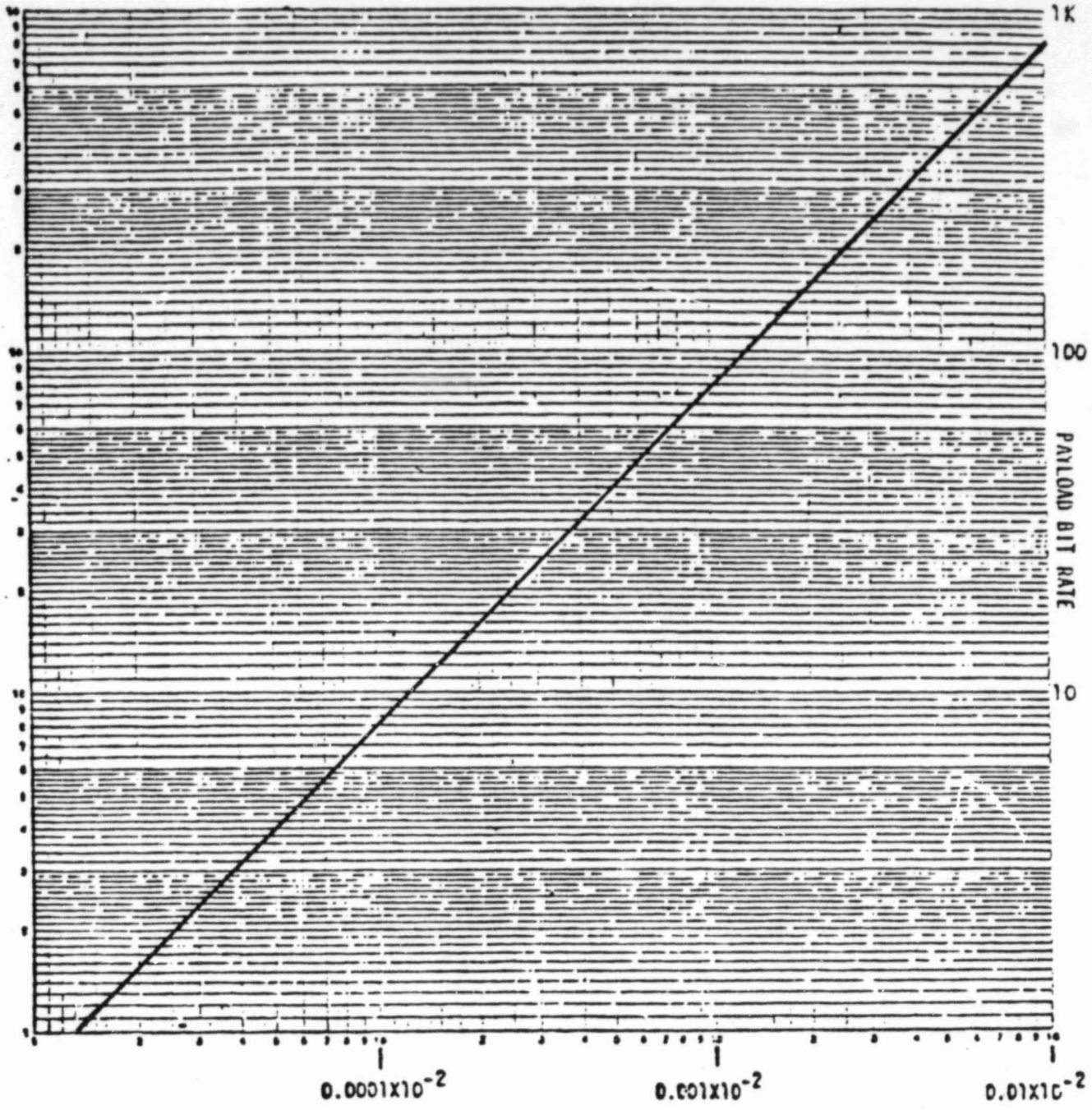

Figure 5-4 10 BPS Payload Bit Rate 500 BPS

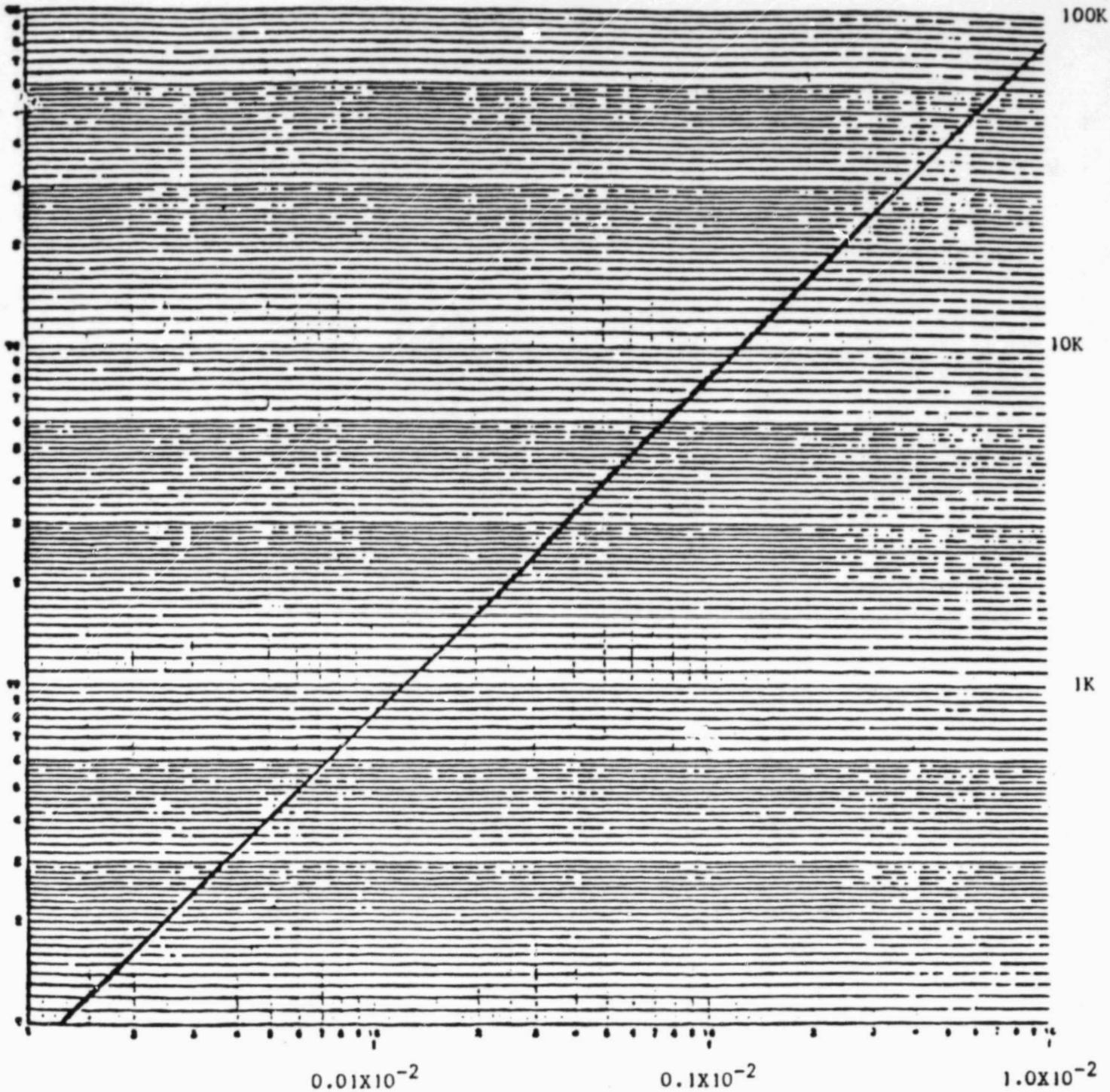

Figure 5-5 500 BPS Payload Bit Rate 64 KBPS

TABLE 6

PDI CLOCK INPUT/CCE TO ORBITER ELECTRICAL INTERFACE CHARACTERISTICS
ALL PARAMETERS REFERENCED TO CISS INTERFACE

Parameter	Dimension	Characteristics Orbiter/CCE Interface	Notes
Signal Type		Differential-Balanced	Refer to Figures 5-1 and 5-2
Amplitute	Volts pk-pk	Min: 2.5 Max: 9.0	Measured line-to-line
Duty Cycle	Percent	50 $\pm$ 5	NRZ bit rate clock
Skew - Data to Clock (NRZ)		Max: $\pm$ 10% of clock period	Bit rate clock to NRZ bit start (1). See Figure 2.10.2.3.2-1
Stability		< 1 part in 10^5 over 60 sec period	
Clock Accuracy	Percent	$\pm$ 3.25	(2)
Waveform Distortion		Overshoot and undershoot less than 20% of peak amplitude level	
Noise	Milivolts	100 pk-pk, differential line-to-line, DC to 100 KHz	CCE transmitting, not transmitting, or failed
Cable		2 conductor twisted, shielded, jacketed, controlled impedance	Rockwell design standard MP572-0328-0002
Cable Impedance	Ohm	75 $\pm$ 5	Characteristic Impedance
Cable Capacitance	Picofarads	2900 max	Capacitance across differential line pair from CISS interface to PDI (18 to 23 pf/ft)
Load Impedance	Ohm	74 min 91 max	DC resistance line-to-line at interface includes cable resistance

TABLE 6

PDI CLOCK INPUT/CCE TO ORBITER ELECTRICAL INTERFACE CHARACTERISTICS
ALL PARAMETERS REFERENCED TO CISS INTERFACE (Continued)

Parameter	Dimension	Characteristics Orbiter/CCE Interface	Notes
Cable Resistance	Ohm	4.4 per conductor (max)	Based on 126 ft. cable length
Cable Length	Feet	126 max	From CISS interface to PDI input
Rise/Fall Time		Max: Refer to Differential Phase Skew	RT/FT are independent of bit rate and data code type (BiØ or NRZ)
Skew-Differential Phase	Nanosecond to Millisecond depending on bit rate	Maximum value shall be the same as that specified for associated NRZ data	
Common Mode	Volt	Min: ±3 pk-pk continuous or ±60 pk-pk for 10 μ sec for damage level	± 3V from EMI, negligible from payload or PDI (3)

(1) Any bit or clock transition point occurs in time at the 50% pk-pk amplitude point.

(2) The PDI shall set an error flag within its BITE Status Register whenever the Payload bit rate exceeds ± 3.25% of its specified center frequency.

(3) Volts across frequency spectrum from DC to 100 KHz.

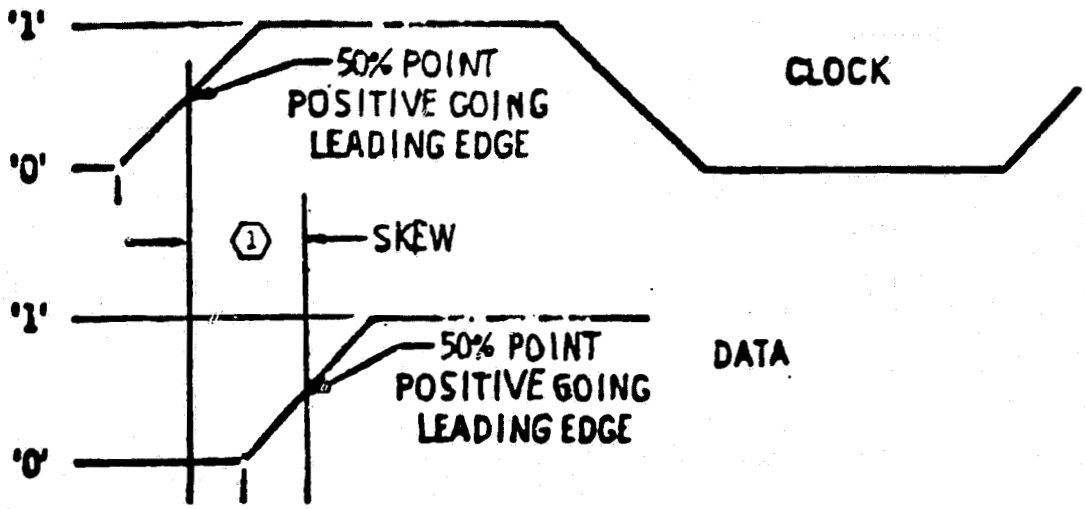

1 The rising edge of each clock signal shall be coincident with the starting edge of the corresponding data bit period within plus or minus 10 percent of the clock period maximum.

Figure 6-1 Skew

TABLE 7

DIGITAL DATA RECORDING ELECTRICAL INTERFACE CHARACTERISTICS
ALL PARAMETERS REFERENCED TO CISS INTERFACE

Parameter	Dimension	Characteristics Orbiter/CCE Interface	Notes
Bit Pate	kbps	64	
Signal Type		Differential	
Data Type		Bi Ø-L	
Rise & Fall Time	Percent Bit Cell Time (BCT)	10 Max	
Signal Amplitude	V, P-P	3.7 Min 9 Max	(3)
Jitter & Assymetry	Percent of BCI	± 2	
Input Impedance (Recorder)	Ohms, L-L	75 ± 10%	
Source Impedance (Payload)	Ohms, L-L	TTI Compatible (4)	
Common-mode Rejection	volts	± 15	(1)
Cable Type		Twisted Shielded Pair	(2)
Cable Impedance (Orbiter)	Ohms	75 ± 5	
Cable Capacitance (Orbiter)	Picofarads	2900 Max (3)	18 to 23 pf per foot
Cable Resistance (Orbiter)	ohms	4.4 per conductor(max) (3)	

(1) Referenced to Signal Ground
(2) FMI class 'RF'. Refer to Table 10.7.1-1
(3) Eased on 126-ft cable length from CISS interface to payload recorder input
(4) such as TI SN55114, or equivalent

TABLE 8

PSP COMMAND DATA OUTPUT, ELECTRICAL INTERFACE CHARACTERISTICS
ALL PARAMETERS REFERENCED AT CISS INTERFACE

Parameter	Dimension	Value	Notes
Subcarrier Frequency	KHz	16 $\pm$ 0.001% (long term) (1)	Sine wave
Subcarrier Harmonic Distortion	Percent	Less than 2% of the power in the subcarrier	Total harmonic distortion
Subcarrier Frequency Stability		$\leq 10^{-7}$ of the subcarrier frequency over a 10 second period (short term) (1)	
Subcarrier Modulation		PSK	
Data Rate	bps	1000 $\pm$ 0.001%(long term (1)	
Data Rate Stability		10^{-7} over a 10 second period (short term) (1)	
Data Types		NRZ-L	
Frequency-to-Bit Rate Ratio		Multiple of data rate	Data waveform shall conform to S/C zero crossings within $\pm$ degrees
Data Transition		Data shall alter S/C phase by $\pm$ 90° $\pm$ 10%	
Amplitude	volts p-p	3.0 to 4.4, line-to-line	Voltage at CISS interface includes orbiter cable losses
Phase Jitter	Percent of bit period	3 max	
Data Asymetry	Percent of bit period	2 max over a 300 bit period	See Fig 9
Channel-to-Channel Isolation	dB	40 min	Between-channel isolation when each channel is terminated with 75 ohms

TABLE 8

PSP COMMAND DATA OUTPUT, ELECTRICAL INTERFACE CHARACTERISTICS
ALL PARAMETERS REFERENCED TO CISS INTERFACE (Continued)

Parameter	Dimension	Value	Notes
Source Impedance	Ohms	< 15	
Load Impedance	ohms	75 ± 10%	
Output Type		Differential	
Load Termination		Differential, Direct Coupled	
Offset	volts	0.0 ± 0.5 either line-to-ground	
Cable Type		Twisted Shielded Pair	EMI class 'RF' refer to Table TBD
Cable Impedance (Orbiter)	Ohms	75 ± 5	
Cable Capacitance (Orbiter)	Picofarads	2900 max (2)	18 to 23 pf per foot
Cable Resistance (Orbiter)	Ohms	4.4 maximum per conductor (2)	
Cable Length (Orbiter	Feet	126 (max)	From PSP to CISS interface

(1) Based on MTU accuracy and stability
(2) Based on 126 foot cable length from PSP output to CISS interface

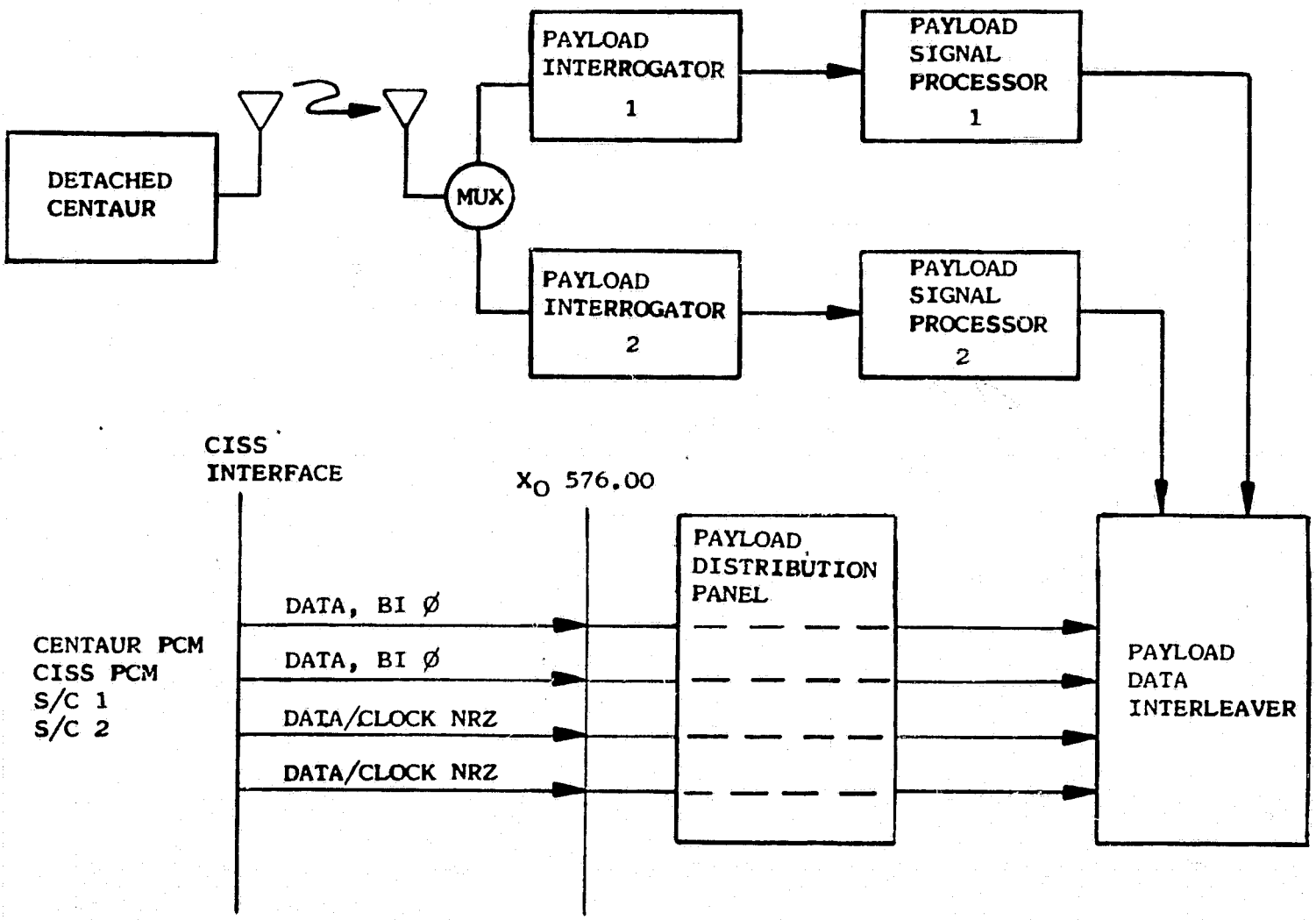

FIGURE 1 PAYLOAD DATA INTERLEAVER DATA FLOW

	N WORDS PER FRAME		
	SYNC	COUNTER	
M FRAMES PER DATA CYCLE	"	"	
	"	"	
	"	"	
	"	"	
	"	"	
	"	"	
	"	"	
	"	"	
	"	"	
	"	"	
	"	"	

- CENTAUR USES A SHUTTLE STANDARD TYPE 3 FORMAT
- WORD LENGTH IS 8 BITS.
- DCU DIGITAL DATA OCCUPIES 3 WORDS (24 BITS).
- SYNC PATTERN IS 01147537 OCTAL - PROGRAMMED BY SOFTWARE.
- FRAME COUNTER COUNTS FROM 1 TO M (COUNTER IS 8 BITS).
- M, N ARE TBD, BUT BOTH WILL BE EVEN.
- DATA CYCLE WILL BE APPROXIMATELY 1 SECOND LONG.

Figure 2 Type 3 Shuttle Standard Format

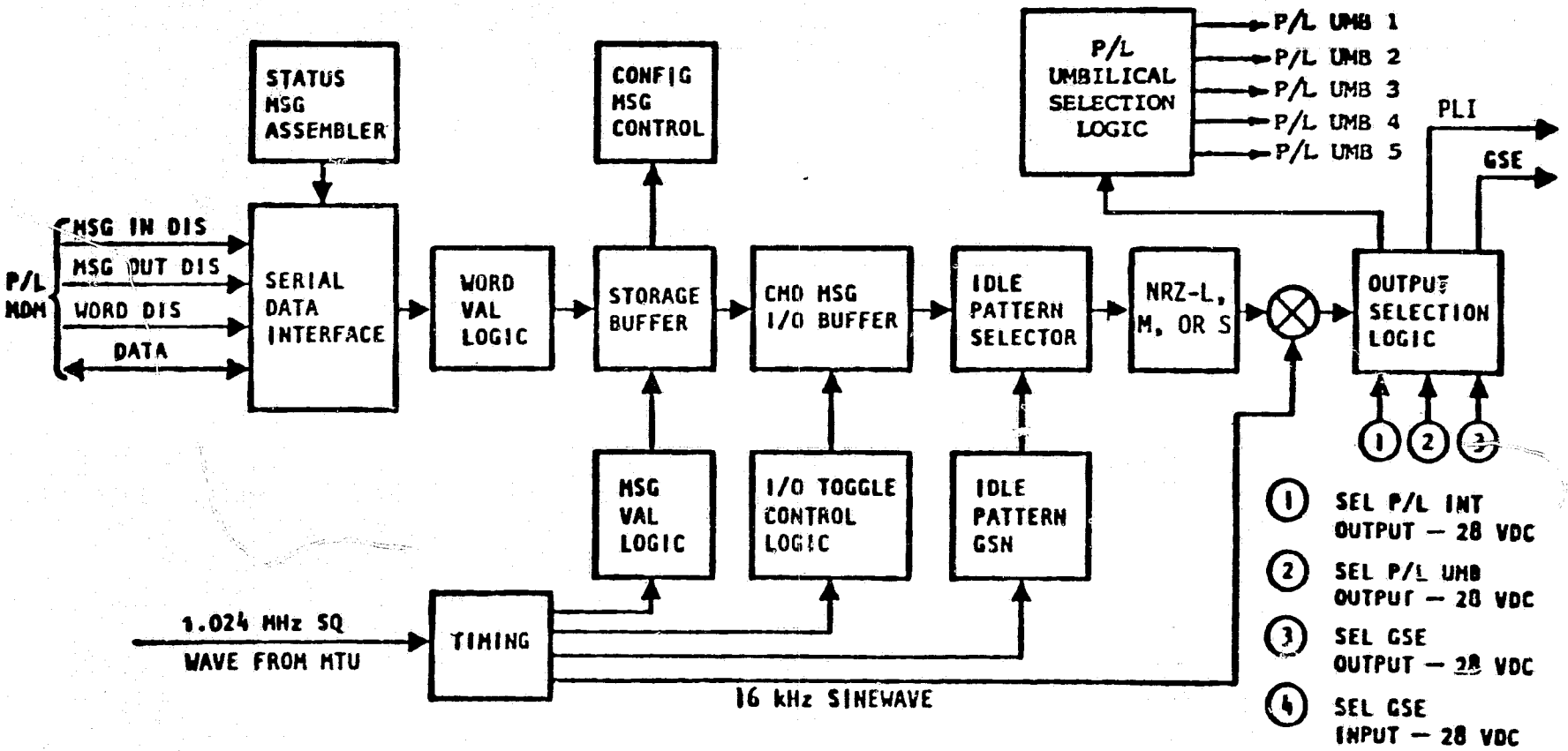

Figure 3 Functional Block Diagram (Command Portion)

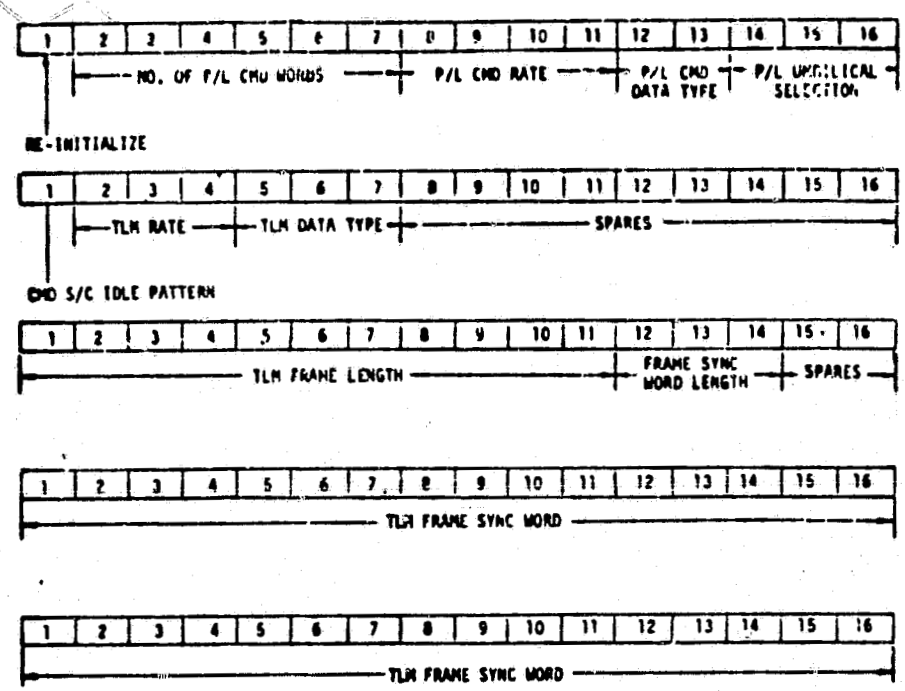

Figure 4 PSP Configuration Message

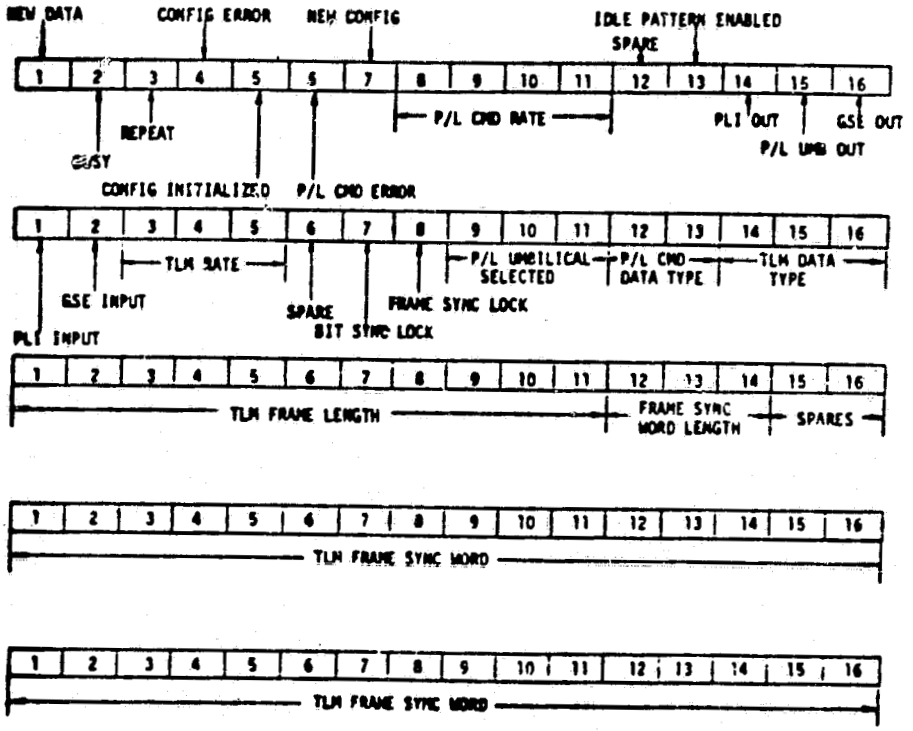

Figure 5 PSP Status Message

GROUNDING AND SHIELDING TERMINATION

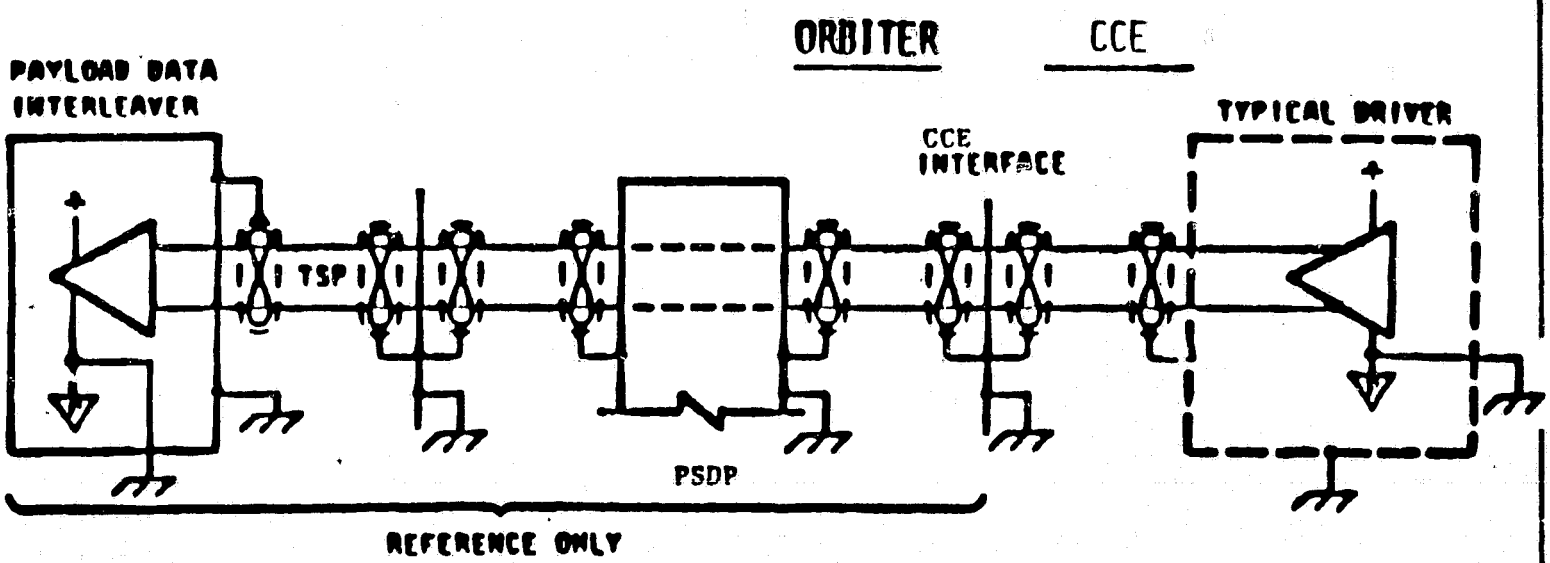

Figure 6 Payload Data Interleaver Grounding and Shielding Interface Data & Clock

GROUNDING AND SHIELDING TERMINATIONS

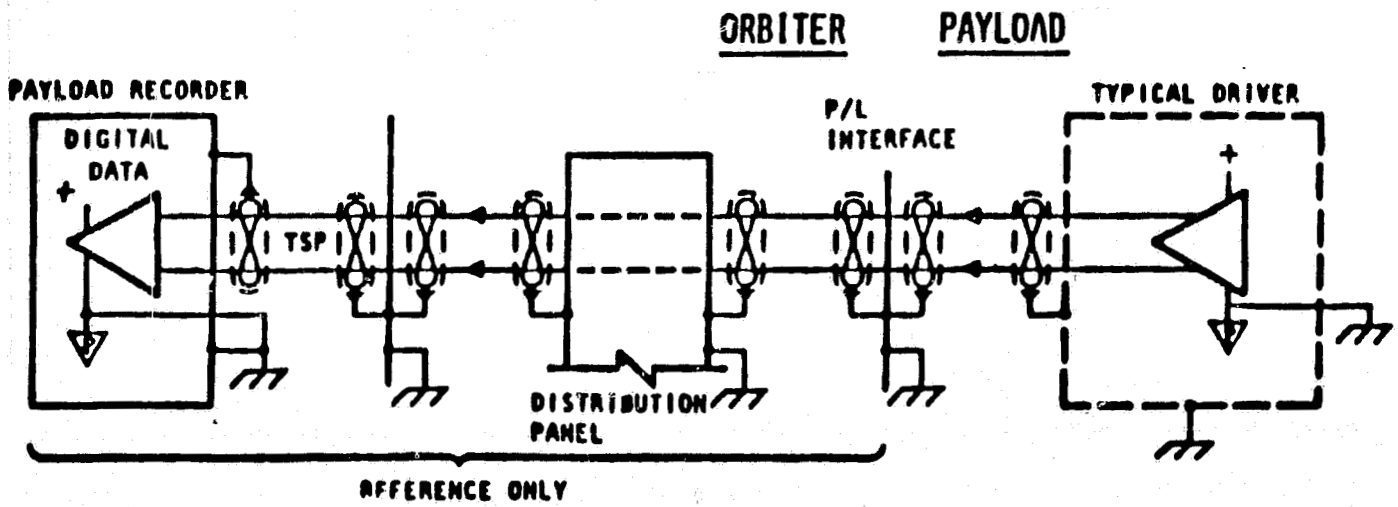

Figure 7 Data Recorder Grounding and Shielding

GROUNDING AND SHIELDING TERMINATION

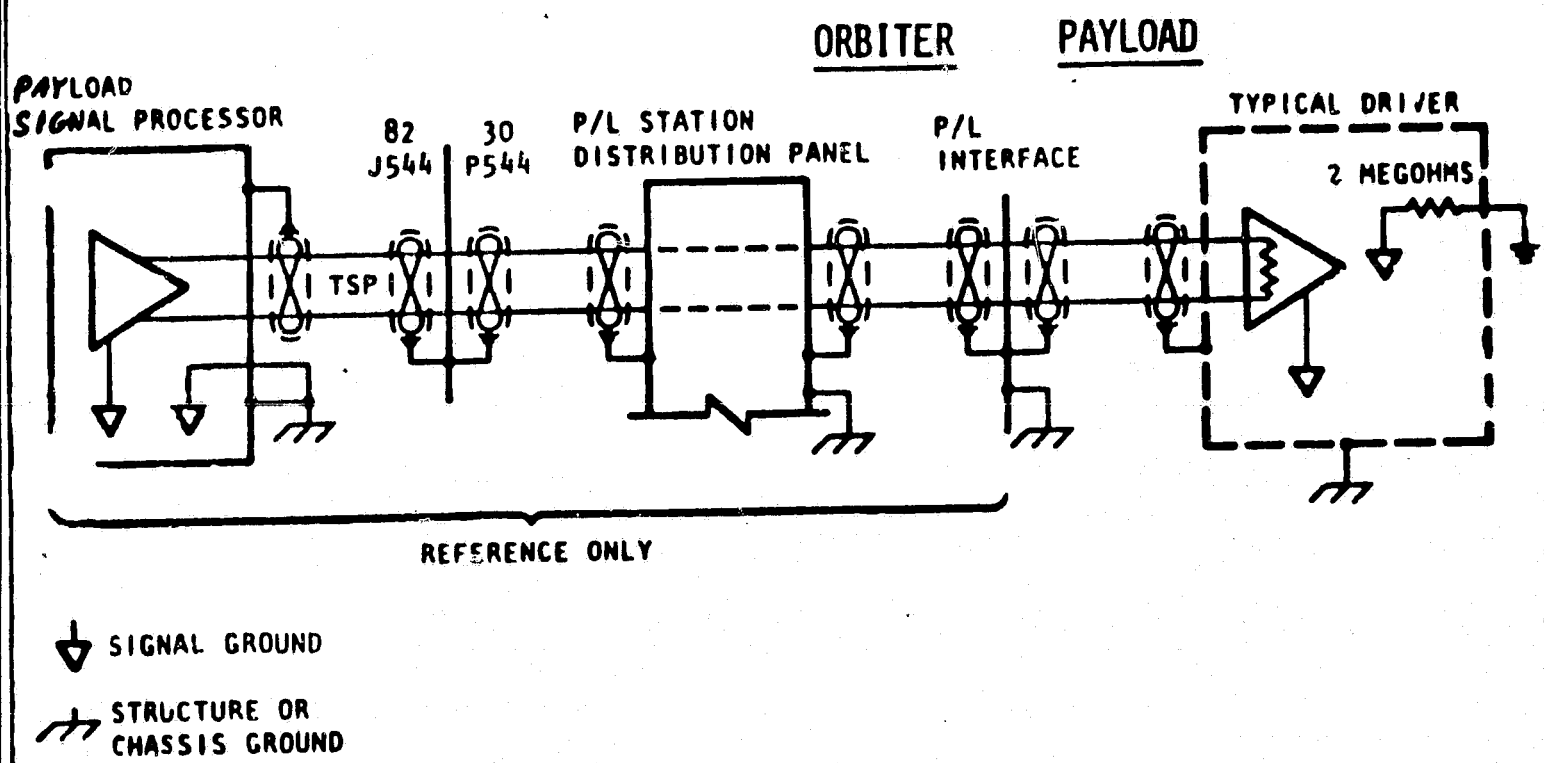

Figure 8 Payload Signal Processor Grounding and Shielding

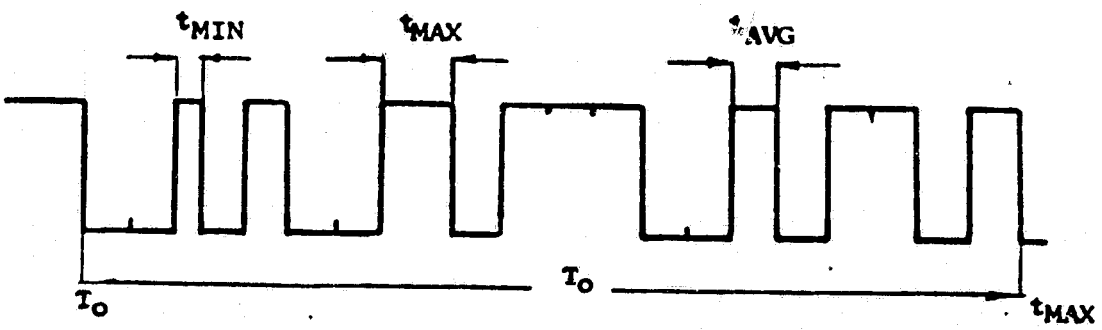

NOTES:

1. t_{MAX} - MAXIMUM SYMBOL PERIOD
2. t_{MIN} - MINIMUM SYMBOL PERIOD
3. t_{AVG} - IS THE AVERAGE SYMBOL PERIOD
4. T_o - IS THE OBSERVATION TIME
5. ASYMMETRY DOES NOT ACCUMULATE (i.e., $t_{AVG} = \frac{1}{R}$ WHERE R IS THE DATA RATE)

$$\text{ASYMMETRY \%} = \frac{t_{MAX} - t_{MIN}}{t_{MAX} + t_{MIN}} \times 100\%$$

Figure 9 Digital Data Asymmetry

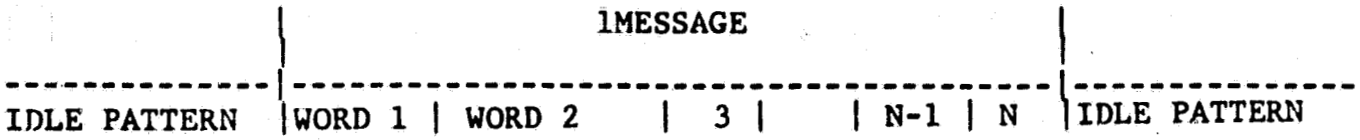

- IDLE PATTERN IS 101010 .. - MINIMUM OF 132 BITS PRECEEDING EACH MESSAGE
- ALL WORDS ARE 16 BITS. THERE ARE NO START OR STOP BITS BETWEEN WORDS.
- WORD 1 IS A FIXED SYNCHRONIZATION PATTERN, REGARDLESS OF THE MESSAGE TYPE. THE SPECIFIC PATTERN IS TBD.
- WORD 2 DEFINES THE MESSAGE TYPE (I.E., COMMAND OR NAVIGATION UPDATE) AND MESSAGE LENGTH (NUMBER OF WORDS).
- WORD N IS A CHECKSUM OF THE PREVIOUS WORDS FOR ERROR DETECTION PURPOSES. THERE IS NO ERROR CORRECTION CAPABILITY.
- THE TOTAL MESSAGE LENGTH IS VARIABLE.
- A CONTINUOUS IDLE PATTERN IS DESIRED BETWEEN MESSAGES TO MAINTAIN SYNCHRONIZATION OF THE COMMAND DETECTOR UNIT IN THE CENTAUR TRANSPONDER.

Figure 10 Preliminary Centaur Command Format

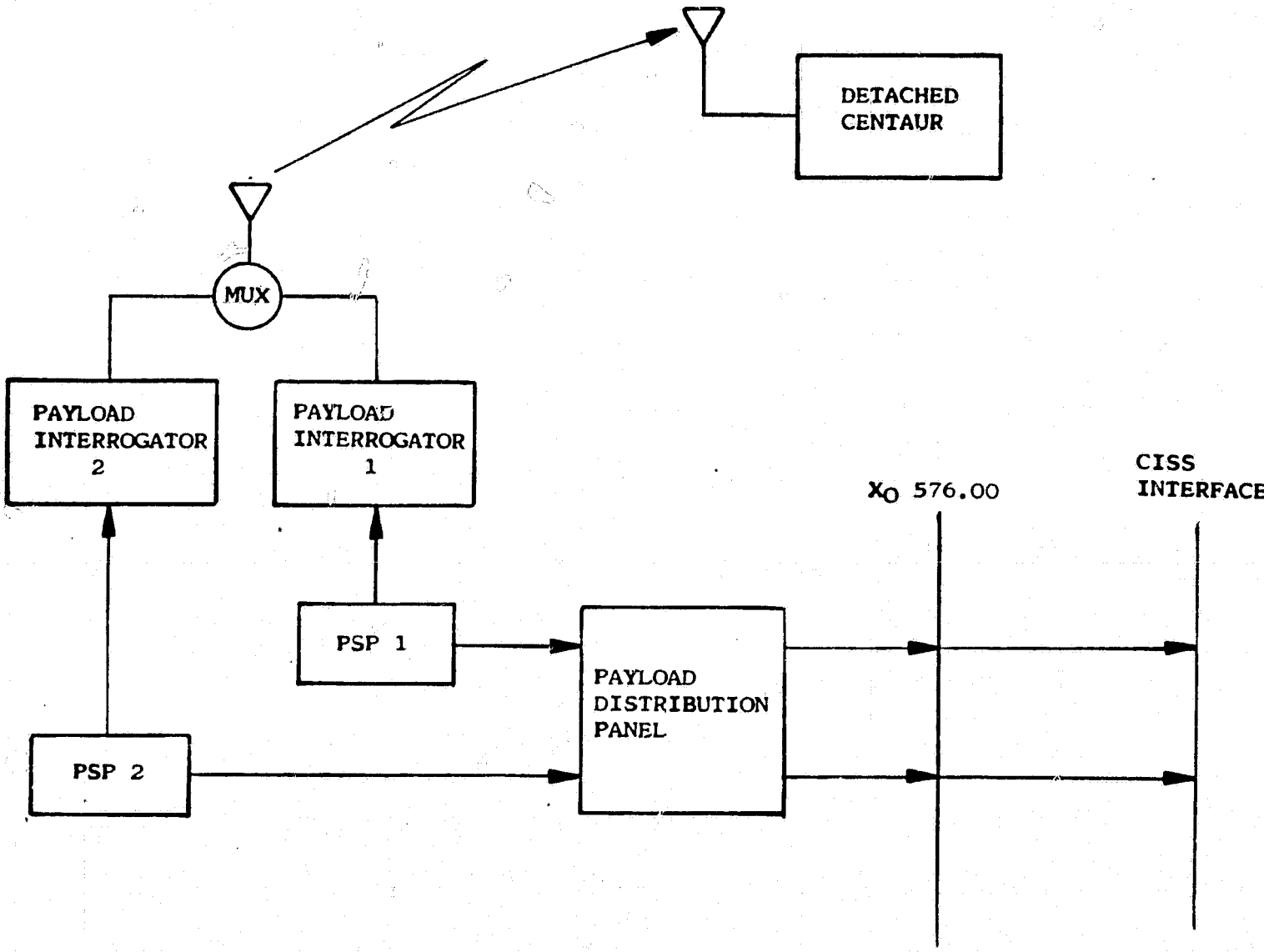

FIGURE 11 PAYLOAD SIGNAL PROCESSOR COMMAND DATA FLOW

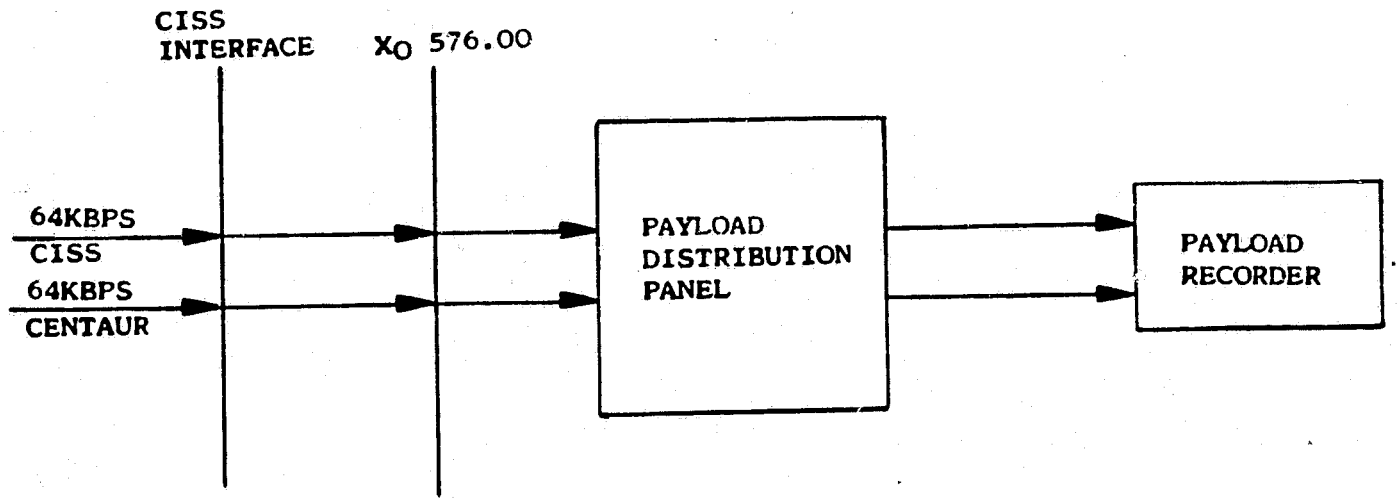

FIGURE 12 PAYLOAD RECORDER DATA FLOW

Figure 12 Payload Recorder Data Flow

9.0 SOFTWARE REQUIREMENTS

9.1 Software Overview. TBD.

9.2 Orbiter General Purpose Computer Standard Software Service. TBD.

9.3 Mission Phase Applicability. TBD.

9.4 Software Constraints. TBD.